Title

Regulation of Plasticity at Individual Dendritic Spine Synapses

Author

Flores, Juan Carlos

Publication Date

2024

Peer reviewed|Thesis/dissertation

Regulation of Plasticity at Individual Dendritic Spine Synapses

By

JUAN C. FLORES
DISSERTATION

Submitted in partial satisfaction of the requirements for the degree of

DOCTOR OF PHILOSOPHY

in

Molecular, cellular, and integrative physiology

in the

OFFICE OF GRADUATE STUDIES

of the

UNIVERSITY OF CALIFORNIA

DAVIS

Approved:

Karen Zito, Chair

John Gray

Johannes Hell

Jie Zheng

Committee in Charge

2024

Regulation of Plasticity at Individual Dendritic Spine Synapses

Abstract

Learning is crucial for survival. Learning involves the remodeling of synaptic connections in the brain which alters the strength of the synapses in response to activity. These changes in synaptic strength are known as synaptic plasticity. Synaptic plasticity has been a heavily studied topic since the discovery of long-term potentiation (LTP) by Bliss and Lomo in 1973. Much of this research focuses on the synaptic plasticity of connections in the hippocampus, a brain region which is critical for learning. It has been observed that learning can be more effective when using the spaced learning technique, where learning sessions are broken up by short breaks. Interestingly, it has been shown that spaced learning paradigms improve learning in animal models of Down's and fragile X, which exhibit impaired learning. It has been proposed that this efficacy of spaced learning is due to saturation of plasticity, a state in which synapses become unresponsive to plasticity stimuli following the initial induction of plasticity. Saturation of plasticity has been observed in the hippocampus and artificial induction of saturation leads to learning deficits in rodents. It has also been shown that following the induction of plasticity at hippocampal circuits, these become unresponsive to further plasticity-inducing stimulation. After some time, these circuits can undergo plasticity again. Yet, how saturation of plasticity is occurring and what molecular mechanisms are responsible for the onset and offset of saturation have not been identified. I hypothesized that saturation of plasticity can occur at individual dendritic spines—membranous protrusions on dendrites which are the postsynaptic site of excitatory neurotransmission in the cortex. In **Chapter 1** of this dissertation, I review the current

literature on the molecular makeup of dendritic spines, their plasticity mechanisms and saturation of plasticity. **Chapter 2** of this work contains experiments which I conducted to elucidate mechanisms which are involved in saturation of plasticity at individual spines. I show that plasticity can be saturated at individual dendritic spines and that after a period of 60 minutes, these same spines are able to undergo further plasticity. This time period of saturation can be described as a refractory period for plasticity. I also show that CaMKII signaling is impaired in saturated spines and that increasing the strength of the plasticity-inducing stimulation is not sufficient to recover their plasticity during the refractory period. Additionally, I show that the refractory period can be shortened by the overexpression of the synaptic scaffolding protein, PSD95. In **Chapter 3**, I explore mechanisms that may be related to saturation of plasticity, including a potential role for an NMDA receptor subunit switch, metabotropic glutamate receptor and the timing of the arrival of PSD95 at potentiated synapses. **Chapter 4** of this work is a reflection of my contributions to the field of plasticity and my thoughts on the future directions on this line of research. Finally, I have included an **Appendix** in which I tested the role of $mGluR_5$ in mGluR-mediated long-term depression (LTD) in spines of different sizes.

Acknowledgements

Pursuing a doctoral degree is no easy feat. I would not have been able to complete my work without the help and guidance of many people. I would like to thank these individuals for their support.

Firstly, I would like to thank my graduate advisor, Dr. Karen Zito, for her endless support and patience. When we first met, Dr. Zito's passion and enthusiasm for her research inspired me to join her lab for my PhD. When I arrived at UC Davis, I did not have much of a background in neuroscience. Dr. Zito is a truly caring advisor, and she took the time to help me navigate this new field and get up to speed as I began my dissertation research. Dr. Zito has helped me develop into a more confident person and an independent scientist. I will be forever grateful to her for this opportunity.

I would also like to thank the other members of my dissertation committee, Drs. Johannes Hell, John Gray and Jie Zheng. Their feedback and advice on my experiments was invaluable to the completion of this work. I would especially like to thank Dr. John Gray for providing me with GluN2 conditional knock-out mouse lines that were used for my research.

I would like to acknowledge the current and former members of the Zito lab for all of their contributions. Dr. Ivar Stein inspired me to be a rigorous scientist and a kind person. Sam Petshow, Lorenzo Tom, Marco Alarcon and Drs. Margo Anisimova, Nicole Claiborne, Jinyoung Jang, Deborah Park and Dipannita Sarkar made my time in the Zito lab fun and kept me in good spirits when my experiments weren't working. I also want to thank them for their feedback and engaging conversations that made me think more deeply about my research and led me to new insights.

Finally, I would like to thank my family for their endless love and unconditional support. My daughter Sophia and my wife Jackie were my motivation and my biggest supporters. I thank them for following me in my journey and motivating me to push myself to achieve my goals. I would not have been able to complete this doctorate without them. The love and support of my parents was also instrumental to my success and I cannot thank them enougeh. To them I say: “Si, se puede!”

Contents

Chapter 1: Literature Review

Introduction

Our brains are remarkable biological structures that allow us to perceive the world around us and generate appropriate responses to outside stimuli. Most importantly, our brains have the ability to rapidly change in response to new experiences and recall prior experiences. Learning can take different forms, such as recalling past events, recognizing familiar faces or learning motor skills. Some memories are explicit, like recalling the name of someone you have just met while others, like riding a bicycle, are implicit. These types of memory are necessary for our survival, and the modification of the brain's synaptic circuitry is required for the formation of both types.

One area of the brain that is important for learning is the hippocampus. A classic example that demonstrates the importance of the hippocampus for learning is that of patient HM, who suffered from anterograde amnesia following bilateral resection of their hippocampus to treat epilepsy (Scoville & Milner, 1957). While HM could recall life events and childhood memories which occurred prior to their surgery, they could not form new declarative memories (Milner et al., 1968; Scoville & Milner, 1957). Despite this deficit, patient HM was capable of acquiring new motor skills (Corkin, 1965). This suggests that while not all learning requires the hippocampus, it is a region that is critical for declarative learning.

The ability to learn is crucial for our survival. This ability relies on the rewiring and modification of the connections between the neurons in the brain, a process known as synaptic plasticity (Bliss & Lømo, 1973). Most of the excitatory connections in the brain find their postsynaptic site at dendritic spines, small membranous protrusions which emanate from the shafts of dendrites. Dendritic spines were first observed by Santiago Ramon y Cajal by using a silver nitrate stain, known as the Golgi stain. Cajal hypothesized that these "espinas", or spines as he described

them, received contacts from the axons of other neurons (Yuste, 2015). Unfortunately for Cajal, his hypothesis was in opposition to the prevailing hypothesis of the time, which proposed that neurons formed a continues network, joined by gap junctions. After Cajal's death in 1934, dendritic spines were first seen under the electron microscope in 1959 (E. G. Gray, 1959a, 1959b). These studies revealed that spines did in fact make contact with axons and formed synapses with a post-synaptic density on the spine and vesicles in the presynaptic axons separated by a small synaptic cleft measuring 25-30 nm (E. G. Gray, 1959a).

Since their discovery, dendritic spines and their function have been a heavily studied topic. Early studies showed that spines are diverse in their head morphology and they were hypothesized to be involved in neuronal signaling and synaptic plasticity (K. M. Harris & Stevens, 1989; K. Harris & Stevens, 1988). These structures are dynamic and can change in number, shape and size (Lendvai et al., 2000; Trachtenberg et al., 2002; Matsuzaki et al., 2004; Holtmaat et al., 2005). Later studies using 2-photon imaging *in vivo* showed that dendritic spines can change in an experience-dependent manner (Grutzendler et al., 2002; Lendvai et al., 2000; Trachtenberg et al., 2002). Dendritic spines were shown to house α-amino-3-hydroxy-5-methyl-4-isoxazolepropionic acid (AMPA)-type glutamate receptors using immunogold labeling (Ottersen & Landsend, 1997; Takumi et al., 1999). Using a newly developed caged glutamate compound and 2-photon microscopy, it was shown that the strength of AMPA receptor currents were tightly correlated with spine size and geometry (Matsuzaki et al., 2001). Using this newly developed tool, individual dendritic spines were shown to undergo long-term potentiation (LTP) in response to high frequency glutamate-uncaging (HFU) stimulation. It was shown that a spine's glutamate-induced excitatory postsynaptic currents (uEPSCs) strengthen in response to HFU stimulation and that this increase in uEPSCs was strongly correlated with an increase in the size of the spine (Matsuzaki et al., 2004). Thus, spines are a site of synaptic contact, they are highly dynamic structures *in vivo* and they can undergo LTP, which is thought to be the cellular

mechanism of learning. These characteristics make dendritic spines a prime candidate to be substrates for learning.

Dendritic spines have been shown to have a significant role in learning. Studies have shown that after learning a novel motor task, mice exhibit an increase in the formation of new spines and elimination of existing spines in the motor cortex (G. Yang et al., 2009). Importantly, the stabilization of new dendritic spines was correlated with improved performance of the learned task. In fact, there is evidence which shows that reversing learning-induced changes of dendritic spines *in vivo* after learning an accelerated rotorod task leads to a loss of the learned behavior (Hayashi-Takagi et al., 2015). In this study, animals expressing a novel photoactivatable Rac1, which was targeted to spines that were activated during learning, was used to selectively shrink spines that were involved in the learned behavior. When the spines that were active during learning were experimentally collapsed, the animals' performance in the learned task returned to pre-training levels.

Much work has also been done to understand the role of dendritic spines in disease (for review see Penzes et al., 2011). Dysregulation of spine dynamics are observed in various neurological disorders like Alzheimer's disease, schizophrenia and some forms of autism spectrum disorder. Post-mortem brains of patients with schizophrenia show a reduction of dendritic spine density compared to healthy, age-matched individuals (Rosoklija et al., 2000). Similarly, post-mortem brain samples from individuals with Alzheimer's disease have a reduction in spine density compared to healthy individuals (Boros et al., 2017). Interestingly, this study found that individuals with Alzheimer's disease pathology, but no cognitive impairment did not exhibit the same reduction in dendritic spines, suggesting that the cognitive deficits found in Alzheimer's are mediated by the loss of dendritic spines. This, however, does not mean that having more dendritic spines is necessarily beneficial. Indeed, some forms of autism spectrum disorder are associated with an elevated number of dendritic spines (Hutsler & Zhang, 2010). These studies

show that normal brain function requires a balanced dendritic spine number and disruption of dendritic spine density is associated with cognitive impairments.

The rich history of research about dendritic spines is well warranted. Dendritic spines play an important physiological role in learning and are associated with disorders that manifest with cognitive dysfunction. Understanding how spines are involved in the formation of new memories and the molecular signaling pathways that lead to synaptic plasticity can further our understanding of normal cognitive function and may elucidate targets for pharmacological interventions for individuals with cognitive impairments associated with dendritic spine dysregulation.

Section 1: Synaptic Plasticity of Dendritic Spines

The Molecular Makeup of Dendritic Spines

Dendritic spines are small membranous protrusions that emanate from the shafts of dendrites. These membranous compartments are supported by an underlying cytoskeleton of actin filaments (Matus, 2000). This network of actin helps to maintain the shape of the spine and it can be modified to support the changes in spine size associated with synaptic plasticity (Honkura et al., 2008; Chazeau & Giannone, 2016). Dendritic spines house the postsynaptic density, a protein dense region of dendritic spines found at the sites of synaptic contact. The postsynaptic density (PSD) consists of neurotransmitter receptors, signaling molecules and scaffolding molecules that recruit and maintain the proteins that constitute the postsynapse. While most dendritic spines contain excitatory synapses, studies show that spines can house multiple synapses (known as perforated synapses; (K. M. Harris et al., 1992; Y. Sun et al., 2021)) and that a small number of spines (~5-10%) house both excitatory and inhibitory synapses (Kleinjan et al., 2023).

Synaptic Scaffolding Proteins in Dendritic Spines

The PSD of dendritic spines is enriched in scaffolding molecules that are important for synaptic transmission. These proteins support synaptic transmission and plasticity by anchoring the receptors and transsynaptic adhesion molecules of spines in the PSD. One class of molecules that is important for synaptic function is the PSD membrane associated guanylate kinases (MAGUKs). Notably, dendritic spines have enriched levels of two important PSD-MAGUKs, PSD95 and PSD93. These two MAGUKs have similar structures, both have 3 PDZ domains, an SH3 and a GK domain with 2 palmitoylation site on their N-terminus (Won et al., 2017). Despite the similarities these two PSD-MAGUKs play vastly different physiological roles. Homeostatic upscaling of synaptic currents requires both PSD95 and PSD93, while scaling down does not require PSD93 (Q. Sun & Turrigiano, 2011). Furthermore, it has been shown that loss of PSD95 prevents maturation of silent synapses (which exhibit NMDA receptors but no AMPA receptors) while loss of PSD93 has the opposite effect, leading to protracted maturation of silent synapses (Favaro et al., 2018). Our lab has previously shown that in nascent dendritic spines PSD93 is enriched to mature levels within 4.5 hours, while PSD95 takes up to 20 hours to reach mature levels (Lambert et al., 2017). My work in **Chapter 2** shows that PSD95, but not PSD93, plays a role in the recovery of plasticity at saturated spines.

Dendritic Spine Glutamate receptors

Spines with excitatory glutamatergic synapses have a variety of receptors on their membranes. Spines have AMPA-type glutamate receptors, N-methyl-D-aspartate (NMDA)-type glutamate receptors and metabotropic glutamate receptors. Even within these broad classifications there are multiple receptor subtypes. These receptors all play different roles in the synaptic signaling and plasticity of dendritic spines (for review see Traynelis et al., 2010 and Scheefhals & MacGillavry, 2018).

The AMPA-type glutamate receptors are heterotetrameric proteins that form a channel pore, which opens in the presence of glutamate. These AMPA receptors are permeable to Na^+ and K^+ and play a role in the depolarization of the postsynaptic neuron during synaptic activity. The AMPA receptors can be modulated by phosphorylation and they can be inserted or removed from synapses upon the induction of plasticity, thereby altering the strength of the synapse. A subset of AMPA-type glutamate receptors are GluA1 homomers, lacking the GluA2 subunit of the receptor. In addition to monovalent cations, these GluA2-lacking AMPA receptors are also permeable to calcium (Hollmann et al., 1991). Receptors lacking the GluA2 subunit are transiently recruited into the synapse following the induction of LTP (Plant et al., 2006).

Another glutamate receptor, the NMDA-type receptor, is found in spines and is critical for the induction of plasticity. Like the AMPA receptor, there are many types of NMDA receptors, depending on their subunit composition. The NMDA receptor is permeable to monovalent cations and more importantly, it is permeable to Ca^{2+}. The NMDA receptor is a heterotetrameric complex with two obligatory GluN1 subunits and 2 GluN2/3 subunits. The GluN1 subunits of the receptor bind to D-serine or glycine as a co-agonist. The GluN2 subunit is responsible for binding glutamate and there are 4 genes encoding variants (GluN2A-D) which give the NMDA receptor different current dynamics and calcium permeabilities (for review see Paoletti et al., 2013). The NMDA receptor is known as a coincidence receptor because it requires simultaneous postsynaptic depolarization and presynaptic glutamate release to open its channel pore. Activation of the NMDA receptor is necessary for the induction of LTP and long-term depression (LTD). The pattern and duration of synaptic stimulation determines the activation and the level of Ca^{2+} elevation in dendritic spines, leading to either LTP or LTD (S.-N. Yang et al., 1999). In addition to its ionotropic signaling, the NMDA receptor has also been observed to have non-ionotropic signaling which occurs when glutamate binds the receptor in the absence

of co-agonist binding (and therefore no ion flux) and biases synapses towards LTD (Nabavi et al., 2013; Aow et al., 2015; Stein et al., 2015, 2020).

A third class of glutamate receptors are the metabotropic receptors (mGluRs). Physiologically, activation of mGluRs can alter the ability of synapses to undergo plasticity, or metaplasticity. It has been observed that $mGluR_5$ but not $mGluR_1$ or $mGluR_7$ activation is necessary for a switch from mGluR and NMDAR-dependent LTP to a form of LTP that only requires activation of the NMDAR (Bortolotto et al., 1994, 2005). The mGluRs are g-protein coupled receptors that activate internal signaling cascades. They are classified (class I-III) by their homology and their G-protein signaling pathway. Group I mGluRs are found postsynaptically and groups II and III are found at presynaptic sites (Niswender & Conn, 2010). The group I mGluRs, $mGluR_1$ and $mGluR_5$ receptors are generally associated with G_q/G_{11} and activate this pathway to induce the downstream release of Ca^{2+} from internal stores and the activation of protein kinase C (PKC). Interestingly, $mGluR_5$ has been shown to be highly localized and regulated by the NMDA receptor in cortical neurons (Alagarsamy et al., 2002). It has been previously shown that mGluRs activation at spines of different sizes has differential effects on LTD (Holbro et al., 2009; Oh et al., 2013). In the **Appendix**, I investigate the role of $mGluR_1$ and $mGluR_5$ in LTD at small and large spines.

Molecular Mechanisms of Spine Plasticity

Role of CaMKII in Spine Plasticity

The changes in synaptic plasticity that are involved in learning have been associated with changes in spine morphology. The induction of LTP and LTD at individual dendritic spines is accompanied by spine growth and spines shrinkage, respectively (Matsuzaki et al., 2004; Oh et al., 2013). These changes are initiated by the release of glutamate from presynaptic terminals into the synaptic cleft. Glutamate can then activate the AMPA receptor to allow postsynaptic

depolarization and thus activation of the NMDA receptors. The opening of the NMDA receptors leads to an influx of calcium. The frequency and duration of calcium influx will determine the type of plasticity that the synapse experiences. Generally, short high-frequency stimuli induce LTP and spine growth, while prolonged low-frequency stimulation induces LTD and spine shrinkage. The influx of calcium activates a key signaling molecule, calcium/calmodulin dependent kinase II α (CaMKIIα) which is involved in the LTP/LTD decision by integrating the calcium signal via its autophosphorylation at reside T286 or T305/306, to promote either LTP when T286 is phosphorylated or LTD when T286 and T305/306 are phosphorylated (Cook et al., 2021). Phosphorylation of T286 allows for CaMKII to maintain some autonomous activity (~15-25% of its maximal activity) after calcium levels return to baseline following glutamatergic activity (Coultrap et al., 2010). Following high-frequency glutamate uncaging, CaMKIIα is recruited to the stimulated spines (Zhang et al., 2008). This recruitment of CaMKII to the PSD is mediated by its interaction with the GluN2B subunit of the NMDA receptor and plays a role in the maintenance of synaptic strength (Barcomb et al., 2016). Live imaging of CaMKII activity using 2-photon FRET-FLIM and glutamate uncaging reveals that CaMKII is rapidly and transiently activated within stimulated spines during LTP-induction (S.-J. R. Lee et al., 2009). The activation of CaMKII leads to a plethora of downstream effects like the phosphorylation of various receptors and proteins which alter the synaptic strength and size spines (for review see Yasuda et al., 2022 and Bayer & Schulman, 2019).

Potentiation of Synaptic Strength

One consequence of CaMKII activation that is thought to be crucial for LTP is the phosphorylation of AMPA receptors at S831 on the intracellular C-terminal tail of the GluA1 receptor subunit (Barria et al., 1997; Mammen et al., 1997). This phosphorylation increases the single channel conductance of AMPA receptors (Derkach et al., 1999). Increases in AMPA receptor conductance are only partially responsible for the increase in synaptic currents after

LTP-induction. In addition, after the chemical induction of LTP, it has been observed that the AMPA receptor content of dendritic spines is increased shortly after their enlargement (Kopec et al., 2006). Increases in AMPA receptor content can be driven by CaMKII activation but does not require the phosphorylation of GluA1 at S831 (Hayashi et al., 2000). It was also shown that the C-terminal tail of the GluA1 subunit is sufficient for spine growth but not synaptic strengthening in response to LTP stimulation (Kopec et al., 2007). It has been suggested that LTP causes an increase in AMPA receptor currents through the trapping of these receptors at the PSD. Indeed, glutamatergic activity has been shown to immobilize GluA1-containing AMPA receptors at active synapses (Ehlers et al., 2007). Phosphorylation of the transmembrane AMPA receptor regulatory protein (TARP), stargazin, promotes synaptic incorporation of AMPA receptors (Tomita et al., 2005). Furthermore, CaMKII-mediated phosphorylation of stargazin during LTP causes the stabilization of AMPA receptors (Opazo et al., 2010). These molecular events result in the increase of synaptic currents following strong glutamatergic activity.

LTP-associated Changes in Spine Size

Changes in spine size in response to glutamatergic activity are also associated with CaMKII activity. Glutamate uncaging-induced spine growth requires the polymerization of actin (Matsuzaki et al., 2004). The NMDA receptor-induced calcium influx results in the activation GTPases which cause the remodeling of the spine's actin cytoskeleton (for review, see Basu & Lamprecht, 2018). Plasticity leads to the activation of Cdc42, Rac1 and RhoA, which through the signaling or WASP, WAVE and LIMK, respectively can act on the actin cytoskeleton to alter the morphology of potentiated spines (Nishiyama & Yasuda, 2015). Activation of the Cdc42 and RhoA during structural plasticity was shown to be downstream of CaMKII by pharmacological inhibition of the kinase (Murakoshi et al., 2011). Downstream of the activation of these GTPases, filamentous actin is polymerized to support the increase in spine size that is associated with LTP. After the induction of LTP, β-actin is recruited to the spine (Bosch et al.,

2014). Cofilin, one of the effector proteins that is activated by GTPases, has been shown to be rapidly recruited to stimulated spines and interact with F-actin (Bosch et al., 2014).

Changes in Spine Composition Induced by Plasticity

Following the induction of plasticity, the protein makeup of spines changes through the delivery of proteins from the dendritic shaft and the synthesis of new proteins for the late phase of LTP (Frey et al., 1988). Bosch et al., propose that following the induction of spine growth by glutamate uncaging, there are three phases of potentiation—reorganization, stabilization and consolidation—each associated with the delivery of different synaptic component proteins (Bosch et al., 2014). Synaptically relevant proteins such as CaMKII and GluA1 arrived rapidly to dendritic spines that had received a high-frequency glutamate uncaging stimulus. Interestingly Bosch *et al.*, also found two PSD-scaffolding molecules, Homer1b and Shank1b, were delivered to stimulated spines after nearly 60 minutes. Ultrastructural studies have revealed that the PSD takes between 30 minutes and 2 hours to grow after induction of LTP (Bourne & Harris, 2011). It has been proposed that synapses recover from saturation via the expansion of nascent zones, regions of the presynaptic bouton that lack glutamate release machinery but are across from a PSD (Bell et al., 2014). In short, synaptic strengthening requires that presynaptic nascent zones are converted into part of the active zone after stimulation. Within about 2 hours, the presynaptic nascent zone reemerges and plasticity is once again possible.

Importantly, it is known that following induction of spine growth, the postsynaptic density (PSD) remains stable for up to 2 hours (Bourne & Harris, 2011). It has been shown that the PSD scaffolding protein, PSD95, arrives to spines more than 1 hour after induction of spine growth (Meyer et al., 2014). Other PSD proteins like Homer1b and Shank1b also arrive to stimulated spines after a delay of approximately 45 minutes (Bosch et al., 2014). This evidence suggests that following glutamate-induced spine growth PSD proteins are de-enriched for a period of time

before they are delivered to the spine and restore the enrichment of PSD proteins to their previous levels.

Activity and changes in the synaptic plasticity threshold

It has been shown that changes in NMDAR subunit composition alters the dynamics of the channel and it's been proposed that a switch from GluN2B- to GluN2A-containing receptors influences their ability to drive plasticity (Gray et al., 2011; Paoletti et al., 2013). Additionally, the prolonged inactivation of glutamatergic synapses in organotypic slices leads to an increase in GluN2B containing NMDARs and a lowered threshold for induction of LTP at the silenced spine (Lee et al., 2010). Lee *et al.,* found that these silenced synapses with their increased GluN2B content, had increased calcium currents and had a reduced threshold for the induction of LTP.

Section 2: Saturation of plasticity

Saturation of Plasticity and Learning

The discovery of LTP and its association with learning lead to many hypotheses of learning. One of these hypotheses was that synaptic strength has an asymptotic ceiling at which synapses can no longer strengthen, and thus LTP becomes saturated. Since LTP is required for learning, this would suggest that saturation of LTP would then lead to learning deficits. Indeed, it was shown that when a stimulating electrode was used to saturate LTP in the hippocampus of rats, their performance on a spatial memory task was impaired (Barnes et al., 1994). Other studies also found that saturation of plasticity caused impaired learning in the Morris water maze task (Moser, 1998). Thus, whole-hippocampus saturation of LTP limits further plasticity and learning.

Saturation of Plasticity in the Hippocampus

Previous studies have shown that the ability of synaptic connections to undergo plasticity can be influenced by their prior plasticity history (Cao & Harris, 2014; Frey et al., 1995; Huang et al.,

1992; Kramar et al., 2012). After the induction of LTP at hippocampal circuits *in vitro* these circuits become resistant to further LTP induction. The ability to undergo LTP becomes saturated in these circuits, and thus further stimulation yields no increase in synaptic strength. Studies show that in the hippocampus, this saturation of LTP lasts approximately 60 minutes, after which these connections can become stronger in response to an LTP-inducing stimulus. Thus, saturation of LTP can be viewed as a refractory period for LTP. Interestingly, there is evidence that suggest that LTD and spine shrinkage can also become saturated following its induction (Parvez et al., 2010; Oh et al., 2013).

It has been shown that LTP can saturate in hippocampal circuits and be recovered when stimuli are sufficiently spaced in time (Cao & Harris, 2014; Frey et al., 1995; Huang et al., 1992; Kramar et al., 2012). The recovery of LTP at previously potentiated synapses is not well understood. It has been proposed that the recovery of plasticity in hippocampal circuits is mediated by the recruitment of new synapses into the circuit. One hypothesis is that synapses with a higher threshold for LTP induction have that threshold reduced such that they become available substrates for subsequent LTP (Kramar et al., 2012; Lynch et al., 2013). It has been shown that induction of LTP at individual synapses does indeed lower the threshold for plasticity at nearby synapses (Harvey & Svoboda, 2007). However, this effect is observed within minutes of the initial LTP induction and it is reported to only persist for ~10 minutes after the initial induction of LTP. Furthermore, if the ability of circuits to undergo subsequent plasticity relied on the recruitment of more synapses to the circuit, it is unclear why it takes ~60 minutes for this recruitment. It is also possible that it is not existing spines lowering their threshold, but rather new nascent spines being generated and recruited to the circuit that allows for the recovery of plasticity after the induction of plasticity.

Another mechanism that has been proposed is that the same synapses that undergo the initial LTP are able to undergo further potentiation after some time due to a recovery of presynaptic

nascent zones (Bell et al., 2014). The nascent zone is a region of the presynaptic bouton, which has been observed to have no neurotransmitter vesicles despite the presence of PSD across the synaptic cleft. Following LTP, these presynaptic nascent zones are filled with vesicles and converted to active zones. After the conversion, the presynaptic bouton is depleted of its nascent zone. This hypothesis proposes that the expansion of the active zone is necessary for LTP and that saturation of LTP is due to a lack in nascent zones, which recover after some time to support further LTP. This would suggest that there is a signal that coordinates the expansion of the nascent zone with the expansion of the postsynaptic density (which happens between 30 and 120 minutes after the induction of LTP (Bell et al., 2014; Bourne & Harris, 2011)). The coordinating signal has not been identified, though it could involve retrograde signaling from the postsynaptic spine to the bouton, coordination of pre- and postsynaptic adhesion molecules or even the mechanical force spine enlargement on the presynaptic bouton (Kasai et al., 2023).

Behavioral Relevance of Saturation of Plasticity

What is the purpose of saturation of plasticity? One possibility is that plasticity is limited at potentiated synapses as a protective mechanism. Neuronal activity in the brain is constant, in the absence of saturation, it is possible for a synapse that was recently potentiated to undergo further activity that is non-specific to the learning at hand. Should this happen, learning would be disrupted and thus, saturation could serve to protect recently encoded memories. Intriguingly, the ability to retain long-term memories in artificial systems has been hindered by the overwriting of past memories by ongoing activity, a process know as catastrophic forgetting (Van De Ven et al., 2020; Kudithipudi et al., 2022). Could the mechanisms that underlie spaced learning be the key to solving the problem of catastrophic forgetting?

One aspect of learning that is often talked about by educators is the concept of spaced learning, where repetition of a task is broken up by short breaks. Spaced learning is a more effective method of learning, compared to uninterrupted learning sessions (Kelley & Whatson, 2013).

One study has demonstrated that spacing can improve the learning outcomes of motor tasks, like learning to perform laparoscopic sutures (Boettcher et al., 2018). Notably, it has been shown that using spaced learning paradigms can improve learning in animal models with learning deficits like Down's and fragile X syndromes (Lauterborn et al., 2019; Seese et al., 2014). Yet, how spaced learning functions on a molecular level remains poorly understood. Some have proposed that the effectiveness of spaced learning is related to the saturation of plasticity of synaptic connections (Cao & Harris, 2014; Kramar et al., 2012).

Studies have shown that ensembles of synapses that are involved in a task are repeatedly activated during learning (Hofer et al., 2006; Hayashi-Takagi et al., 2015; Glas et al., 2021). In fact, when spines that are involved in the learning of a task are optically shrank, relearning of the task causes the same subset of spines to grow again (Hayashi-Takagi et al., 2015). The temporary saturation of plasticity at these synapses could cause them to become ineffective as substrates for learning. It would be feasible that the breaks used in spaced learning allow for spines to be released from their saturated states and become suitable for plasticity once again. This limitation of learning seems to be detrimental.

Conclusions

The ability to learn relies on the modification of synaptic circuits. Spaced learning has been shown to improve learning in animal models that have learning impairments (Seese et al., 2014; Lauterborn et al., 2019). It has been hypothesized that saturation of LTP after learning may plays a role in the efficacy of spaced learning. Indeed, saturation of LTP can lead to impaired learning in animal models (Barnes et al., 1994; Moser, 1998). Yet how saturation of LTP occurs remains ill-understood. In this **Chapter 2**, I show that saturation of LTP can occur at individual synapses in the hippocampus and can be recovered after some time. The molecular mechanisms that underlie the onset and subsequent release of saturation at individual synapses still remains a mystery. I set out to elucidate a molecular mechanism and potential

therapeutic targets that may facilitate learning in populations with learning deficits. Though I identify PSD95 as a protein that is involved in the recovery of plasticity, much remains to be discovered about its specific role in allowing previously stimulated spines to undergo plasticity once again.

Chapter 2: Prior potentiation initiates a synapse-specific refractory period for plasticity at individual dendritic spines

Preface

The following chapter has been submitted for publication with the title: “Prior potentiation initiates a synapse-specific refractory period for plasticity at individual dendritic spines.” This chapter is the submitted version of the manuscript, only the layout has been altered to fit the format of this thesis. The authors of the manuscript are Juan C. Flores and Karen Zito. Jennifer Jahncke and Lorenzo Tom aided in the preparation and maintenance of hippocampal slice cultures. Samuel Petshow, Marco Alarcon, and Drs. Johannes Hell, John Gray, Margarita Anisimova, Dipannita Sarkar provided critical input and/or reading of the manuscript.

Abstract

How newly formed memories are preserved while brain plasticity is ongoing has been a source of debate. One idea is that synapses which experienced recent plasticity become resistant to further plasticity, a type of metaplasticity often referred to as saturation. Here, we probe the mechanisms that limit plasticity at recently potentiated synapses. Using two-photon imaging and glutamate uncaging, we show that potentiation-inducing stimulation at a single synapse is sufficient to initiate a synapse-specific refractory period for further potentiation. The refractory period is associated with reduced CaMKII activity; however, stronger stimulation is only partially able to rescue potentiation. Importantly, the refractory period is released after one hour, a timing that coincides with the enrichment of several postsynaptic proteins to pre-plasticity levels. Intriguingly, increasing the level of the postsynaptic scaffold, PSD95, but not of PSD93, overcomes the refractory period. Our results support a model in which potentiation at a single synapse is sufficient to initiate a postsynaptically-induced, synapse-specific refractory period that persists until key postsynaptic proteins regain their steady-state synaptic levels.

Introduction

Learning and memory formation are thought to rely upon long-term changes in neural circuit connections, both via alterations in the strength of existing synapses and through formation of new synapses (Grutzendler et al., 2002; Hayashi-Takagi et al., 2015; Trachtenberg et al., 2002). One challenge for synaptic models of learning and memory has been how synapses can be both plastic, in order to encode new memories, and stable, in order to retain old memories (Abraham et al., 2019; Bailey et al., 2015; Bliss & Collingridge, 1993; Magee & Grienberger, 2020; Martin et al., 2000; Mongillo et al., 2017). A prominent hypothesis posits that synapses that have recently been recruited for learning are protected from further modification (Fusi et al., 2005; Van De Ven et al., 2020, 2022). Indeed, there is evidence that when animals learn two distinct tasks over a close period of time, non-overlapping populations of synapses encode the two distinct tasks (Fu et al., 2012; Hayashi-Takagi et al., 2015).

An important component of synaptic learning models therefore would be mechanisms that support the selection of predominantly distinct sets of labile synapses to encode distinct tasks when learned close in time. One such mechanism would be through the existence a period of time in which recently potentiated synapses are unable to undergo further potentiation; this type of metaplasticity has often been referred to as saturation of plasticity (Abraham et al., 2019; Barnes et al., 1994; Fusi et al., 2005; Moser, 1998). Indeed, in vitro studies at the circuit level have shown that recently potentiated hippocampal circuits are unable to undergo further potentiation within the first few hours after potentiation (Cao & Harris, 2014; Frey et al., 1995; Huang et al., 1992; Kramar et al., 2012). Furthermore, in vivo studies have shown that after inducing saturation of potentiation in the hippocampus of live rats, learning is impaired compared to control animals (Barnes et al., 1994). However, the cellular and molecular mechanisms that inhibit further plasticity at recently potentiated synapses, and the spatial and temporal scales over which they act, are not well understood.

Here, we show that prior potentiation at individual dendritic spines is sufficient to initiate a refractory period that prevents additional structural and functional plasticity. We further show that the refractory period is limited to synapses receiving prior potentiation, and that it is accompanied by reduced activation of CaMKII. Increasing the strength of the potentiating stimulus at 30 min is not sufficient to overcome the refractory period at individual spines; however, it is fully released within 60 min. Finally, we show that increasing levels of the postsynaptic scaffolding protein PSD95, but not of PSD93, is sufficient to release the refractory period, such that previously potentiated synapses are again able to exhibit robust plasticity at a time when they would typically be refractory.

Results

Individual potentiated spine synapses are refractory to further plasticity

To test whether recently potentiated individual synapses can exhibit further plasticity, our strategy was to induce long-term potentiation (LTP) at a single target spine and then attempt to induce further potentiation at the same target spine 30 min later (**Fig. 1A**). After two baseline images, individual spines on EGFP-expressing CA1 neurons in hippocampal slice cultures were stimulated with high-frequency uncaging of MNI-glutamate (HFU: 60 pulses, 2 ms pulse duration, 2 Hz, ~8.5 mW at 720 nm in 2.5 mM MNI-glu, 2 mM Ca^{2+} and 0 mM Mg^{2+}), which has been shown to induce concurrent long-term increases in spine size and synaptic strength (Hill & Zito, 2013; Matsuzaki et al., 2004). As expected, following an initial HFU at time 0 (HFU_0), we observed that stimulated target spines exhibited a long-term increase in size (**Fig. 1B,C,E**; 210% ± 20%; $p < 0.001$). Notably, an identical HFU stimulus at the same target spine 30 min later (HFU_{30}) induced no further long-term growth (**Fig. 1B-E**; 102% ± 12%; $p > 0.99$). Importantly, previously unstimulated, size-matched (**Fig. S1A**) control spines on different dendrites of the same cells exhibited a robust long-term increase in size in response to HFU_{30} (**Fig. 1B,D,E**; 170% ± 18%; $p < 0.01$), supporting that the lack of plasticity observed in the re-

stimulated target spine was not due to either (i) a decay in ability to undergo plasticity after 30 min in the bath chamber and/or (ii) the increased spine size following the first round of plasticity. Our results demonstrate that prior potentiation initiates a refractory period for further plasticity at individual dendritic spines.

In addition to a long-term increase in spine size, potentiation at single spines also drives a long-term increase in surface AMPARs (Hill & Zito, 2013; Matsuzaki et al., 2004; Oh et al., 2015). To examine whether insertion of surface AMPARs also exhibits a refractory period following potentiation at single dendritic spines, we transfected CA1 neurons with super ecliptic pHluorin (SEP)-tagged GluA2 to monitor surface expression of AMPARs (Kopec et al., 2006; Miesenböck et al., 1998; Oh et al., 2015) along with tDimer-dsRed as a red cell fill (**Fig. 1F**). Importantly, by monitoring the red cell fill, we observed that the presence of SEP-GluA2 did not alter establishment of the refractory period for plasticity (**Fig. S1D-F**). By monitoring the SEP-GluA2 fluorescence, we observed that an initial HFU (HFU_0) drove a long-term increase in surface GluA2 compared to baseline, as expected (**Fig. 1F,G,I**; 142 ± 9%, $p < 0.001$). An identical HFU stimulus at the same target spine 30 min later (HFU_{30}) induced no further GluA2 insertion (**Fig. 1F-I**; 102 ± 4%, $p > 0.99$), despite that a second previously unstimulated, size-matched (**Fig. S1C**) control spine on a different dendrite of the same cell exhibited a robust long-term increase in GluA2 insertion in response to HFU_{30} (**Fig. 1F,H,I**; 139 ± 11%, $p < 0.001$). Thus, prior potentiation initiates a refractory period for both long-term spine growth and insertion of surface AMPARs.

CaMKII activation is reduced in recently potentiated spines

To elucidate a molecular mechanism for the refractory period following prior potentiation, we first focused on whether CaMKII signaling was altered in recently potentiated spines. CaMKII is a key integrator of synaptic activity and plays a role in both LTP and LTD (Hell, 2014; Bayer & Schulman, 2019; Yasuda et al., 2022; Cook et al., 2021). Furthermore, it has been shown that

CaMKII activation is sufficient to induce LTP (Shibata et al., 2021). Using 2-photon fluorescence lifetime imaging (FLIM) of Camui-α, a genetically-encoded CaMKII activity reporter in response to an established glutamate uncaging protocol (HFU: 30 pulses, 4-6 ms pulse duration, 0.5 Hz, 4 mW at 720 nm in 4 mM MNI-glu, 4 mM Ca^{2+} and 0 mM Mg^{2+}) (S.-J. R. Lee et al., 2009), we imaged CaMKII activation (**Fig. 2A**) during and immediately following potentiation and saturation (**Fig. S2A-C**) of an individual dendritic spine. In response to the initial potentiating stimulation (HFU_0), we saw a robust CaMKII activation, as detected by a sensor lifetime change of 120 ± 25 ps (**Fig. 2A,B, D**). Notably, a second identical potentiating stimulus 30 min later (HFU_{30}) elicited a dramatically reduced change in CaMKII sensor lifetime (**Fig 2C, D**; 77 ± 14 ps, p = 0.029 compared to HFU_0). Peak sensor lifetime change (**Fig 2C, D**; 130 ±14 ps) of size-matched control spines (**Fig. S2D**) was not different than the initial response (p = 0.65 compared to HFU_0). Importantly, red fluorescence (**Fig. S2E**) and donor photon counts (**Fig. S2F**) in the target spines at 25-30 min after HFU_0 was not different from that of size-matched control spines, and initial spine size also did not influence the measured lifetime change during an HFU (**Fig S2G**). In sum, results show that CaMKII activation is reduced in recently potentiated spines.

Refractory period for plasticity at previously potentiated spines is partially released by a stronger stimulus.

Because we found that CaMKII activation was decreased in recently potentiated spines, we tested whether plasticity could be recovered by increasing the strength of the second stimulus to drive stronger activation of CaMKII. We therefore increased the strength of the HFU_{30} stimulation by increasing the duration of the uncaging laser pulses from 2 ms to 4 ms. As expected, spines grew in response to HFU_0 (**Fig 3B, D**; 183 ± 21%, p = 0.003). In response to this second stronger stimulation at 30 min (HFU_{30+}) after the first HFU (HFU_0), target spines showed a trend toward growth (**Fig 3C, D**; target: 136 ± 6% p = 0.14), but in a much smaller magnitude than that observed in size-matched (**Fig. S3A**) control spines on a different dendrite

from the same cell (230 ± 35%, $p < 0.001$). We further tested increasing the strength of the second stimulation to 5-6 ms pulses (HFU_{30++}; **Fig. S3D-F**). As expected, spines grew in size in response HFU_0 (**Fig S3D, F**; 188 ± 10%, $p < 0.001$). Notably, despite the further increase in stimulus strength with HFU_{30++}, the size increase of the target spine (144 ± 12%, $p = 0.02$), remained significantly reduced compared to that of the control spines (195 ± 26%, $p < 0.001$). Our results show that increasing the strength of second potentiating stimulus can partially overcome the refractory period, it does cannot fully recover plasticity to the level of spines which had not experienced prior stimulation.

Refractory period for single spine plasticity is released within 60 min

We instead wondered if full recovery from the refractory period was a function of time. To test whether doubling the time interval between the first HFU and the second HFU would permit recovery of plasticity, we repeated our experiments now with a 60 min interval between the two HFU stimuli (**Fig. 4**). As expected, target spines exhibited a long-term increase in size in response to the HFU_0 stimulus (**Fig. 4A,B,D**; 171% ± 13%, $p < 0.001$). In contrast to the lack of additional plasticity observed at 30 min, a second identical HFU stimulus at 60 min (HFU_{60}) resulted in an additional long-term increase in size of target spines (**Fig. 4A-D**; 135% ± 11%, $p < 0.01$). Importantly, recovery of plasticity was not due to secondary effects caused by a decay in size of target spines back toward their initial value over the 60 min interval, as the long-term increase in size induced by HFU_0 was maintained for the full 60 min prior to HFU_{60} (20-30 min: 171 % ± 13%; 55-60 min: 166% ± 17%; $p = 0.8$). Furthermore, previously unstimulated, size-matched (**Fig. S4A**) control spines on a different dendrite of the same cells grew to a comparable magnitude in response to HFU_{60} (**Fig 4A,C, D**; 137% ± 9%, $p < 0.01$), suggesting complete recovery of plasticity in the target spine. Our results support that the target spine was released from the refractory period for further plasticity within 60 min.

Increased PSD95 expression level is sufficient to release the refractory period for plasticity at previously potentiated spines

Our data support the existence of a refractory period for plasticity at single spines that is released between 30 and 60 min after potentiation. In addition, because our glutamate uncaging stimulus bypasses presynaptic vesicle release, our results support that the refractory period is initiated via postsynaptic mechanisms. Ultrastructural studies have demonstrated that the PSD of potentiated spines does not increase in size for the first 30 min after LTP induction, but does so within 2 hrs (Bourne & Harris, 2011), suggesting that delayed PSD enlargement at potentiated synapses could contribute to limiting plasticity (Bell et al., 2014). Furthermore, live imaging studies have shown that the synaptic expression level of several GFP-tagged postsynaptic scaffolding proteins does not increase within 30 min of LTP induction, despite a rapid increase in spine volume (Bosch et al., 2014). We therefore hypothesized that acceleration of the post-LTP PSD expansion through increasing the availability of key PSD proteins might allow for faster recovery from the refractory period. To test our hypothesis, we manipulated the expression level of PSD95, one of the most abundant PSD scaffolding proteins (Cho et al., 1992; Kennedy, 1997) with important roles in regulating spine stabilization (Cane et al., 2014; De Roo et al., 2008; Ehrlich et al., 2007; Okabe et al., 2001; Taft & Turrigiano, 2014), and which increases at newly potentiated spines only after a delay (Bosch et al., 2014; Meyer et al., 2014).

We postulated that the optimal approach for testing our hypothesis would be to select a time interval between the two HFU stimuli at which the refractory period persisted, but such that synaptic molecular configuration would be close to recovered, and therefore increasing the expression of a single PSD protein might expedite the recovery of plasticity. We therefore chose to examine a 45 min interval – at the halfway time point between completely refractory (30 min) and full recovery of plasticity (60 min). We found that in spines from neurons expressing a red

cell fill, there was an initial long-term increase in target spine size after the HFU_0 stimulus (**Fig. 5A,B,D**; 200% ± 19%, $p < 0.01$), but no long-term increase in response to a second HFU at 45 min (**Fig. 5A-D**; HFU_{45}; 103% ± 5%, $p = 0.6$), although previously unstimulated, size-matched (**Fig. S5E**) control spines on the same cells did exhibit a long-term increase in size in response to HFU_{45} (**Fig. 5A,C,D**; 151% ± 18%, $p < 0.01$). Our results indicate that recovery from the refractory period at single spines occurs between 45 and 60 min after potentiation.

To determine whether increased expression of PSD95 would accelerate recovery from the refractory period, we stimulated CA1 neurons transfected with GFP-tagged PSD95α (N. W. Gray et al., 2006) (PSD95-GFP) and a red cell fill (**Fig. 5E**). As expected, target spines exhibited a long-term increase in size in response to HFU_0 (**Fig. 5F,H**; 180 ± 19%, $p < 0.001$). Notably, target spines with excess PSD95 exhibited an additional long-term increase in size in response to the second HFU at 45 min (**Fig. 5F-H**, 136 ± 10%, $p < 0.05$) that was comparable to that of previously unstimulated, size-matched (**Fig. S5F**) control spines (**Fig 5G,H**; 140% ± 13%, $p < 0.05$), suggesting complete recovery of plasticity in the target spine. Importantly, the initial size of target spines (**Fig. S5A,B**) and the magnitude of long-term spine growth in response to HFU_0 (**Fig. S5C,D**) were not altered in cells with excess PSD95. Furthermore, increased synaptic AMPAR currents associated with excess PSD95 (Ehrlich & Malinow, 2004; Schnell et al., 2002) did not contribute to the shorter refractory period, because even in the presence of NBQX to block AMPAR currents, target spines exhibited additional long-term growth in response to HFU_{45} (**Fig. 5J-L**; 148 ± 14%, $p < 0.05$) comparable to that of previously unstimulated, size-matched (**Fig. S5G**) control spines. Thus, increased expression of PSD95 is sufficient to shorten the refractory period for plasticity induced by prior potentiation at single spines.

Increased PSD93 expression level is not sufficient to release the refractory period for plasticity at previously potentiated spines

Because PSD95 and PSD93 have extensive sequence identity (~70% overall (Brenman et al., 1996)), especially in the 3 PDZ binding motifs (86%), but have distinct functional roles (Favaro et al., 2018; Q. Sun & Turrigiano, 2011), we wondered whether increased PSD93 levels would also shorten the refractory period for plasticity at single spines. We therefore repeated the experiment with GFP-tagged PSD93α (Schnell et al., 2002) (PSD93-GFP; **Fig. 6A**). As expected, target spines from neurons co-transfected with DsRedExpress and PSD93-GFP exhibited long-term increase in size in response to HFU_0 (**Fig. 6B,D**; 202 ± 28%; $p < 0.001$). In contrast to the rescue of plasticity observed with PSD95-GFP, spines from cells with excess PSD93-GFP failed to exhibit long-term growth in response to a second HFU stimulus at 45 min (**Fig. 6B-D**; 109 ± 7%; $p > 0.99$). Importantly, initial size of target spines and spine expression of GFP-tagged proteins were not different between PSD95- and PSD93-expressing spines (**Fig. S6A-D**). Altogether, our data show that increased expression of PSD95, but not PSD93, overcomes the refractory period for plasticity at single spines.

Discussion

That synapses which have experienced recent plasticity should become temporarily resistant to further plasticity has been proposed as a mechanism through which newly formed memories can be preserved at the synaptic level while brain plasticity is ongoing (Abraham et al., 2019; Bailey et al., 2015; Bliss & Collingridge, 1993; Fusi et al., 2005; Magee & Grienberger, 2020; Martin et al., 2000). Earlier studies established that this type of metaplasticity is indeed observed at the circuit level (Cao & Harris, 2014; Frey et al., 1995; Huang et al., 1992; Kramar et al., 2012). Here, we provide new information on the cellular and molecular mechanisms that regulate this refractory period for plasticity. We show that potentiation even at single synapses is sufficient to establish a refractory period for further potentiation that is synapse-specific, lasts

between 45-60 minutes, and is regulated by the expression level of the postsynaptic scaffolding protein, PSD95.

Initiation, time-course, and synapse-specificity of refractory period for potentiation

We demonstrate that a single LTP-inducing stimulus at an individual spine was sufficient to initiate a refractory period for further potentiation, consistent results from circuit level studies activating multiple axons using a variety of protocols to induce LTP, including tetanic, theta-burst, and pairing stimulation (Cao & Harris, 2014; Frey et al., 1995; Huang et al., 1992; Kramar et al., 2012). Importantly, because our glutamate uncaging stimulation bypassed the presynaptic vesicle release, our results support a postsynaptic locus of initiation for the refractory period. Furthermore, we found that the refractory period for potentiation was fully recovered by 45-60 min after the initial LTP induction, a similar but shorter interval than that observed in circuit level studies, which showed that further potentiation can be achieved 1-2 hrs following LTP induction (Cao & Harris, 2014; Frey et al., 1995; Huang et al., 1992; Kramar et al., 2012). Notably, because our experimental paradigm focused on single synapses, we were able to distinguish that full recovery occurred without the need to recruit additional naïve synapses[18]. It is likely that the success of induction and duration of the refractory period will be dependent on the pattern, strength, and duration of synaptic activity at single synapses. Indeed, it has been recently reported that different naturalistic patterns of activity influence the duration of long-term synaptic structural plasticity (Argunsah & Israely, 2023).

We show that LTP induction at single spines initiates a refractory period for further potentiation at the potentiated spine, but not at previously unstimulated, size-matched control spines on a different dendrite of the same cell, suggesting that the refractory period is synapse-specific. Although our studies do not exclude that immediate neighbors of potentiated spines also exhibit a refractory period for potentiation, we think that this is unlikely as other studies have shown that

LTP at an individual target spine lowers, rather than increases, the threshold for plasticity at spines that are within 10 μm of the potentiated spine (Harvey & Svoboda, 2007).

Molecular mechanisms of refractory period for potentiation

Although several studies have characterized the time-course of activation and enrichment of synaptic signaling and scaffolding molecules following LTP (Bosch et al., 2014; Bourne & Harris, 2012; Hayashi, 2022; Kramar et al., 2012; Nakahata & Yasuda, 2018; Perez-Alvarez et al., 2020), which molecular signaling components contribute to the refractory period for potentiation is unknown. We found that increased expression of the postsynaptic scaffolding protein PSD95 was sufficient to restore plasticity to recently potentiated synapses in the refractory period, suggesting that the lower levels of PSD95 in recently potentiated synapses contributes to the refractory period. Indeed, following the induction of LTP, the PSD takes between 30 min and 2 hrs to grow (Bourne & Harris, 2011), and PSD-scaffolding molecules arrive only after a delay of ~60 min (Bosch et al., 2014). Our results provide experimental evidence in support of models based on ultrastructural studies positing that delayed expansion of the PSD limits further potentiation at recently potentiated synapses (Bell et al., 2014).

Intriguingly, we show that increased expression of PSD93 is not sufficient to restore plasticity to recently potentiated synapses. This could be viewed as surprising, as these two MAGUKs have a high level of sequence identity, and share 3 PDZ domains, an SH3 and a GK domain with 2 palmitoylation sites (Won et al., 2017), and both have demonstrated roles in spine stabilization (Cane et al., 2014; De Roo et al., 2008; Ehrlich et al., 2007; Okabe et al., 2001; Taft & Turrigiano, 2014). However, despite the similarities, PSD95 and PSD93 have distinct physiological roles. For example, homeostatic upscaling of synaptic currents requires both PSD95 and PSD93, while scaling down does not require PSD93 (Q. Sun & Turrigiano, 2011). In addition, loss of PSD95 prevents maturation of silent synapses, while loss of PSD93 has the opposite effect, instead leading to accelerated maturation of silent synapses (Favaro et al.,

2018). Furthermore, in nascent dendritic spines, PSD93 is enriched to mature levels within several hours, whereas PSD95 takes over 12 hours to reach mature levels, suggesting sequential roles in nascent spine stabilization (Lambert et al., 2017). How increased PSD95 levels overcomes the refractory period remains undefined.

We considered the possibility that a switch in NMDAR subunit composition could contribute to the refractory period. Perhaps PSD95 acts to increase the level of GluN2B subunit containing NMDARs through its direct interaction with GluN2B (Sanz-Clemente et al., 2010) and by excluding $STEP_{61}$, a tyrosine phosphatase that targets GluN2B for endocytosis(Won et al., 2016). Indeed, induction of LTP in young acute hippocampal slices drives a rapid change from GluN2B- to GluN2A-containing NMDARs, which carry less Ca^{2+} current and are less favorable to induction of LTP (Bellone & Nicoll, 2007). This switch is likely to occur also at single synapses, as prolonged inactivation of synaptic transmission at individual synapses on cultured hippocampal neurons induces the opposite switch from GluN2A to GluN2B (M.-C. Lee et al., 2010). However, we think that this mechanism is unlikely to contribute to our observations for two reasons: the LTP-induced subunit switch observed by Bellone and colleagues shows no recovery within one hour and, most importantly, it is not observed in slices from older animals comparable in age range to that used for our experiments.

Implications for learning of refractory period for plasticity

We and others have postulated that a refractory period for plasticity during learning at recently potentiated synapses exists to exclude those synapses from incorporation into distinct subsequently-learned tasks, thus prevent overwriting of recently established memories still in the labile phase. As there is considerable evidence that repeated learning bouts activate the same sets of synapses (Glas et al., 2021; Hayashi-Takagi et al., 2015; Hofer et al., 2009), another consequence of a refractory period on learning would be to temporarily prevent synapses from undergoing further potentiation related to the same task. Indeed, several have

proposed that a refractory period for plasticity could be the basis for increased success of a type of learning known as spaced learning, in which breaks are incorporated into learning sessions (Bell et al., 2014; Kramar et al., 2012). Such breaks during spaced learning could serve to allow synapses to recover their ability to undergo plasticity. Indeed, spaced learning approaches have been shown to improve learning outcomes over traditional learning in which repetitions are temporally clustered in both humans and rodents (Boettcher et al., 2018; Glas et al., 2021; Smolen et al., 2016), and to improve learning under conditions where learning is challenged in disease (Lauterborn et al., 2019; Seese et al., 2014). It follows that manipulation of the molecular signaling mechanisms that regulate the refractory period could serve to improve learning outcomes associated with disease.

Methods

Preparation and transfection of organotypic hippocampal slice cultures

Cultured hippocampal slices (300-400 µm) were prepared from P6-P8 C57BL/6 mice of both sexes, as described(Stoppini et al., 1991), and as approved by the UC Davis Institutional Animal Care and Use Committee (IACUC). Cultured slices were transfected at 8-16 DIV using biolistic gene transfer (180-210 psi), as described (G. Woods & Zito, 2008). 6-8 mg of 1.6 µm gold beads (BioRad) were coated with 15 µg of EGFP-N1 (Clontech), or 10 µg of tDimer-dsRed together with 16 µg SEP-GluA2 (Kopec et al., 2006), or 10 µg of DsRedExpress alone, or 10 µg DsRedExpress (Clontech) together with 1-2 µg of GFP-tagged PSD95α (N. W. Gray et al., 2006) or PSD93α (Schnell et al., 2002). Slices were transfected 2-3 days (EGFP), 3-4 days (SEP-GluA2/tDimer-dsRed), or 24 hrs (PSD95/93/DsRedExpress) prior to imaging.

Time-lapse two-photon imaging

Transfected CA1 pyramidal neurons at depths of 10–50 µm in slice cultures (10-18 DIV) were imaged using a custom two-photon microscope (G. F. Woods et al., 2011) controlled with

ScanImage (Pologruto et al., 2003). Image stacks (512 x 512 pixels; 0.02 µm/pixel) with 1 µm z-steps were collected. For each neuron, one segment of secondary or tertiary basal dendrite was imaged at 5 min intervals at 29°C in recirculating ACSF (in mM): 127 NaCl, 25 $NaHCO_3$, 1.2NaH_2PO_4, 2.5 KCl, 25 D-glucose, aerated with 95% O_2/5% CO_2, 310 mOsm, pH 7.2, with 0.001 TTX, 0 Mg^{2+}, and 2 Ca^{2+}. Dendrites of transfected cells were selected under epifluorescence and MNI-glutamate (2.5 mM) was added at least 15 min prior to uncaging stimulation.

High frequency uncaging (HFU) of glutamate

HFU consisted of 60 pulses (720 nm; ~7.5–9.5 mW at the sample) of 2 ms duration at 2 Hz delivered in ACSF containing the following (in mM): 2 Ca^{2+}, 0 Mg^{2+}, 2.5 MNI-glutamate, and 0.001 TTX. Because earlier studies established that spine size can influence the magnitude of potentiation (Matsuzaki et al., 2004), we selected target spines with an initial size range in the 25-50% quartile of sizes. The laser beam was parked at a point ~0.5–1 µm from the spine head in the direction away from the dendrite. Cells with no noticeable transients in response to HFU_0 were discarded and not further pursued.

Image analysis

Images were analyzed using a custom MATLAB software, as described (G. F. Woods et al., 2011). In brief, following application of a 3 x 3 median filter, background-subtracted integrated green and/or red fluorescence intensity was calculated from a boxed region surrounding the spine head. Spine volume was estimated using fluorescence from a cell fill (EGFP, tDimer-dsRed, or DsRedExpress) (Holtmaat et al., 2005). Bar graphs show the average values from the three time points occurring at 20-30 min after the most recent HFU (HFU_0: 20-30min; HFU_{30}: 50-60 min; HFU_{45}: 65-75 min; HFU_{60}: 80-90 min). Relative spine size was calculated by normalizing

the individual spine fluorescence to the mean for all spines on the same dendrite using the two time points immediately prior to HFU.

Statistics

All data are represented as mean ± standard error of the mean (SEM). All statistics were calculated across cells using GraphPad Prism. Statistical significance level (α) was set to $p < 0.05$ for all tests. When comparing only two groups, paired or unpaired (as appropriate) Student's t-tests were used. When multiple comparisons were made, a one or two-way ANOVA with Bonferroni post-hoc test was performed. All p values are in the text and n values are in the figure legends.

Supplemental Information

Supplemental Information can be found attached.

Acknowledgments

This work was supported by the National Institutes of Health (R01 NS062736, T32 GM099608, F99 NS125772) and an ARCS fellowship to JF. We thank J. Jahncke and L. Tom for support with experiments, J. Hell, J. Gray, J. Zheng, M. Navedo, M. Anisimova, S. Petshow, D. Sarkar, and M. Alarcon for critical input and/or reading of the manuscript.

Author Contributions

JF and KZ designed the study. JF performed the experiments and analyzed the data. JF and KZ wrote the manuscript.

Declaration Of Interests

The authors declare no competing financial interests.

Figures and Legends

Figure 1. A single LTP-inducing stimulus initiates a synapse-specific refractory period for long-term growth and synaptic strengthening at individual dendritic spines

(A) Schematic of the experimental approach. An individual dendritic spine (target) was stimulated (yellow crosses) to induce LTP and then imaged every 5 min. At 30 min, the target spine was stimulated again along with a previously unstimulated, size-matched control spine (control) on the same cell. **(B)** Representative images of dendrites from an EGFP-transfected hippocampal CA1 pyramidal neuron directly prior to and 25 min after HFU_0 and HFU_{30} at target (left images) and control (right images) spines. **(C-E)** The initial HFU stimulus (HFU_0) resulted in long-term growth of target spines (filled blue circles/bars; n=8 spines/cells), but an identical HFU at 30 min (HFU_{30}) did not drive additional growth. A size-matched control spine on the same cell grew in response to HFU_{30} (gray circles/bar; n=8 spines/cells). Neighboring spines were unchanged (open circles; n=73 spines/8 cells). Target spine data in **D** is from **C** re-normalized to the new baseline. **(F)** Images of dendrites from a CA1 pyramidal neuron transfected with SEP-GluA2 (green) and tDimer-dsRed (magenta) directly prior to and 25 min after HFU_0 and HFU_{30} at target (left images) and control (right images) spines. **(G-I)** An initial HFU stimulus (HFU_0) resulted in a long-term increase in surface expression of SEP-GluA2 in target spines (filled blue circles/bars; n=7 spines/cells), but an identical HFU at 30 min (HFU_{30}) did not drive an additional increase. In contrast, HFU_{30} drove a long-term increase in surface SEP-GluA2 on a size-matched control spine on the same cell (gray circles/bar; n=7 spines/cells). Target spine data in **H** is from **G** re-normalized to the new baseline. Data represent mean ± SEM. Statistics: 2-way ANOVA with Bonferroni test. $^{**}p < 0.01$, $^{***}p < 0.001$. See also **Figure S1**.

Figure 1

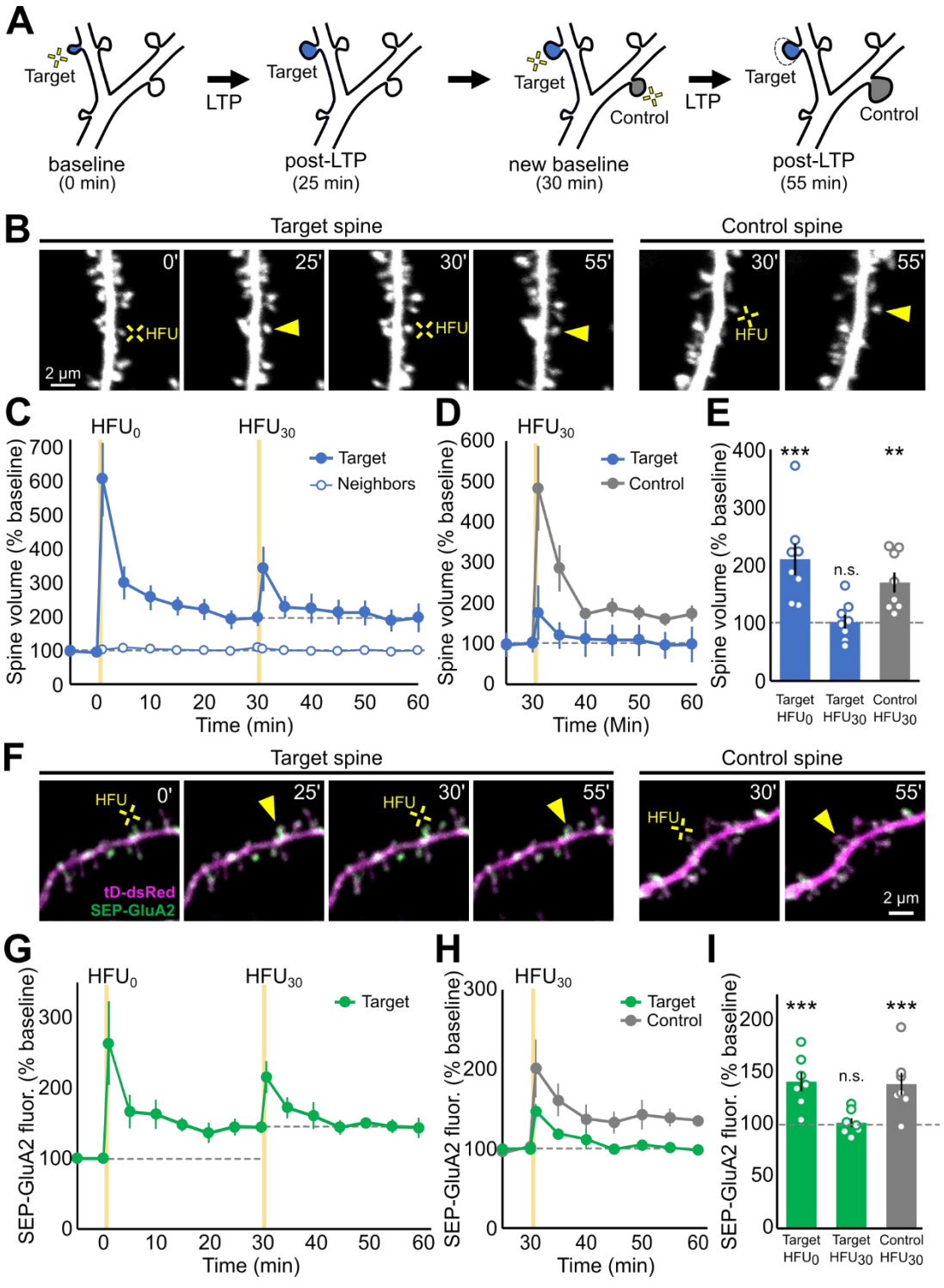
A
Target
baseline
(0 min)
LTP
Target
post-LTP
(25 min)
Target
Control
new baseline
(30 min)
LTP
Target
Control
post-LTP
(55 min)
B
Target spine
Control spine
0'
25'
30'
55'
HFU
2 µm
C
HFU0
HFU30
Target
Neighbors
Spine volume (% baseline)
Time (min)
D
HFU30
Target
Control
Spine volume (% baseline)
Time (Min)
E
***
**
n.s.
Spine volume (% baseline)
Target HFU0
Target HFU30
Control HFU30
F
Target spine
Control spine
tD-dsRed
SEP-GluA2
2 µm
G
HFU0
HFU30
Target
SEP-GluA2 fluor. (% baseline)
Time (min)
H
HFU30
Target
Control
SEP-GluA2 fluor. (% baseline)
Time (min)
I
***
***
n.s.
SEP-GluA2 fluor. (% baseline)
Target HFU0
Target HFU30
Control HFU30

Figure 2. CaMKII activation is reduced in previously potentiated spines.

(A) Representative lifetime maps from neurons in slice culture expressing CaMKII FRET sensor prior to and during high frequency uncaging (HFU, yellow cross) at 0 min (HFU_0) and 30 min later (HFU_{30}) at target (left) and control spine (right). **(B)** The initial HFU stimulus (HFU_0) resulted in robust activation of CaMKII at target spines (blue circles; n = 10 spines/cells). **(C, D)** CaMKII activation in response to the second HFU stimulus (HFU_{30}) was reduced previously potentiated target spines, but not in size-matched control spines (gray circles/bars; n = 10 spines/cells). Target spine data in **C** is from **B** re-normalized to the new baseline. Data represent mean ± SEM. Statistics: Student's t-test. *p <0.05, **p < 0.01. See also **Figure S2**.

Figure 2

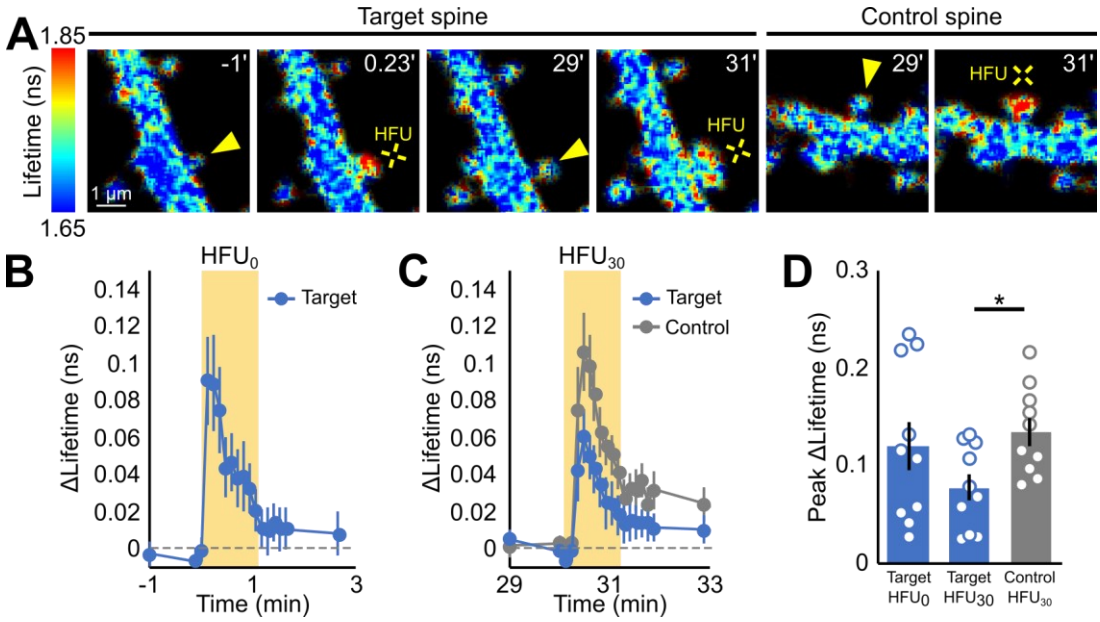
A
Target spine
Control spine
1.85
Lifetime (ns)
1.65
-1'
0.23'
29'
31'
29'
31'
HFU
HFU
HFU
1 µm
B
HFU0
Target
ΔLifetime (ns)
0.14
0.12
0.1
0.08
0.06
0.04
0.02
0
-1
1
3
Time (min)
C
HFU30
Target
Control
ΔLifetime (ns)
0.14
0.12
0.1
0.08
0.06
0.04
0.02
0
29
31
33
Time (min)
D
Peak ΔLifetime (ns)
0.3
0.2
0.1
0
*
Target HFU0
Target HFU30
Control HFU30

Figure 3. Refractory period for plasticity at previously potentiated spines is partially released with stronger stimulus.

(A) Images of dendrites from an EGFP-transfected CA1 neuron in slice culture directly prior to and 30 min after HFU_0 at target (left images) and HFU_{30}^+ at target (left images) and control (right images) spines. **(B-D)** A second stronger HFU at 30 min (HFU_{30}) resulted in a trend toward additional growth in target spines (blue circles/bars; n = 6 spines/cells), yet that was still greatly reduced compared to that of control spines (gray circles/bars; n = 6 spines/cells). Target spine data in **C** is from **B** re-normalized to the new baseline. Data represent mean ± SEM. Statistics: 2-way ANOVA with Bonferroni test. *p <0.05, **p < 0.01, ***p < 0.001. See also **Figure S3**.

Figure 3

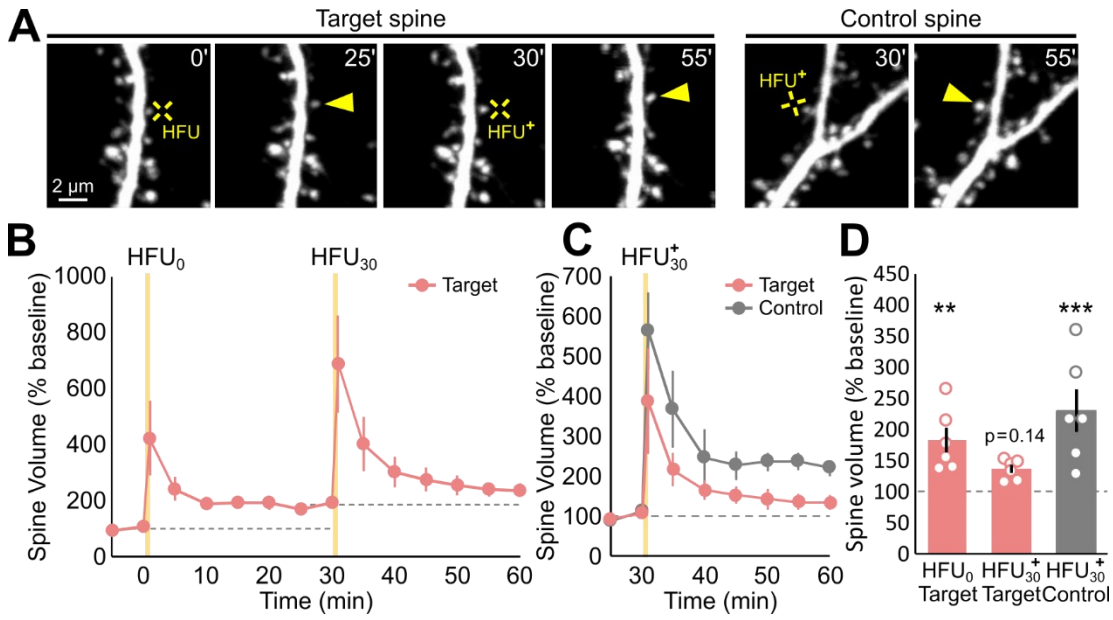
A
Target spine
Control spine
0'
25'
30'
55'
HFU
HFU+
2 µm
B
HFU0
HFU30
Target
Spine Volume (% baseline)
Time (min)
C
HFU+30
Target
Control
Spine Volume (% baseline)
Time (min)
D
Spine volume (% baseline)
**
***
p=0.14
HFU0 Target
HFU+30 Target
HFU+30 Control

Figure 4. Refractory period for plasticity at previously potentiated spines is released within 60 min.

(A) Images of dendrites from an EGFP-transfected CA1 neuron in slice culture directly prior to and 30 min after HFU_0 at target (left images) and HFU_{60} at target (left images) and control (right images) spines. **(B-D)** A second HFU at 60 min (HFU_{60}) resulted in additional growth (filled blue circles/bars, n=7 spines/cells; HFU_0: $p<0.0001$ HFU_{30}), comparable to that observed from a size-matched control spine on the same cell (gray circles/bar; n=7 spines/cells). Neighboring spines were unchanged throughout (open circles; n=64 spines/7 cells). Target spine data in **C** is from **B** re-normalized to the new baseline. **(E)** Images of dendrites from an DsRedExpress-transfected CA1 neuron in slice culture directly prior to and 30 min after HFU_0 at target (left images) and HFU_{45} at target (left images) and control (right images) spines. **(F-H)** The initial HFU stimulus (HFU_0) resulted in long-term growth of target spines on cells expressing DsRedExpress (black circles/bars; n=9 spines/cells), but an identical HFU at 45 min (HFU_{45}) did not drive additional growth. In contrast, a size-matched control spine on the same cell grew in response to HFU_{45} (gray circles/bar; n=9 spines/cells). Target spine data in **G** is from **F** re-normalized to the new baseline. Data represent mean ± SEM. Statistics: 2-way ANOVA with Bonferroni test. *$p < 0.05$, **$p < 0.01$. See also **Figure S4**.

Figure 4

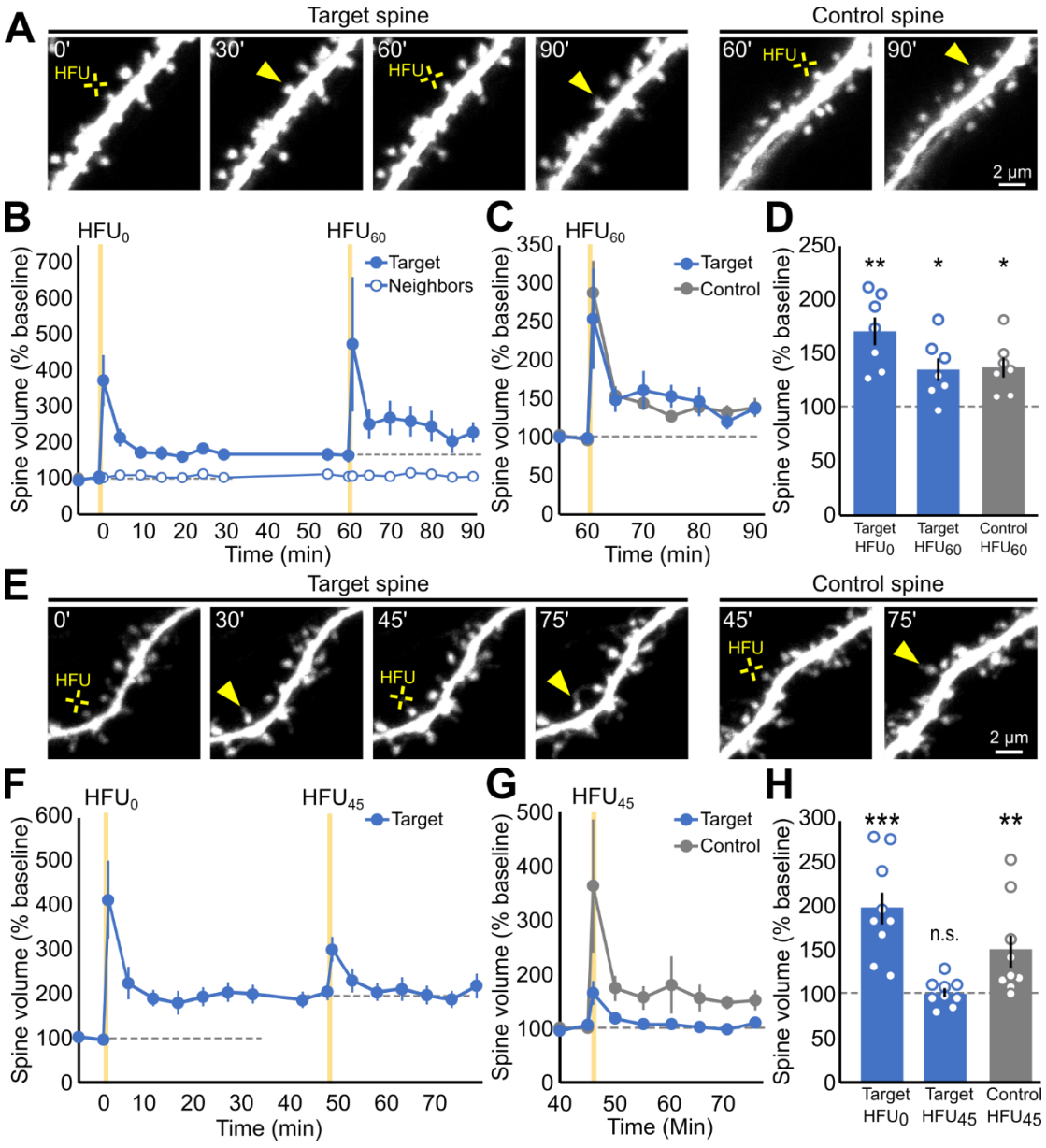
A
Target spine
Control spine
0'
30'
60'
90'
HFU
2 µm
B
HFU0
HFU60
Target
Neighbors
Spine volume (% baseline)
Time (min)
C
HFU60
Target
Control
D
Target HFU0
Target HFU60
Control HFU60
E
45'
75'
F
HFU45
G
Time (Min)
H
n.s.
Target HFU45
Control HFU45

Figure 5. Increased PSD95 expression level is sufficient to release the refractory period for plasticity at previously potentiated spines.

(A, E) Images of dendrites from CA1 pyramidal neurons transfected with DsRedExpress (magenta) and PSD95-GFP (green) directly prior to and 30 min after HFU_0 and HFU_{45} at target (left images) or control (right images) spines. **(B-D)** Notably, a second HFU at 45 min (HFU_{45}) resulted in additional growth (blue circles/bars; n=10 spines/cells) of target spines on dendrites of cells expressing PSD95-GFP and dsRedExpress, comparable to that observed in a size-matched control spine on the same cell (gray circles/bar; n=10 spines/cells). Target spine data in **C** is from **B** re-normalized to the new baseline. **(F-H)** Even when NBQX was added to the bath 30 min after HFU_0, both the target spine and the control spine (gray circles/bars; n = 5 spines/cells) grew in response to HFU_{45}. Target spine data in **G** is from **F** re-normalized to the new baseline. Data represent mean ± SEM. Statistics: 2-way ANOVA with Bonferroni test. *p <0.05, **p < 0.01, ***p < 0.001. See also **Figure S5**.

Figure 5

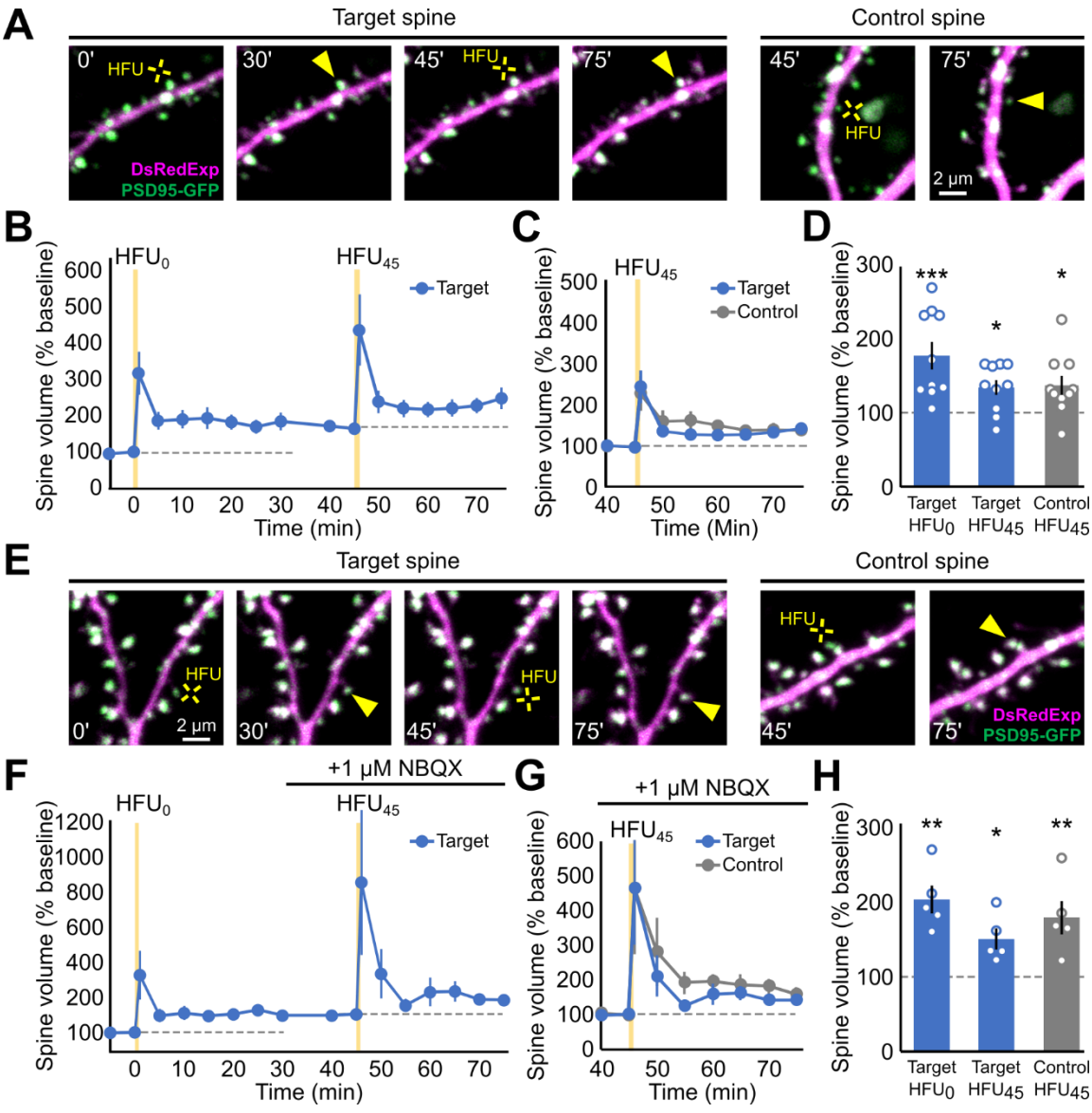
A
Target spine
Control spine
0'
HFU
30'
45'
HFU
75'
45'
HFU
75'
2 µm
DsRedExp
PSD95-GFP
B
HFU0
HFU45
Target
Spine volume (% baseline)
Time (min)
C
HFU45
Target
Control
Spine volume (% baseline)
Time (Min)
D
***
*
*
Spine volume (% baseline)
Target HFU0
Target HFU45
Control HFU45
E
Target spine
Control spine
HFU
0'
2 µm
30'
45'
HFU
75'
HFU
45'
75'
DsRedExp
PSD95-GFP
F
+1 µM NBQX
HFU0
HFU45
Target
Spine volume (% baseline)
Time (min)
G
+1 µM NBQX
HFU45
Target
Control
Spine volume (% baseline)
Time (min)
H
**
*
**
Spine volume (% baseline)
Target HFU0
Target HFU45
Control HFU45

Figure 6. Increased PSD93 expression level is not sufficient to release the refractory period for plasticity at previously potentiated spines.

(A) Images of dendrites from CA1 pyramidal neurons transfected with DsRedExpress and PSD93-GFP directly prior to and 45 min after HFU_0 and HFU_{45} at target (left images) and control (right images) spines. **(B-D)** The initial HFU stimulus (HFU_0) resulted in long-term growth of target spines (filled blue circles/bars; n=6 spines/cells), but an identical HFU at 45 min (HFU_{45}) did not drive additional growth. In contrast, a size-matched control spine on the same cell grew in response to HFU_{45} (gray circles/bar; n=6 spines/cells). Target spine data in **C** is from **B** re-normalized to the new baseline. Data represent mean ± SEM. Statistics: 2-way ANOVA with Bonferroni test. *p <0.05, ***p < 0.001. See also **Figure S6**.

Figure 6

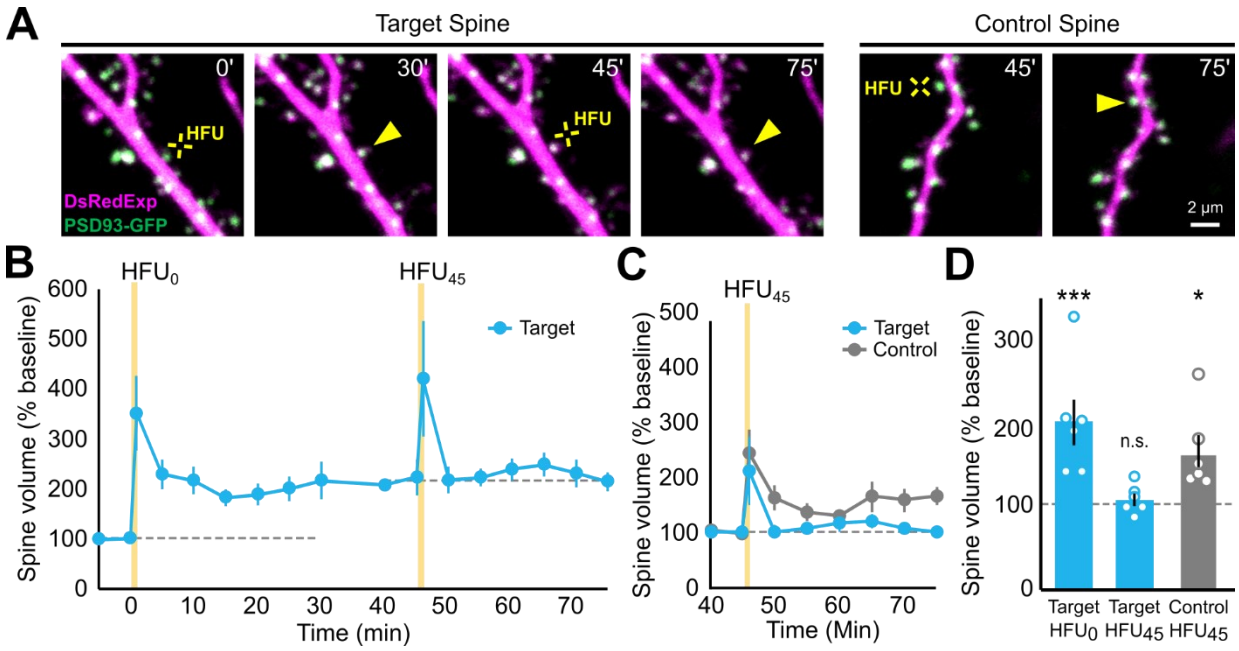
A
Target Spine
Control Spine
0'
30'
45'
75'
HFU
HFU
45'
75'
HFU
2 µm
DsRedExp
PSD93-GFP
B
HFU0
HFU45
Target
Spine volume (% baseline)
Time (min)
C
HFU45
Target
Control
Spine volume (% baseline)
Time (Min)
D
***
*
n.s.
Spine volume (% baseline)
Target HFU0
Target HFU45
Control HFU45

Figure S1: Related to Figure 1

(A) Quantification of spine size relative to neighbors for the target spine at baseline and 25-30 and control spine prior to HFU. There are no significant differences between the target's post-stimulus and the control spine's relative size (target: 108 ± 13%, control: 102 ± 16%; p = 0.68). **(B)** Initial spine size did not correlate with saturation (p = 0.38). **(C)** The relative size of the control spine in the SEP-GluA2 and tD-dsRed condition is not significantly different to the target spine post-HFU (target: 92 ± 6%, control: 85 ± 2%, p= 0.53). **(D-F)** Spines from SEP-GluA2 experiments grew in response to HFU_0 (measured as tD-dsRed fluorescence; black circles/bars; n = 7 spines/cells; 175 ± 13%; p<0.0001) but not HFU_{30} (111 ± 7%; p>0.99). Control spine grew in response to HFU_{30} (gray circles/bar; n = 7 spines/cells; 163 ± 14%). Statistics: paired Student's t-test used in **A** and **C**; simple linear regression used in **B**. 2-way ANOVA with Bonferroni Test used in **F**.

Figure S1

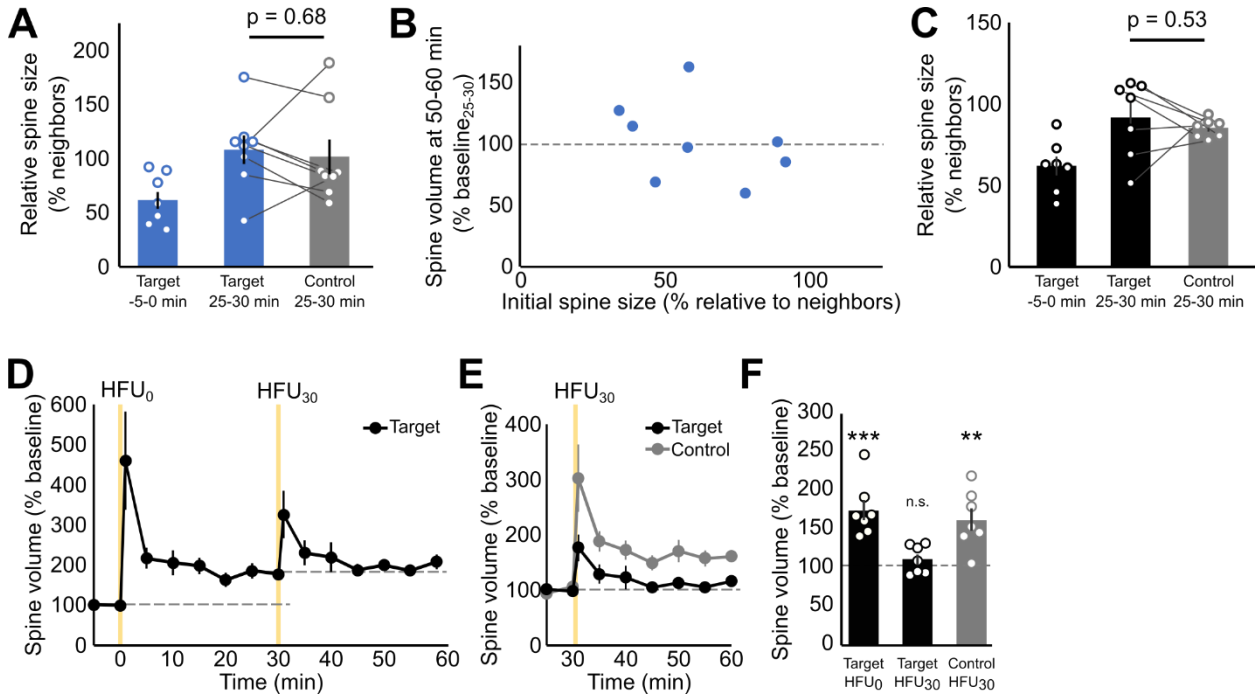
A
p = 0.68
Relative spine size (% neighbors)
200
150
100
50
0
Target -5-0 min
Target 25-30 min
Control 25-30 min
B
Spine volume at 50-60 min (% baseline25-30)
150
100
50
0
0
50
100
Initial spine size (% relative to neighbors)
C
p = 0.53
Relative spine size (% neighbors)
150
100
50
0
Target -5-0 min
Target 25-30 min
Control 25-30 min
D
HFU0
HFU30
Target
Spine volume (% baseline)
600
500
400
300
200
100
0
0
10
20
30
40
50
60
Time (min)
E
HFU30
Target
Control
Spine volume (% baseline)
400
300
200
100
0
30
40
50
60
Time (min)
F
Spine volume (% baseline)
300
250
200
150
100
50
0
***
n.s.
**
Target HFU0
Target HFU30
Control HFU30

Figure S2: Related to Figure 2

(A-C) Spines from CaMKII FRET-FLIM experiments grew in response to HFU_0 (measured from CyRFP1 fluorescence; blue circles/bars; n = 10 spines/cells; 278 ± 30%; $p<0.0001$) but not HFU_{30} (113 ± 7%; $p>0.99$). Control spine grew in response to HFU_{30} (gray circles/bar; n = 10 spines/cells; 213 ± 19%; $p<0.0001$). **(D)** There was no significant difference in the relative size of the target spine at 25-30 min and the control spine (target: 139 ± 23%, control: 129 ± 19%, p = 0.51). **(E)** There was no significant difference in the integrated red fluorescence of target spine at 25-30 min and the control spine (target: 77808 ± 17845 AU, control: 72579 ± 19973, p = 0.42). (F) The photon counts of the target spine and the control spine prior to HFU_{30} was not significantly different (target: 14627 ± 1656, control: 13696 ± 2158, p = 0.71). **(G)** We found no correlation between peak CaMKII activation and relative spine size (n = 15 spines/cells, p = 0.53). Statistics: 2-way ANOVA with Bonferroni Test used in **C**. paired Student's t-test used in **D-F**; simple linear regression used in **G**.

Figure S2

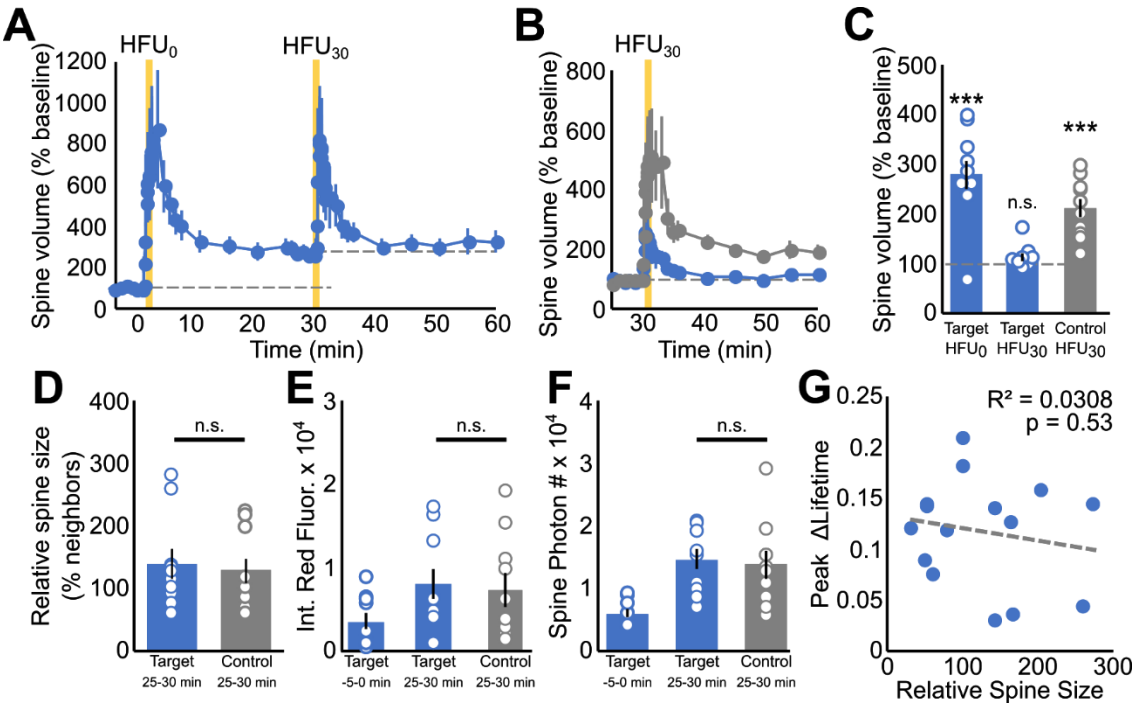
A
HFU0
HFU30
Spine volume (% baseline)
Time (min)
B
HFU30
Spine volume (% baseline)
Time (min)
C
Spine volume (% baseline)
***
n.s.
***
Target HFU0
Target HFU30
Control HFU30
D
Relative spine size (% neighbors)
n.s.
Target 25-30 min
Control 25-30 min
E
Int. Red Fluor. x 10^4
n.s.
Target -5-0 min
Target 25-30 min
Control 25-30 min
F
Spine Photon # x 10^4
n.s.
Target -5-0 min
Target 25-30 min
Control 25-30 min
G
R² = 0.0308
p = 0.53
Peak ΔLifetime
Relative Spine Size

Figure S3: Related to Figure 3

(A) Quantification of relative spines sizes for the target and control spines prior to HFU_{30}^{+}. There was no significant difference in the sizes of the target spine after its initial growth and the control spines (target: 107 ± 10%, control: 96 ± 9%, p = 0.43). **(B)** Quantification of relative spines sizes for the target and control spines prior to HFU_{30}^{++}. There was no significant difference in the sizes of the target spine after its initial growth and the control spines (target: 105 ± 16%, control: 118 ± 17%, p = 0.39). **(C-E)** HFU_{30}^{++} caused significant growth of both the control spines (gray circles/bars; n = 7 spines/cells) and the target spines (blue circles/bars; n = 7 spines/cells). The growth of the target spines was reduced compared to that of the control spines. Target spine data in **G** is from **D** re-normalized to the new baseline. Statistics: paired Student's t-test used in **A** and **B**; 2-way ANOVA with Bonferroni Test used in **E**.

Figure S3

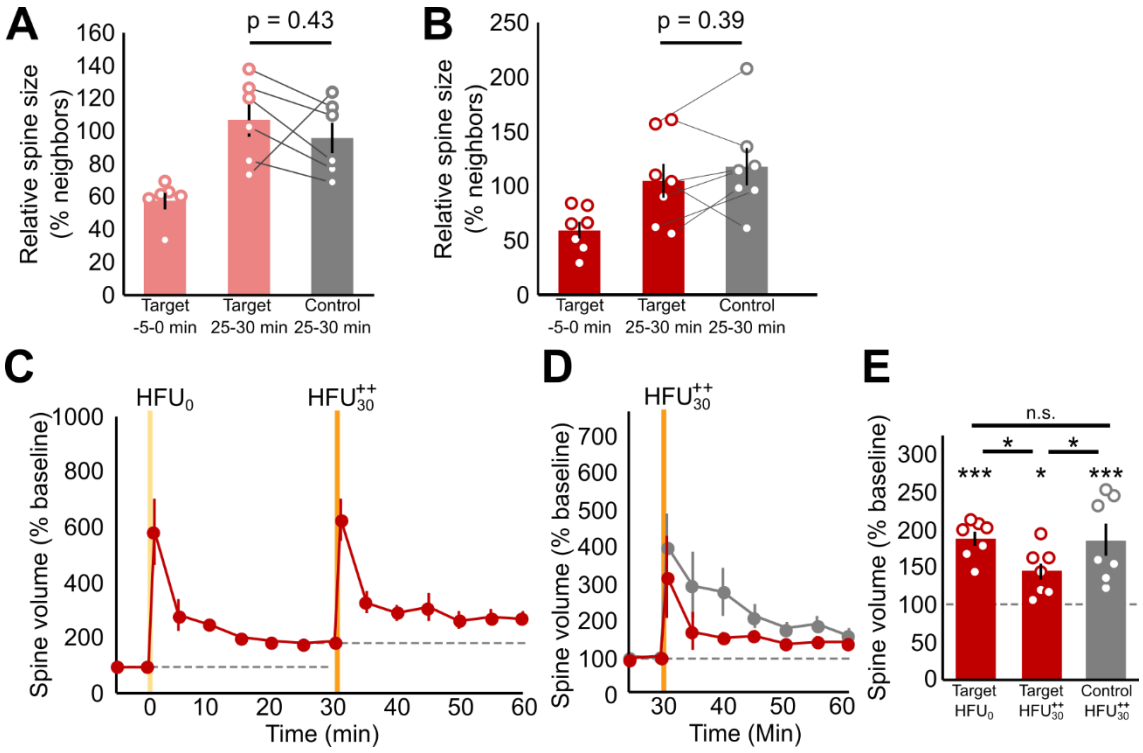
A
p = 0.43
Relative spine size (% neighbors)
Target -5-0 min
Target 25-30 min
Control 25-30 min
B
p = 0.39
Relative spine size (% neighbors)
Target -5-0 min
Target 25-30 min
Control 25-30 min
C
HFU0
HFU30++
Spine volume (% baseline)
Time (min)
D
HFU30++
Spine volume (% baseline)
Time (Min)
E
n.s.
Spine volume (% baseline)
Target HFU0
Target HFU30++
Control HFU30++

Figure S4: Related to Figure 4

(A) Quantification of spine size relative to neighbors for the target spine at baseline and 55-60 and control spine prior to HFU_{60}. There are no significant differences between the target's post-stimulus and the control spine's relative size (target: 91 ± 11%, control: 110 ± 10%; p = 0.31). **(B)** Quantification of spine size relative to neighbors for the target spine at baseline and 40-45 and control spine prior to HFU_{45}. There are no significant differences between the target's post-stimulus and the control spine's relative size (target: 101 ± 10%, control: 96 ± 9%; p = 0.75). Statistics: paired Student's t-test used in **A** and **B.**

Figure S4

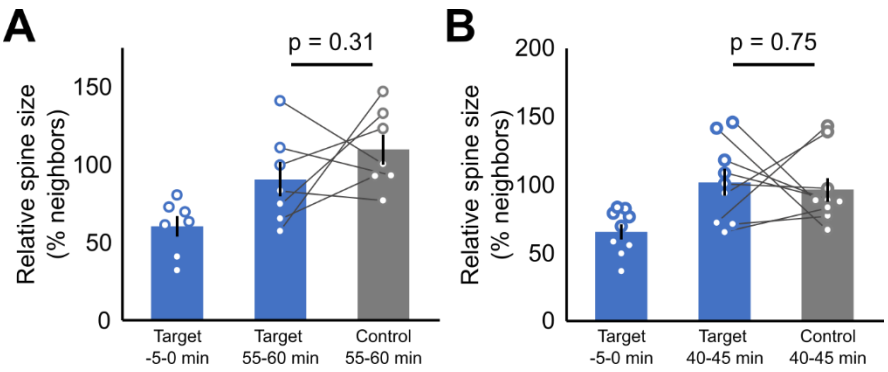
A
p = 0.31
Relative spine size
(% neighbors)
150
100
50
0
Target
-5-0 min
Target
55-60 min
Control
55-60 min
B
p = 0.75
Relative spine size
(% neighbors)
200
150
100
50
0
Target
-5-0 min
Target
40-45 min
Control
40-45 min

Figure S5: Related to Figure 5

(A) Comparison of red intensity from target spines at baseline shows no difference between the DsRedExpress alone and the DsRedExpress with PSD95-GFP groups (p=0.15). **(B)** Initial relative spine size compared to neighbors was no different between the DsRedExpress alone and DsRedExpress with PSD95-GFP (DsRedExp: 92 ± 16%, DsRedExp + PSD95-GFP: 67 ± 7%, p=0.56). **(C)** Transfection with PSD95GFP does not affect growth of previously unstimulated spines. Spines from cells expressing DsRedExpress alone (filled black circles, n = 9 spines/cells), DsRedExpress and PSD95-GFP (filled blue circles, n = 10 spines/cells) or DsRedExpress and PSD95-GFP prior to NBQX addition (open blue circles, n = 5 spines/cells) all grew following HFU_0. **(D)** No significant differences observed in the magnitude of spine volume at 20-30 min (DsRedExp: 199 ± 19%, DsRedExp + PSD95-GFP: 180 ± 19%, DsRedExp + PSD95-GFP + NBQX: 200 ± 18%, p=0.71). **(E)** Control spines matched the post-HFU size of the target spines for the DsRedExpress and PSD95-GFP (target: 93 ± 6%, control: 90 ± 12%, p = 0.87). **(F)** Control spines matched the post-HFU size of the target spines for DsRedExpress and PSD95-GFP with NBQX (target: 87 ± 17%, control: 84 ± 22%, p = 0.75) conditions. Statistics: unpaired Student's t-tests used in **A** and **B**; one-way ANOVA with Bonferroni test used in **D**; paired Student's t-tests used in **E, F**.

Figure S5

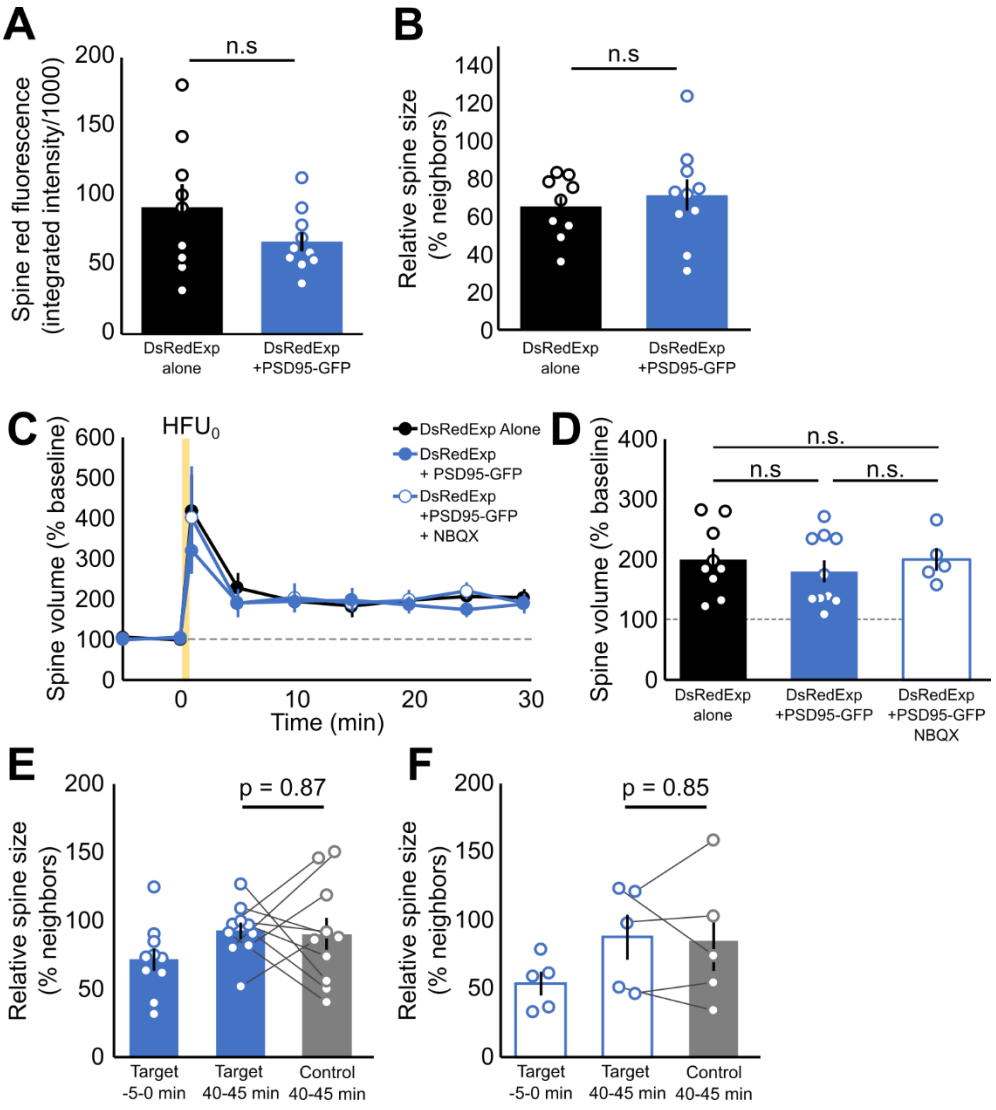
A
Spine red fluorescence (integrated intensity/1000)
n.s
DsRedExp alone
DsRedExp +PSD95-GFP
B
Relative spine size (% neighbors)
n.s
DsRedExp alone
DsRedExp +PSD95-GFP
C
HFU0
DsRedExp Alone
DsRedExp + PSD95-GFP
DsRedExp +PSD95-GFP + NBQX
Spine volume (% baseline)
Time (min)
D
Spine volume (% baseline)
n.s.
n.s
n.s.
DsRedExp alone
DsRedExp +PSD95-GFP
DsRedExp +PSD95-GFP NBQX
E
Relative spine size (% neighbors)
p = 0.87
Target -5-0 min
Target 40-45 min
Control 40-45 min
F
Relative spine size (% neighbors)
p = 0.85
Target -5-0 min
Target 40-45 min
Control 40-45 min

Figure S6: Related to Figure 6

(A) The red fluorescence of the target spines was no different between the DsRedExp with PSD95-GFP (67 ± 7) and DsRedExp and PSD93-GFP (82 ± 14) conditions (p = 0.32). **(B)** The initial relative size of target spines was no different between the groups (DsRedExp+PSD95-GFP: 65 ± 5%, DsRedExp+PSD93-GFP: 63 ± 8%, p = 0.53). **(C)** The green fluorescence of the target spines was no different (DsRedExp+PSD95-GFP: 42 ± 7, DsRedExp+PSD93-GFP: 41 ± 11, p = 0.94). **(D)** The ratio of green to red signal in the target spines was no different (DsRedExp+PSD95-GFP: 0.63 ± 0.08, DsRedExp+PSD93-GFP: 0.58 ± 0.14, p = 0.74). **(E)** Relative size of control spine matched that of the target spine 40-45 min after HFU_0 (target: 115 ± 15%, control: 96 ± 9%, p = 0.15). Statistics: unpaired Student's t-test used in **A-D**; paired Student's t-test used in **E**.s

Figure S6

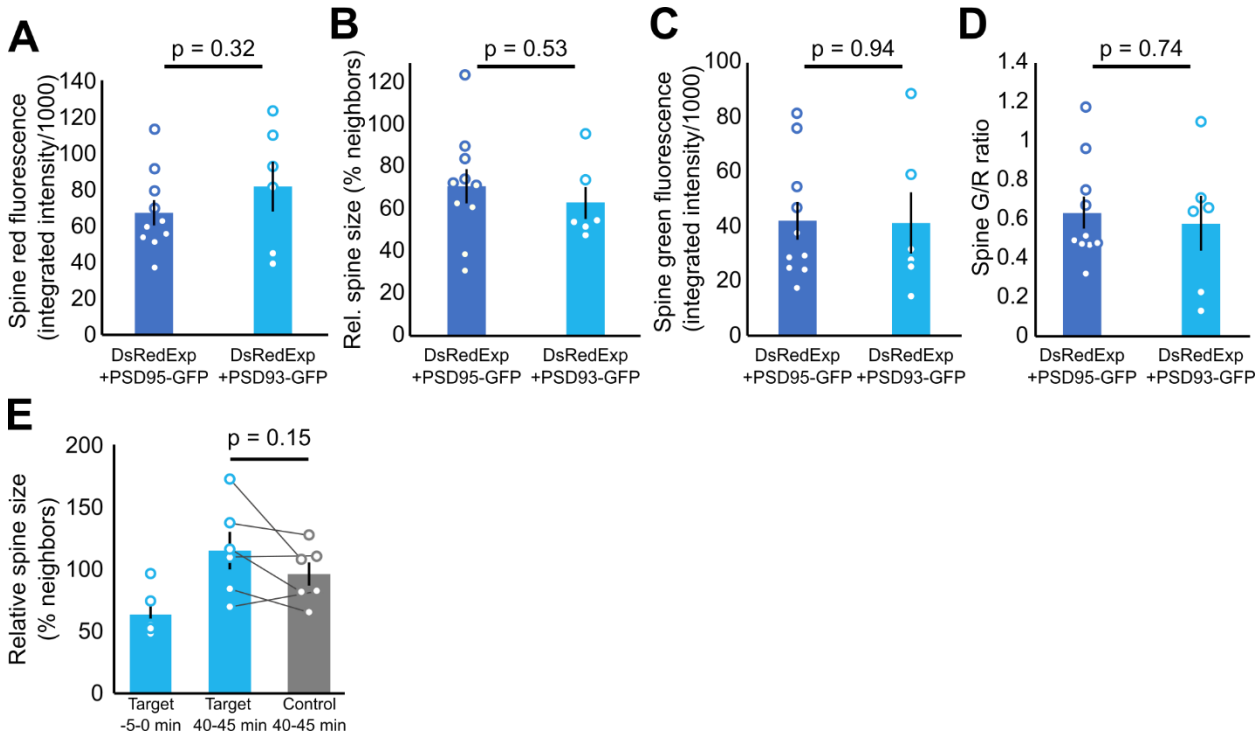
A
p = 0.32
Spine red fluorescence (integrated intensity/1000)
DsRedExp +PSD95-GFP
DsRedExp +PSD93-GFP
B
p = 0.53
Rel. spine size (% neighbors)
C
p = 0.94
Spine green fluorescence (integrated intensity/1000)
D
p = 0.74
Spine G/R ratio
E
p = 0.15
Relative spine size (% neighbors)
Target -5-0 min
Target 40-45 min
Control 40-45 min

Chapter 3: Mechanisms related to saturation of plasticity at individual dendritic spines

Preface

The following chapter contains unpublished and preliminary data related to the focus of my thesis. These experiments were conducted in the pursuit of a molecular mechanism that underlies saturation of plasticity at individual dendritic spines. Many of these experiments have intriguing preliminary results and may be worth pursuing further. The first section of these results focuses on the potential role of the GluN2A subunit of NMDA receptor in saturation of plasticity. The second section of this chapter focuses on $mGluR_5$ and its involvement in saturation of plasticity. Finally, this chapter contains experiments conducted to further elucidate the role of PSD95 in the early recovery of plasticity, which I described in **Chapter 2**. I would like to thank Dr. John Gray for providing me with the GluN2A conditional knockout animals used to start the colony for some of the experiments in this chapter and the Cre-GFP fusion protein plasmid used to induce KO. Dr. Dipannita Sarkar aided in data collection and analysis for the PSD95-AAAA-GFP experiments.

Introduction

Learning is a critical function which requires the ability to process and store information. There is strong evidence that learning depends on synaptic plasticity, or the ability to change the strength of neuronal connections, in the hippocampus. It has been observed that LTP can become saturated in the hippocampus (Cao & Harris, 2014; Huang et al., 1992; Kramar et al., 2012). It has also been shown that saturation of LTP in the hippocampus can lead to learning impairment in rodents (Barnes et al., 1994; Moser, 1998). Notably, saturation of LTP is temporary and it has been observed that given enough time, saturated hippocampal circuits can once again potentiate (Cao & Harris, 2014; Kramar et al., 2012). Yet, the mechanisms by which LTP is saturated and then released from saturation at a later time point has not been clearly defined. It has been proposed that the release of saturation of LTP is due to the recruitment of high threshold synapses into the circuit (Kramar et al., 2012). Others have proposed that the recovery of plasticity involves a presynaptic component, the nascent zone, which acts as a substrate for plasticity at synapses (Bell et al., 2014). My work in **Chapter 2** demonstrates that saturation of plasticity occurs at individual dendritic spine synapses and that these same spines can undergo further plasticity 60 minutes after they are initially potentiated.

To find the molecular mechanism for saturation and release, I hypothesized that changes in the glutamate receptors of dendritic spines played a role in shaping the plasticity response by altering the threshold of plasticity, which is called metaplasticity. Indeed, it has been shown that metaplasticity can occur at individual synapses following a prolonged silencing of those synapses, by changing the composition of NMDA receptors at those synapses to increase their calcium currents (Lee et al., 2010). Interestingly, activity at individual synapses can cause a change to the fractional calcium current of spine NMDA receptors (Sobczyk & Svoboda, 2007). It has also been shown that at synapses from very young animals (P2-P9), induction of LTP can induce a reversible switch of GluN2B-containing NMDA receptors to GluN2A-containing

receptors (Bellone & Nicoll, 2007). Other forms of metaplasticity have also been observed to require the activity of the metabotropic glutamate receptor, $mGluR_5$ (Bortolotto et al., 2005). In this chapter, I explore the potential role of the NMDA receptor's GluN2A subunit and $mGluR_5$ on saturation of plasticity at individual dendritic spines.

One promising set of experiments in **Chapter 2** demonstrated that overexpression of PSD95 can allow dendritic spines to grow in response to a second glutamatergic stimulation after 45 minutes. PSD95 is a key scaffolding protein found in the PSD of dendritic spines. PSD95 is involved in homeostatic plasticity and synapse maturation (Favaro et al., 2018; Q. Sun & Turrigiano, 2011). It has also been shown that PSD95 does not arrive at dendritic spines within 30 minutes of glutamatergic stimulation (Bosch et al., 2014). However, others suggest that additional PSD95 arrives at stimulated spines more than one hour after stimulation (Meyer et al., 2014). Due to the stability of PSD95 at synapses, Meyer *et al*., found that PSD95-GFP bleached and after correction, observed that PSD95 enrichment in stimulated spines became renormalized in spines 60-80 minutes after LTP induction. Although the expansion of the PSD has been observed the arrival, if any, of PSD95 at potentiated synapses is still unclear. In this chapter I also explore the arrival of PSD95 at stimulated spines using live nanobody imaging of PSD95-FingR-GFP (Gross et al., 2013). I also show the initial results of experiments seeking to define the structural domains of PSD95 which may be involved in its role for the recovery of plasticity at previously stimulated spines. We focused on a mutation of the PDZ1 and PDZ2 domains (PDZ1: R70A and G71A, PDZ2: K165A., K168A) which interfere with binding of AMPA and NMDA receptors to PSD95 (Ehrlich & Malinow, 2004; Kornau et al., 1995; Niethammer et al., 1996).

Methods

Preparation and transfection of organotypic hippocampal slice cultures

Cultured hippocampal slices (300-400 µm) were prepared from P6-P8 C57BL/6 mice of both sexes, as described (Stoppini et al., 1991), and as approved by the UC Davis Institutional Animal Care and Use Committee (IACUC). Cultured slices were transfected at 8-16 DIV (or 3-4 DIV for GluN2A cKO) using biolistic gene transfer (180-210 psi), as described (G. Woods & Zito, 2008). 6-8 mg of 1.6 µm gold beads (BioRad) were coated with 10 µg of tDimer-dsRed together with 20 µg SEP-GluN2A and 10 µg of untagged GluN1 (both gifts from Dr. Andres Barria), or 5 µg of FUGW-GFP and 5 µg of FUGW-Cre-GFP (both gifts from Dr. John Gray), or 15 µg of EGFP-N1 (Clontech), or 10 µg DsRedExpress (Clontech) together with 10 µg of GFP-tagged PSD95-FingR-GFP (Gross et al., 2013). Slices were transfected 12-14 days (GFP and Cre-GFP), 1-3 days (EGFP; PSD95-FingR-GFP and DsRedExpress), 2-4 days (SEP-GluN2A and tDimer-dsRed), or 24 hrs (PSD95-AAAA-GFP and DsRedExpress) prior to imaging.

Time-lapse two-photon imaging

Transfected CA1 pyramidal neurons at depths of 10–50 µm in slice cultures (10-18 DIV) were imaged using a custom two-photon microscope (G. F. Woods et al., 2011) controlled with ScanImage (Pologruto et al., 2003). Image stacks (512 x 512 pixels; 0.02 µm/pixel) with 1 µm z-steps were collected. For each neuron, one segment of secondary or tertiary basal dendrite was imaged at 5 min intervals at 29°C in recirculating ACSF (in mM): 127 NaCl, 25 $NaHCO_3$, 1.2NaH_2PO_4, 2.5 KCl, 25 D-glucose, aerated with 95% O_2/5% CO_2, 310 mOsm, pH 7.2, with 0.001 TTX, 0 Mg^{2+}, and 2 Ca^{2+}. Dendrites of transfected cells were selected under epifluorescence and MNI-glutamate (2.5 mM) was added at least 15 min prior to uncaging stimulation.

High frequency uncaging (HFU) of glutamate

HFU consisted of 60 pulses (720 nm; ~7.5–9.5 mW at the sample) of 2 ms duration at 2 Hz delivered in ACSF containing the following (in mM): 2 Ca^{2+}, 0 Mg^{2+}, 2.5 MNI-glutamate, and 0.001 TTX. Because earlier studies established that spine size can influence the magnitude of potentiation (Matsuzaki et al., 2004), we selected target spines with an initial size range in the 25-50% quartile of sizes. The laser beam was parked at a point ~0.5–1 μm from the spine head in the direction away from the dendrite. Cells with no noticeable transients in response to HFU_0 were discarded and not further pursued.

Image analysis

Images were analyzed using a custom MATLAB software, as described (G. F. Woods et al., 2011). In brief, following application of a 3 x 3 median filter, background-subtracted integrated green and/or red fluorescence intensity was calculated from a boxed region surrounding the spine head. Spine volume was estimated using fluorescence from a cell fill (EGFP, tDimer-dsRed, or DsRedExpress) (Holtmaat et al., 2005). Bar graphs show the average values from the three time points occurring at 20-30 min after the most recent HFU (HFU_0: 20-30min; HFU_{30}: 50-60 min; HFU_{45}: 65-75 min).

Quantification of PSD95 enrichment in dendritic spines

The integrated fluorescence of the PSD95-FingR-GFP and DsRedExpress in the target spine and three regions of interest in the dendrite were quantified. The enrichment of PSD95 in dendritic spines was calculated as follows:

$$Erichment = (\frac{G_{spine}}{R_{spine}})/(\frac{G_{dendrite}}{R_{dendrite}})$$

Where G is the integrated fluorescence of PSD95-FingR-GFP in the spine/dendrite and R is the integrated fluorescence of DsRedExpress in the spine/dendrite. The enrichment of PSD95 was then normalized to the average of the baseline for each individual cell.

Statistics

All data are represented as mean ± standard error of the mean (SEM). All statistics were calculated across cells using GraphPad Prism. Statistical significance level (α) was set to $p < 0.05$ for all tests. When comparing only two groups, paired or unpaired (as appropriate) Student's t-tests were used. When multiple comparisons were made, a one or two-way ANOVA with Bonferroni or Tukey post-hoc test was performed. All p values are in the text and n values are in the figure legends.

Results

Role of the GluN2A NMDA receptor subunit in saturation of LTP

It has been shown that, in very young animals (P2-P9), the induction of LTP can cause GluN2B-containing receptors can be rapidly switched with GluN2A-containing receptors (Bellone & Nicoll, 2007). This change can lead to significant alteration of the channel's conductance, leading to reduced calcium influx. These alterations result in a decrease in the NMDAR's ability to drive LTP (Paoletti et al., 2013). Thus, a temporary switch in receptor subunit composition could lead to the temporary inability of spines to undergo LTP. In fact, it has been shown that disrupting the localization of GluN2B prevents LTP and disruption of GluN2A increases the magnitude of LTP in hippocampal circuits (Kellermayer et al., 2018). To test whether a switch from GluN2B- to GluN2A-containing receptors at spines plays a role in saturation of plasticity at individual dendritic spines, I expressed super-ecliptic phluorin (SEP)-tagged GluN2A and an untagged GluN1. The SEP tag on the GluN2A subunit is pH sensitive and thus is quenched when the receptor subunit is in vesicles but can fluoresce when the receptor is inserted into the

cell's membrane (Miesenböck et al., 1998). I then stimulated spines with a high-frequency glutamate uncaging (HFU) stimulus and monitored their SEP-GluN2A content. I hypothesized that SEP-GluN2A would temporarily increase in stimulated spines and then decrease within 60 minutes, at which time spines can undergo plasticity again.

After glutamate uncaging, spine volume was increased and maintained (**Figure 1B, D**; 20-30 min: 195 ± 26%, p = 0.021; 50-60 min: 207 ± 31%, p = 0.024; n = 8 spines/cells, 7 biological replicates). There was no significant difference in spine size between 20-30 minutes and 50-60 minutes (**Figure 1D**; p = 0.95). SEP-GluN2A was increased in stimulated spines at 20-30 minutes which became non-significant from baseline at 50-60 minutes (**Figure 1C-D**; 20-30 min: 149 ± 15%, p = 0.0.033; 50-60 min: 134 ± 22%, p = 0.33). This establishes a trend towards a decrease in spine GluN2A content over time following HFU, however, there was no significant change in SEP-GluN2A between 20-30 minutes and 50-60 minutes (p = 0.73). Combining the caveats that (i) there was low expression of SEP-GluN2A in the imaged cells (**Figure 1A**), (ii) only two of the individual traces matched the average trend of SEP-GluN2A and (iii) a small (~10%) trend toward bleaching of SEP-GluN2A in the unstimulated neighbor spines (**Figure 1C**), conclusions from this experiment are difficult to make but these experiments are worth pursuing further.

To further test this hypothesis, I also explored saturation of plasticity in a Cre-driven conditional GluN2A KO model (Gray et al., 2011). I transfected slices for 12-14 days with a Cre-GFP fusion protein to induce KO of GluN2A and cytosolic GFP to measure spine volume. I then visually identified CA1 pyramidal neurons in organotypic slice culture which had elevated GFP fluorescence in their nucleus relative to the rest of the soma (**Figure 2A**) and stimulated a spine with an HFU stimulus (HFU_0). I monitored the fluorescence of the stimulated spine for 30 minutes and then stimulated the same spine a second time, with an identical HFU stimulus (HFU_{30}). The results of this experiment are preliminary. In these experiments, I observed spine

growth which did not reach significance in response to HFU_0 (**Figure 2B-D**; 210 ± 34%; p = 0.25; n = 3 spines/cells, 3 biological replicates), likely due to the small number of spines in the dataset. Spines did not grow in response to HFU_{30} (**Figure 2 B-D**; 90 ± 25, p > 0.99). Though the change in spine size in response to HFU_0 was not significant compared to baseline, there is a significant difference in the change between HFU_0 and HFU_{30} (**Figure 2D**; p = 0.02). Interestingly, rather than showing no response or a small transient increase in size (as seen in **Chapter 2**), spines from GluN2A cKO neurons temporarily shrank in response to HFU_{30} (**Figure 2C**; not quantified). Together, these results suggest that a switch to GluN2A and reversal is not likely to be the molecular mechanism that underlies the refractory period for plasticity that spines exhibit but could play a role in shaping their plasticity response after their initial growth.

Role of $mGluR_5$ on saturation of spine growth

The class I metabotropic glutamate receptor, $mGluR_5$, has been implicated in metaplasticity (Bortolotto et al., 2005; El-Hassar et al., 2011). I hypothesized that saturation of LTP could be controlled by $mGluR_5$. To test this hypothesis, I blocked $mGluR_5$ by incubating my slices for 15 minutes in 15 μM MPEP prior to HFU_0. I then stimulated a spine with an HFU and monitored its size for 30 minutes before stimulating the spine a second time and stimulating a control spine on the same cell. This experiment was also carried out in the absence of MPEP. In the vehicle condition, spines had a trend towards growth in response to HFU_0 (**Figure 3B, D**; 190 ± 49%, p= 0.15; n = 3 spines/cells, 2 biological replicates) but failed to grow in response to a second stimulus (**Figure 3B-D**; 111 ± 16%, p = 0.54), as expected. The lack of significant growth after HFU_0 is likely due to the low number of spines collected for this experiment. Control spines in the vehicle condition also trended towards growth but failed to achieve significance (**Figure 3G, H**; 154 ± 3%, p = 0.15), likely also due to the small number of spines in the dataset. Spines had a growth trend in response to HFU_0 in the presence of MPEP (**Figure 3F, H**; 205 ± 25%, p = 0.08; n = 3 spines/cells, 3 biological replicates) and did not grow significantly in response to

HFU_{30} (**Figure 3F-H**; 140 ± 21%, p = 0.75). Notably, control spines grew significantly in response to HFU_{30} (**Figure 3G, H**; 226 ± 35%, p = 0.03). The growth of the control spine was greater in the MPEP condition than the vehicle condition (Student's t-test: p = 0.11), suggesting that that $mGluR_5$ activation may play a role in the plasticity of naïve spines, adding a caveat to the interpretation of these results. Indeed, mGluR plays a different role in LTD on spines of different sizes (Holbro et al., 2009; Oh et al., 2013).

Time-course of PDS95 enrichment following LTP

Previous studies have shown that while spines grow quickly following the induction of LTP, the PSD of these spines grows with a delay between 1 and 3 hours (Bosch et al., 2014; Bourne & Harris, 2011; Meyer et al., 2014). I hypothesized that the building up of the PSD was the limiting step in the recovery of plasticity at dendritic spines. I tested this hypothesis by using a novel PSD95 probe, PSD95-FingR-GFP (Gross et al., 2013), to monitor changes in endogenous PSD95 in live cells. I transfected cells with PSD95-FingR-GFP and DsRedExpress as a volume marker. I stimulated spines with a single HFU and monitored changes in spine size and PSD95 content for 75 minutes. If the delayed arrival of PSD95 to potentiated synapses limits plasticity, we would expect to see PSD95 arrive at stimulated spines within 60 minutes, a time point at which spines can once again undergo HFU-induced growth.

As expected, stimulation of dendritic spines expressing PSD95-FingR-GFP and DsRedExpress, led to an increase in spine size (**Figure 4A, B, E**; 20-30 min: 191 ±59%, p < 0.001; 50-60 min: 214 ± 82%, p <0.001). There was no significant change in PSD95 at 20-30 minutes or 50-60 minutes (**Figure 4A, C, E**; 20-30 min: 105 ±4%, p =0.95; 50-60 min: 99 ± 5%, p > 0.99). I measured the enrichment of PSD95 relative to the dendrite (**Figure 4D, F**). Immediately after stimulation, PSD95 became de-enriched in the stimulated spine, and did not recover within the 75-minute imaging period (**Figure 4D, F**; 20-30 min: 0.67 ± 0.09, p > 0.99; 50-60 min: 0.69 ± 0.11, p >0.99). This de-enrichment fails to meet significance at the current number of replicates.

These results are consistent with previous results showing that PSD95 takes more than an hour to arrive at spines that have undergone LTP (Meyer et al., 2014). This also suggests that overexpression of PSD95 can facilitate the recovery of plasticity, though this is may not be due to its arrival at stimulated spines but rather its ability to regulate the localization of other proteins which may destabilize glutamate receptors at the synapses like $STEP_{61}$ (Won et al., 2016). The PSD95-FingR-GFP intrabody is autoregulates its own expression though its ZF-KRAB domains when all of the antibody is bound to endogenous PSD95 (Gross et al., 2013). This may be a confounding factor as it is unclear whether the intrabody is being upregulated quickly enough to bind newly transcribed PSD95. It would be important to show that the FingR intrabody can detect changes in endogenous protein levels on our timescale through imaging of a protein which is know to rapidly arrive at stimulated spines such as CaMKII (Bosch et al., 2014).

Role of PDZ1 and 2 of PSD95 in recovery of plasticity after saturation

In **Chapter 2**, I show that overexpression of PSD95 allowed spines to grow in response to a second stimulus administered at 45 minutes. To test what interactions of PSD95 are relevant for the recovery of plasticity at previously stimulates spines, we induced four point-mutations in the PDZ1 and PDZ2 regions of PSD95 (R70A, G71A, K165A and K168A; PSD95-AAAA), which render these 2 domains null, thus preventing their interactions with other synaptic proteins (Ehrlich & Malinow, 2004). We transfected neurons with PSD95-AAAA-GFP and DsRedExpress and stimulated them with an HFU (HFU_0) and monitored spine size for 45 minutes before stimulating a second time (HFU_{45}). These experiments are preliminary and ongoing.

An initial HFU leads to an increase spine size, as expected (**Figure 5B, D**; 189 ± 45%, p = 0.01; n = 4 spines/cells, 4 biological replicates). In response to HFU_{45} spines failed to show significant growth (**Figure 5B-D**; 117 ± 37%, p = 0.55). Control spines on these cells also failed to grow significantly (**Figure 5 C, D**; 129 ± 12%, p = 0.32), likely due to the small number of spines in this preliminary experiment. In **Chapter 2**, I observed growth at this timepoint when cells were

overexpressing a WT PSD95-GFP. The mutation of PSD95's PDZ1 and PDZ2 domains appears to ablate the recovery effect of PSD95 overexpression. This suggests that PSD95 may play a role in the recovery of plasticity through its interactions at these at one or both of these two domains.

Discussion

Role of the glutamate receptors in saturation of plasticity

I have observed that plasticity is saturated and released at individual dendritic spine synapses. I had initially hypothesized that this saturation could be due to changes in the threshold for synaptic plasticity at these spines. The NMDA receptors containing the GluN2B subunit are important for LTP and disrupting their synaptic localization can prevent LTP (Kellermayer et al., 2018). Receptors that contain the GluN2A subunit, have altered channel dynamics and calcium permeability, making the NMDA receptor subunit switch a promising mechanism to be involved in saturation of plasticity. My preliminary experiments show that following HFU stimulation, spines did not have a significant increase in GluN2A, though a trend was observed for increased GluN2A content at the 20-30 minute time point with a small reduction by the 50-60 minute time point. It has been previously shown that induction of LTP induces a reversible switch in NMDA receptor subunit composition in slices from P2-P9 animals, but not in older animals (Bellone & Nicoll, 2007). Bellone and Nicoll found that LTP does not induce a change in NMDA receptor composition in older animals. It is possible that this is caused by a developmental change in NMDA receptor composition occluding the effect of LTP-induction of NMDA receptor composition (Sans et al., 2000). Further preliminary experiment show that spines in GluN2A cKO neurons grew in response to an initial HFU, though has not reached significance due to a small sample size. The KO of GluN2A did not allow for spines to grow in response to a second stimulus, as I had hypothesized. Interestingly, saturation experiments in slices from GluN2A-cKO animals revealed an interesting transient shrinking behavior. This

result suggests that the GluN2A subunit is not responsible for the saturation of LTP. Together both of my preliminary results suggest that GluN2A is not responsible for the onset of saturation of plasticity, but it is involved in the plasticity of previously stimulated synapses. These results warrant further investigation.

Metabotropic glutamate receptors, specifically $mGluR_5$, have been shown to play a role in metaplasticity (Bortolotto et al., 2005). Intriguingly, $mGluR_5$ activity can modulate neuronal excitability by activating the Ca^{2+}-activated potassium channel, SK2 (El-Hassar et al., 2011). The SK2 channel can modulate the NMDA receptor's Ca^{2+} current and blocking SK2 can facilitate LTP by lowering the threshold for plasticity (Ngo-Anh et al., 2005). Experiments blocking $mGluR_5$ activity show that while previously stimulated spines may grow more when $mGluR_5$ is inhibited, the larger control spines also had enhanced HFU-induced growth. Our lab has previously shown that mGluR activity plays a different role in spine shrinkage in large spines (Oh et al., 2013). The different role of mGluR function in spines of different sizes could explain the confounding effect I observed on control spines in the MPEP condition. Furthermore, because $mGluR_5$ can drive SK2 channel activity, and SK2 channel activity can reduce NMDA receptor Ca^{2+} currents, it is likely that the additional growth I observed is due to stronger NMDA receptor currents, causing the stimulus to be stronger. Thus, the additional growth that I observed in the presence of $mGluR_5$ inhibitor is caused by this stronger stimulus, as I show in **Chapter 2**.

Role of synaptic scaffolding in saturation of plasticity

One interesting hypothesis about saturation of plasticity is that it occurs due to the lack of available slots for AMPA receptor insertion. AMPA receptors are anchored at synapses by an indirect interaction with PSD95 through stargazin (Schnell et al., 2002). The phosphorylation of stargazin is mediated by CaMKII and PKC and is important for its localization at synapses (Tomita et al., 2005). The PDZ domains of PSD95 act as slots for AMPA receptors to be

stabilized at synapses. Furthermore, the observation that the expansion of the PSD in potentiated spines is delayed makes this an interesting hypothesis (Bourne & Harris, 2011). I hypothesized that the lack of plasticity at previously stimulated spines could be a result of available PSD95 becoming occupied by an initial stimulus and depleting the pool of available AMPA receptor slot. I have observed that overexpression of PSD95 can indeed allow for spines to undergo plasticity at an earlier time point. In my preliminary live nanobody imaging of PSD95, I found that PSD95 is not increased in potentiated spines within the time frame that plasticity recovers. This would suggest that it is not the arrival of PSD95 itself that allows for plasticity to be recovered but rather some other interaction. With the aid of Dr. Dipannita Sarkar, I also find, in my preliminary studies, that overexpression of a PDZ1/2 null mutant of PSD95 does not allow for the same recovery of plasticity as overexpression of WT PSD95. One of the many roles of these domains of PSD95 is in anchoring AMPA receptors at the synapse (Ehrlich & Malinow, 2004; Won et al., 2017).

If the arrival of PSD95 is not required for the recovery of plasticity, how does PSD95 overexpression allow for this recovery? It could be that PSD95 could be playing a role by recruiting some other protein to synapses that is depleted by LTP. This would likely be a protein which interacts with PDZ1/2 of PSD95, as mutation of these domains causes a failure of spines to grow in response to a second HFU. It has also been observed that overexpression of PSD95 causes accumulation of AMPA-type glutamate receptors at synapses (Ehrlich & Malinow, 2004). I have shown that AMPA receptor activation is not required for the recovery of plasticity when WT PSD95 is overexpressed (**Chapter 2**). This does not rule out the possibility that AMPA receptors may be involved in the recovery of plasticity as they could be playing a separate role that does not involve their channel opening. Indeed, it has been observed that the AMPA receptor GluA1 c-tail is sufficient for spine structural plasticity (Kopec et al., 2007). Another possibility is that overexpression of PSD95 brings more binding slots than are required for

plasticity. It has been suggested that spine size follows a discreet distribution and that potentiation at single hippocampal CA3-CA1 synapses exhibits an all-or-none behavior (Bartol et al., 2015; Petersen et al., 1998). If this is the case, it could be possible that LTP induces insertion of a set number of AMPA receptors at spines. With the excess availability of PSD95, this could cause only a partial occupation of available AMPA receptor binding slots and leave excess unoccupied slots for subsequent plasticity. Though the role of PSD95 in saturation of plasticity is not fully understood, identifying the interactions of PSD95 that are relevant for recovery of plasticity could yield further clues into this elusive mechanism.

Figures and Legends

Figure 1: Time course of GluN2A in dendritic spines following the induction of LTP.

(A) Representative time-lapse images of a dendrite of a CA1 pyramidal neuron expressing SEP-GluN2A (green) and tD-DsRed (magenta) in organotypic hippocampal slice cultures after a single HFU stimulus. **(B)** Spines grew in response to HFU stimulus. **(C)** SEP-GluN2A signal in the stimulated spine was significantly increased from baseline at 20-30 minutes but not 50-60 minutes. **(D)** Spines showed persistent significant increase in size (20-30 min: 195 ± 26%, $p = 0.021$; 50-60 min: 207 ± 31%, $p = 0.024$). SEP-GluN2A was significantly increased by HFU at the 20-30 minute timeframe (149 ± 15%, $p = 0.033$) but was not significantly different from baseline at the 50-60 minute timeframe (134 ± 22%, $p = 0.33$). Scalebar: 2 μm. n = 8 cells/spines; 7 biological replicates. Statistics: significance was determined using a one-way ANOVAs with Tukey's multiple comparisons test. *$p < 0.05$, **$p < 0.01$, ***$p < 0.001$.

Figure 1

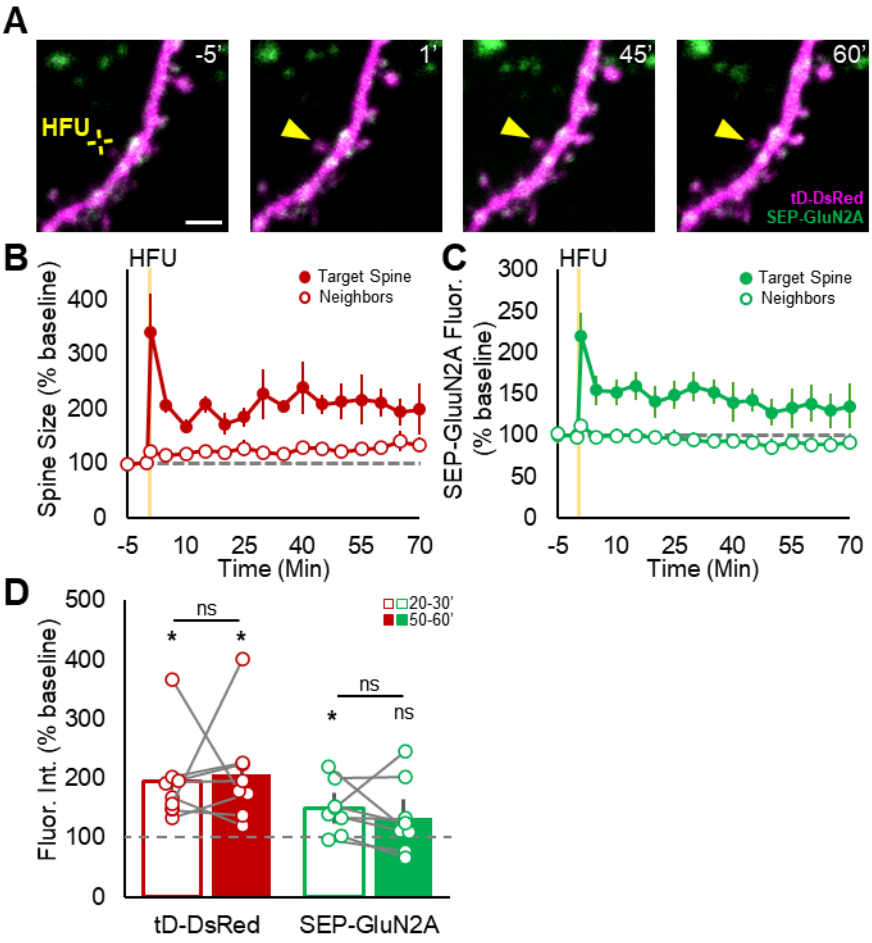
A
-5'
HFU
1'
45'
60'
tD-DsRed
SEP-GluN2A
B
HFU
Target Spine
Neighbors
Spine Size (% baseline)
400
300
200
100
0
-5
10
25
40
55
70
Time (Min)
C
HFU
Target Spine
Neighbors
SEP-GluuN2A Fluor. (% baseline)
300
250
200
150
100
50
0
-5
10
25
40
55
70
Time (Min)
D
20-30'
50-60'
Fluor. Int. (% baseline)
500
400
300
200
100
0
ns
*
*
ns
*
ns
tD-DsRed
SEP-GluN2A

Figure 2: Role of GluN2A in saturation of spine structural plasticity.

(A) Image of the soma of a CA1 pyramidal neuron expressing cytosolic GFP and Cre-GFP in organotypic hippocampal slice culture. **(B)** Representative time-lapse images of a spine before and 25 min after HFU stimulation at 0 and 30 minutes. **(C)** Spines trend towards growth (210 ± 34%; $p = 0.25$) in response to HFU_0 but did not have significant growth in response to HFU_{30} (90 ± 25%; $p > 0.99$). **(D)** The change in spine size between HFU_0 and HFU_{30} is significantly different ($p = 0.02$). Scalebar: 2 μm. n = 3 cells/spines; 3 biological replicates. Statistics: significance was determined using a one-way ANOVA with Bonferroni's multiple comparisons test. *p <0.05, **p < 0.01, ***p < 0.001.

Figure 2

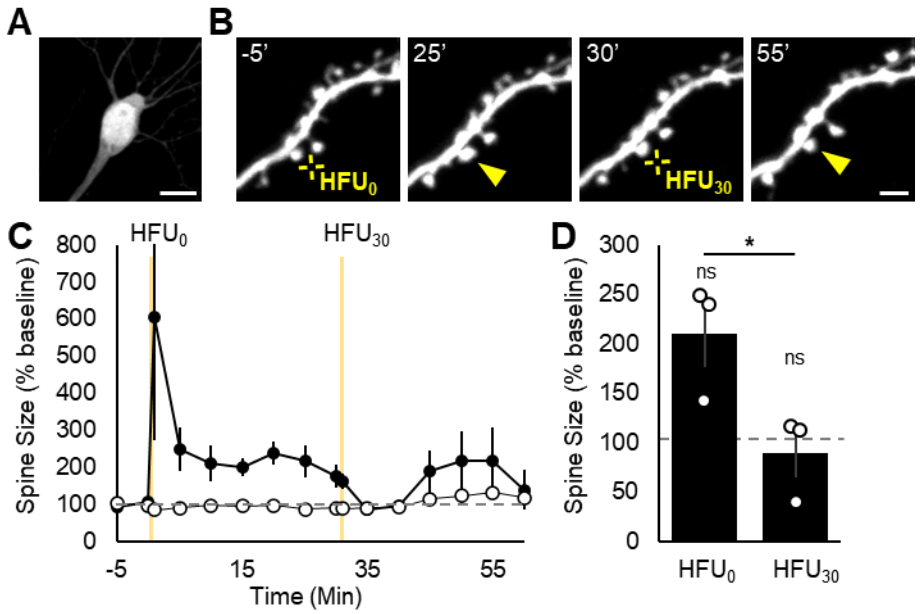
A
B
-5'
25'
30'
55'
HFU0
HFU30
C
HFU0
HFU30
Spine Size (% baseline)
800
700
600
500
400
300
200
100
0
-5
15
35
55
Time (Min)
D
300
250
200
150
100
50
0
ns
ns
*
HFU0
HFU30

Figure 3. Role of $mGluR_5$ in saturation of spine structural plasticity.

(A) Left: Representative time-lapse images of a target spine in vehicle (H_2O) before and after HFU_0 and HFU_{30} (left) and a control spine after HFU_{30} (right). **(B-D)** Target spines (blue circles/bars, n = 3 spines/cells; 3 biological replicates) trend towards growth in response to HFU_0 (190 ± 49%; p = 0.15) but no significant growth in response to HFU_{30} (111 ± 16%; p = 0.54). Control spines (gray circles/bars, n = 3 spine/cells; 3 biological replicates) did not have a significant increase in size in response to HFU_{30} (154 ± 3%; p = 0.15). **(E)** Left: Representative time-lapse images of a target spine in 15 μM MPEP before and after HFU_0 and HFU_{30} (left) and a control spine after HFU_{30} (right). **(F-H)** Target spines (blue circles/bars, n = 3 spines/cells; 2 biological replicates) trend towards growth in response to HFU_0 (205 ± 25%; p = 0.08) but no significant growth in response to HFU_{30} (140 ± 21%; p = 0.75). Control spines (gray circles/bars, n = 3 spine/cells; 2 biological replicates) had a significant increase in size in response to HFU_{30} (226 ± 35%; p = 0.03). Scalebar: 2 μm. Statistics: significance was determined using a two-way ANOVA with Tukey's multiple comparisons test. *p <0.05, **p < 0.01, ***p < 0.001.

Figure 3

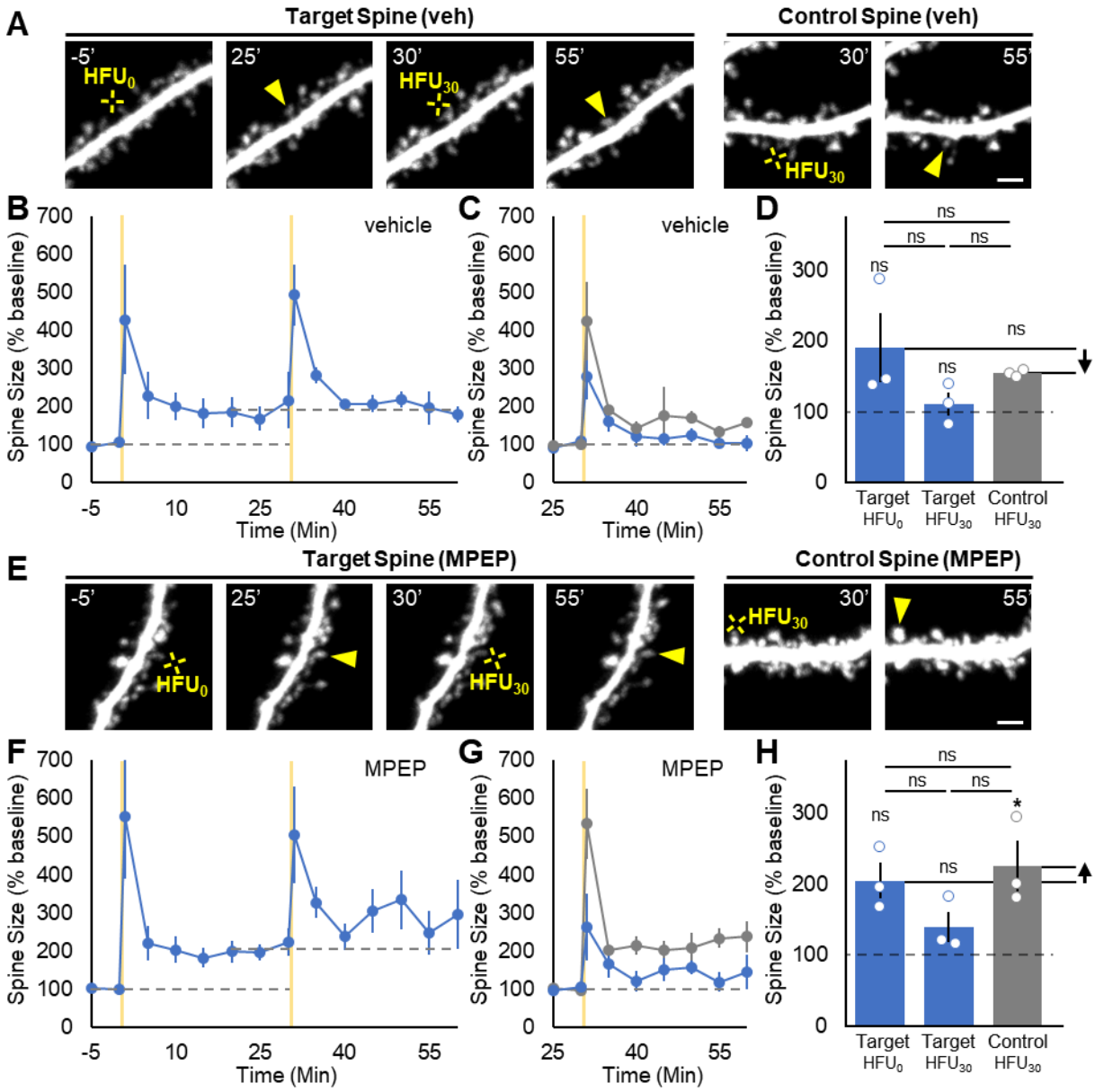
A
Target Spine (veh)
Control Spine (veh)
-5'
HFU0
25'
30'
HFU30
55'
30'
HFU30
55'
B
vehicle
Spine Size (% baseline)
Time (Min)
C
vehicle
Spine Size (% baseline)
Time (Min)
D
ns
Spine Size (% baseline)
Target HFU0
Target HFU30
Control HFU30
E
Target Spine (MPEP)
Control Spine (MPEP)
-5'
HFU0
25'
30'
HFU30
55'
30'
HFU30
55'
F
MPEP
Spine Size (% baseline)
Time (Min)
G
MPEP
Spine Size (% baseline)
Time (Min)
H
ns
*
Spine Size (% baseline)
Target HFU0
Target HFU30
Control HFU30

Figure 4: Time-course of PSD95 enrichment in dendritic spines following the induction of LTP.

(A) Representative time-lapse images of a dendrite of a CA1 pyramidal neuron expressing PSD95-FingR-GFP (green) and DsRedExpress (magenta) in organotypic hippocampal slice cultures after a single HFU stimulus. **(B, E)** Target spines (filled circles) grew in response to HFU stimulus (20-30 min: 191 ± 59%, $p < 0.001$; 50-60 min: 214 ± 82%, $p < 0.001$). **(C, E)** The PSD95-FingR-GFP content was not changed in target spines (filled circles) following HFU (20-30 min: 105 ± 4%, $p = 0.95$; 50-60 min: 99 ± 5%, $p > 0.99$). **(D, F)** The enrichment of PSD95 in target spines was reduced after stimulation and did not recover (20-30 min: 0.67 ± 0.09, $p > 0.99$; 50-60 min: 0.69 ± 0.11, $p > 0.99$). Scalebar: 2 µm. n = 5 spines/cells, 4 biological replicates. Statistics: significance was determined using a two-way ANOVA with Tukey's multiple comparisons test. *$p < 0.05$, **$p < 0.01$, ***$p < 0.001$.

Figure 4

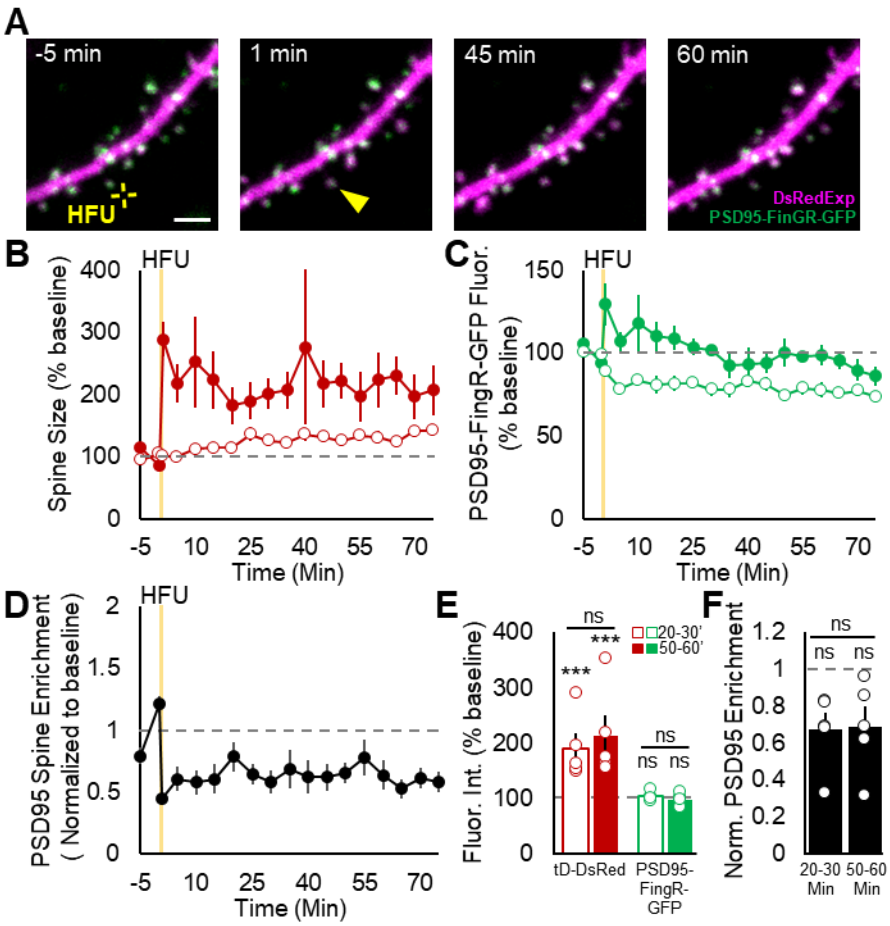
A
-5 min
1 min
45 min
60 min
HFU
DsRedExp
PSD95-FinGR-GFP
B
HFU
Spine Size (% baseline)
400
300
200
100
0
-5 10 25 40 55 70
Time (Min)
C
HFU
PSD95-FingR-GFP Fluor. (% baseline)
150
100
50
0
-5 10 25 40 55 70
Time (Min)
D
HFU
PSD95 Spine Enrichment (Normalized to baseline)
2
1.5
1
0.5
0
-5 10 25 40 55 70
Time (Min)
E
Fluor. Int. (% baseline)
400
300
200
100
0
ns
***
***
20-30'
50-60'
ns
ns ns
tD-DsRed
PSD95-FingR-GFP
F
Norm. PSD95 Enrichment
1.2
1
0.8
0.6
0.4
0.2
0
ns
ns ns
20-30 Min
50-60 Min

Figure 5: Role of PDZ1 and 2 of PSD95 in recovery of plasticity after saturation.

(A) Left: Representative time-lapse images of a target spine in expressing PSD95-AAAA-GFP (green) and DsRedExpress (magenta) before and after HFU_0 and HFU_{45} (left) and a control spine on the same cell after HFU_{45} (right). **(B-D)** Target spines (blue circles/bars, n = 4 spines/cells; 4 biological replicates) grew in response to HFU_0 (189 ± 43%; p = 0.01) but no significant growth in response to HFU_{45} (117 ± 37%; p = 0.55). Control spines (gray circles/bars, n = 4 spine/cells; 4 biological replicates) did not show a significant increase in size in response to HFU_{45} (129 ± 12%; p = 0.32). Scalebar: 2 μm. Statistics: significance was determined using a two-way ANOVA with Bonferroni's multiple comparisons test. *p <0.05, **p < 0.01, ***p < 0.001.

Figure 5

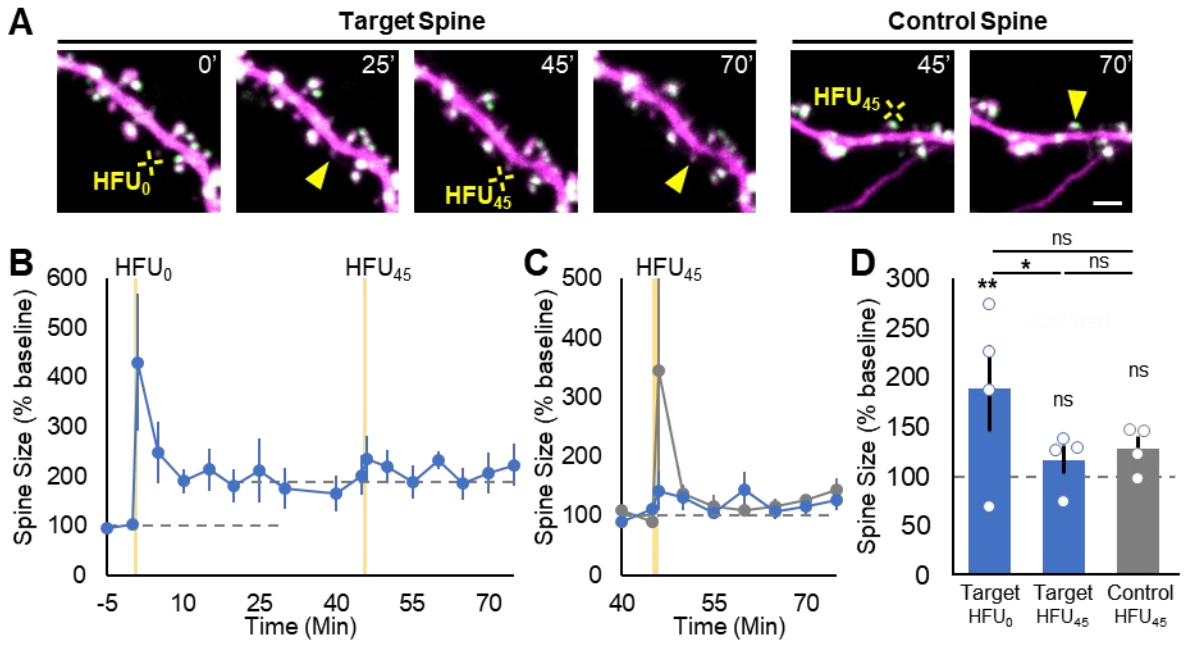
A
Target Spine
Control Spine
0'
25'
45'
70'
45'
70'
HFU0
HFU45
HFU45
B
HFU0
HFU45
Spine Size (% baseline)
Time (Min)
C
HFU45
Spine Size (% baseline)
Time (Min)
D
ns
*
ns
**
ns
ns
Spine Size (% baseline)
Target HFU0
Target HFU45
Control HFU45

Chapter 4: Concluding Remarks

Contributions to the field

It has been known that plasticity can saturate in hippocampal circuits for decades (Frey et al., 1995; Huang et al., 1992). Yet, the mechanisms that underlie saturation and its subsequent release remain ill-defined. In one study, the authors proposed that once a spine becomes saturated, subsequent plasticity in the hippocampus depends on the recruitment of high-threshold synapses to the circuit (Kramar et al., 2012). This would suggest that individual dendritic spines have a one-and-done type of plasticity where upon having undergone LTP, they are unable to potentiate further. My work shows that plasticity is saturated at individual synapses following the induction of LTP. Stimulating individual spines within 45 minutes of an initial LTP-induction does not cause an increase in spine size, despite the fact that of size-matched spines which had not previously undergone structural LTP do increase in size. However, the release from saturation after 60 minutes is observed at the same spines that had been previously stimulated (**Chapter 2**). Thus, LTP can occur again at these synapses, but saturation serves as a refractory period, during which the spines recover their ability to undergo plasticity.

I hypothesized that the saturation we were observing could be due to an increase in the threshold for stimulation to lead to LTP. In fact, It has been shown that HFU-induced spine enlargement is accompanied by the enlargement of the presynaptic bouton (Meyer et al., 2014). It would follow then, that the larger spines may need more stimulation in order to undergo plasticity. This was not the case. I found that when individual dendritic spine synapses are stimulated with a stronger stimulation, they do not undergo normal spine growth during the refractory period. Though some additional spine growth can be observed, this growth is not comparable to that of a spine receiving this stronger stimulus without having been previously

stimulated. This suggests that the saturation of plasticity is not due to a shift in the threshold for plasticity but points to a different mechanism. How then does plasticity saturate?

One interesting hypothesis is that the molecular mechanisms that are responsible for spine growth are limited after having undergone LTP. It is well known that the induction of LTP leads to the alteration of many of the key molecules involved in synaptic plasticity. Such alterations to these proteins could lead to their inability to participate in LTP until they return to their basal states—before the induction of LTP. I showed that in spines that have been previously stimulated, the activity of the key signaling molecule, CaMKII, is reduced. It is unclear whether the reduction of CaMKII activity is due to the inability of CaMKII to activate or if it is because there is a reduction in the Ca^{2+} entering the spine during a second stimulation which is insufficient to drive the same level of CaMKII activation observed in spines that have not previously undergone plasticity. I found that stimulating spines with a stronger stimulus was not sufficient for spines to grow. Though some growth was observed, this grow was significantly reduced compared to that of previously unstimulated spines of the same size. This may suggest that the reduced activation of CaMKII is not dependent on the amount of Ca^{2+}, but rather a different form of CaMKII regulation.

My preliminary results in **Chapter 3** show that the GluN2A subunit of the NMDA receptor may play a role in plasticity at previously stimulated spines. I had originally hypothesized that the reconfiguration of NMDA receptor composition at the synapse could lead to the spines' inability to undergo plasticity. I observed that the GluN2A subunit is increased in stimulated spines but due to low expression, variable response profiles and bleaching of the fluorophore it is unclear if GluN2A leaves the spine within a time frame that is consistent with the end of the refractory period. Additionally, experiments in GluN2A conditional KO animals show that spines still saturate after an initial HFU even in the absence of GluN2A. Intriguingly, these preliminary results show that the GluN2A subunit of the NMDA receptor is not required for the initial

induction of LTP, but it does play some role in the plasticity of spines that have recently undergone plasticity. In fact, the absence of GluN2A caused a transient shrinkage of the saturated spines! I believe this result warrants further investigation into what role GluN2A plays in the plasticity of previously stimulated spines.

Finally, I also show in **Chapter 2** that overexpression of PSD95 was sufficient to drive spine enlargement 45 minutes after an initial HFU. It has been shown that overexpression of PSD95 causes an increase in synaptic AMPA receptor content (Ehrlich & Malinow, 2004). We asked if the shortened refractory period in these conditions may be due to increased AMPA receptor currents. I showed that when AMPA receptor currents are blocked by NBQX there is still a significant increase in spine size at the 45 minute timepoint. I also show that this recovery of plasticity is specific to PSD95, as a comparable overexpression of PSD93, did not have the same effect on the refractory period of saturated spines. In my preliminary studies, I performed time-lapse imaging of endogenous PSD95 (**Chapter 3**), I did not observe the arrival of PSD95 at stimulated spines within 60 minutes, unlike previous studies, which used bleaching corrections to determine the arrival of PSD95 at stimulated spines within 60-80 minutes (Meyer et al., 2014). The lack of an increase in PSD95-FingR-GFP signal in stimulated spines may be due to the intrabody being self-regulating. Shortly, this intrabody is expressed until it binds all endogenous PSD95 and once it is fully bound, it prevents its own expression through the action of its ZF-KRAB domain. Thus, it is unclear if PSD95-FingR-GFP fluorescence can label endogenous PSD95 immediately or if there is a time delay. We could address this caveat by imaging FingR-intrabodies for proteins that are known to rapidly arrive at stimulated spines, like CaMKII. Interestingly, preliminary results in **Chapter 3** suggest that the PDZ1 and PDZ2 domains of PSD95 are required for the earlier recovery of plasticity. Yet, PSD95 does not arrive at dendritic spines within the 60-minute timeframe that I've established as the refractory period for plasticity at individual dendritic spines. It has also been observed that overexpression of

PSD95 causes accumulation of AMPA-type glutamate receptors at synapses (Ehrlich & Malinow, 2004). The observation that PSD95 can aid in the recovery of plasticity, could be due not to the arrival of PSD95 itself, but rather the interaction between PSD95 and other synaptic proteins.

In conclusion, I believe that my experiments have brought the field closer to an answer as to how saturation of plasticity functions. I show that structural plasticity and AMPA receptor insertion can be saturated at individual dendritic spines by the induction of LTP and that these same spines are released from saturation after 60 minutes. My FRET-FLIM data show that saturation occurs by a mechanism that results in the reduction of CaMKII activity in saturated spines. I also show that a stronger stimulus is not sufficient to recover plasticity at saturated spines. Additionally, I elucidated a role for PSD95, but not PSD93, in recovering plasticity at these synapses. Much remains to be done to find the definitive mechanism that underlies the saturation of plasticity. Uncovering these mechanisms will increase our understanding of limitations of synaptic plasticity and their impacts on learning.

Future Directions

I have broadened our understanding of saturation as a refractory period for plasticity, however, the exact mechanisms remain unclear. One key experiment that would help elucidate why spines fail to grow in response to a second LTP stimulus delivered within 45 minutes of potentiation, would be Ca^{2+} imaging. I have shown that CaMKII activation in a saturated spine in response to a second stimulus is lower than the activity induced at size-matched naïve spines. It remains unclear whether this lower activity is due to a reduction in Ca^{2+} influx during the plasticity stimulus, or due to some other regulatory mechanism that feeds back onto CaMKII. If Ca^{2+} influx changes, this could suggest that the intrinsic excitability of the spine has been altered. This could be caused by a number of things. One possibility is that a feedback loop between the NMDA receptor and the SK2 K^{+} channel could lead to this reduction in the amount

of Ca^{2+} (Ngo-Anh et al., 2005). Should Ca^{2+} be unchanged, the reduction in CAMKII activity in saturated spines could be due to the upregulation of endogenous CaMKII inhibitors, such as CaMKII inhibitor 1 (CaMK2N1), which has been shown to be upregulated after the induction of LTP (Astudillo et al., 2020). It would also be interesting to test the sufficiency of CaMKII for plasticity in saturated spines. Can saturated spines grow if CaMKII is activated to the same level that is observed during an initial LTP-inducing stimulus? An enzymatically active photoactivatable CaMKII has been recently developed (Shibata et al., 2021). If identical activation of CaMKII is sufficient to drive plasticity at previously potentiated spines, this would show that saturation of plasticity is, in part, driven by a reduction in CaMKII activity stemming from a regulatory mechanism upstream of CaMKII activation. If activation of CaMKII does dot allow for saturated spines to undergo LTP, this may suggest that CaMKII activity is not sufficient to drive LTP in saturated spines and would point to a mechanism downstream of CaMKII being the limiting factor in the plasticity of previously stimulated spines.

My work has identified PSD95 as a protein with a role in controlling the saturation of plasticity at individual synapses. Yet, a specific role for PSD95 in the recovery of plasticity at dendritic spines remains to be identified. One experiment that might lead to a clearer idea of how PSD95 acts on spines to allow them to recover their plasticity is the overexpression of mutant forms of PSD95. Indeed, we have collected preliminary data which suggest that PDZ1/2 of PSD95 are important for this effect. Beyond this, it would be interesting to observe if either of these two domains are sufficient to recover plasticity on their own. I showed that PSD93, another MAGUK in the PSD95 family, does not recover plasticity in previously stimulated spines. Interestingly, PDZ 1 and 2 of PSD95 interact with the C-terminal region of GluN2A-C, while PSD93's PDZ1 and 2 domains have only been observed to bind GluN2B (Niethammer et al., 1996; Won et al., 2017). The conditional KO of the GluN2A subunit does not appear to be necessary for the induction of LTP in naïve spines, but its absence appears to destabilize potentiated spines in

response to a second stimulation. I believe an interaction between PSD95 and the GluN2A subunit of the NMDA receptor may be important for the ability of dendritic spines to recover their plasticity after they have potentiated.

It is still expected that other molecules which I have not studied are involved in saturation of plasticity. One interesting molecule is striatal-enriched protein tyrosine phosphatase 61 ($STEP_{61}$), a protein phosphatase that has been shown to destabilize NMDA receptors by inducing dephosphorylation of GluN2B on an endocytic motif at Y1472 (Snyder et al., 2005). It has been shown that hippocampus-dependent learning is enhance in $STEP_{61}$ KO mice (Venkitaramani et al., 2011). Intriguingly, PSD95 has been shown to stabilize NMDA receptors at extrasynaptic sites by inducing proteasomal degradation $STEP_{61}$ (Won et al., 2016). Additionally, Won *et al.,* show that knockdown of PSD95 increased the amount of $STEP_{61}$ present in the PSD. It may be possible that PSD95 shortens the refractory period of LTP by keeping $STEP_{61}$ out of the spines.

There is much that remains to be uncovered about the mechanisms that regulate plasticity. In my work I identified some key characteristics and molecules that are involved in the refractory period for LTP. I believe the role of the GluN2A subunit of the NMDA receptor in the recovery of plasticity in saturated spines is intriguing. I also believe that the specific role that PSD95 plays in the recovery of plasticity should also be pursued, whether that role is in the synapse itself or elsewhere in the dendrite.

Saturation of plasticity limits learning and functions as a refractory period. It is possible that the efficacy of spaced learning may involve the saturation of the synapses involved in the learned behavior. Because spaced learning has been shown to improve learning in models of disorders which present with cognitive impairments, understanding saturation of plasticity an important endeavor. It is also possible that saturation is a protective mechanism that prevents living brains from undergoing the catastrophic forgetting that is observed in learning models. Furthering our

understanding of the mechanisms that underlie learning could offer a solution to catastrophic forgetting in learning models and provide therapeutic targets to improve learning in individuals with learning impairments.

Appendix: Role of $mGluR_5$ in mGluR-LTD at small and large spines

Preface

The following appendix contains my unpublished data about the involvement of mGluRs 5 and 1 in mGluR-LTD. It has been shown that mGluRs have a role in the induction of LTD at large spines but not small spines. However, specific group I mGluR that is involved in this type of LTD was not identified. In this appendix, I show that both $mGluR_1$ and $mGluR_5$ may play a role in the LTD of large spines. Dr. Ivar Stein mentored me and provided me with technical guidance as I began to conduct these whole-cell patch experiments.

Introduction

Changes in the strength of synaptic connection in the brain are associated with learning and memory formation. Long-term potentiation (LTP) is an increase in synaptic strength and long-term depression (LTD) is a reduction in synaptic strength. Both LTP and LTD have been associated with learning (Martin et al., 2000). One form of LTD that has been recently identified to be enhanced in fragile X syndrome is mGluR-mediated LTD (Huber et al., 2002; Nakamoto et al., 2007). Interestingly, mGluR-LTD is deficient in $mGluR_5$ KO animals, suggesting that mGluR-LTD is mediated specifically through $mGluR_5$ (Y.-M. Lu et al., 1997). It has been shown through EM that $mGluR_5$ is highly expressed in area CA1 of the hippocampus and it confined to the perisynaptic region of postsynaptic sites (Luján et al., 1996).

It has been shown that mGluR-LTD does not occur at all synapses, but rather at the synapses associated with the large dendritic spines (Holbro et al., 2009; Oh et al., 2013). The results from our lab showed that a low-frequency uncaging (LFU) induced spine shrinkage in spines of all sizes, large spines required mGluR and NMDA receptor activity for shrinkage, while small spines only required NMDA receptor activation. Holbro *et al.*, found that functional depression of synaptic strength at large endoplasmic reticulum (ER)-containing spines only required mGluR activation. While Holbro et al., identified exclusively large ER-containing spines, our data do not distinguish between large spines that contain ER and those that don't. It is possible that spine size and ER content are both factors in the transition from NMDA receptor and mGluR-dependent forms of LTD as they experience activity-dependent increases in size over time. In this appendix, I review my data which show that $mGluR_5$ is required for mGluR-LTD in large dendritic spines. My data also suggests that there may be a role for $mGluR_1$ in mGluR-LTD of large spines.

Methods

Preparation of organotypic hippocampal slice cultures

Cultured hippocampal slices (400 µm) were prepared from P6-P8 Sprague-Dawley rats of both sexes, as described (Stoppini et al., 1991), and as approved by the UC Davis Institutional Animal Care and Use Committee (IACUC).

Measurement of single spine currents

Pyramidal neurons in area CA1 of cultured hippocampal slices (DIV 14-18) were patched with 5-10 MΩ recording pipettes at 25°C in ACSF containing (in mM): 2 CaCl, 1 $MgCl_2$, 0.001 TTX, 0.001 CPP, and 2.5 mM MNI-caged-glutamate. Patch pipettes were filled with a Cs-based internal solution (in mM: 135 Cs-methanesulfonate, 10 HEPES, 10 Na_2-phosphocreatine, 4 $MgCl_2$,4 Na_2-ATP, 0.4 Na-GTP, 3 Na-L-ascorbate, 0.2 Alexa Fluor 488; ~300 mOsm; pH 7.25). Neurons were held at -65 mV and allowed to fill for 10 minutes prior to any stimulation. To record single spine currents, a 720 nM laser was parked ~0.5 µM from the head of the spine and 6 1-ms pulses of ~10 mW were delivered at 0.1 Hz to induce single spine EPSCs (uEPSCs). These responses were averaged together for analysis. uEPSC amplitudes from individual spines were quantified as the average from a 2 ms window centered on the maximum current amplitude within 50 ms following uncaging pulse.

Induction of mGluR LTD and mGluR pharmacology

We used 100 µM DHPG (Tocris) treatment for 5 minutes to induce LTD. We used 15 µM (MPEP (Tocris) to selectively block $mGluR_5$. To selectively inhibit $mGluR_1$, 0.2 µM JNJ-16259685 (Tocris) was used. Slices were incubated in inhibitors for at least 15 minutes before application of DHPG. All drugs were prepared and aliquoted in stock solutions of 1000X. MPEP and DHPG were dissolved in H_2O and JNJ was dissolved in DMSO.

Statistics

All data are represented as mean ± standard error of the mean (SEM). All statistics were calculated across cells using Microsoft Excel. Statistical significance level (α) was set to $p < 0.05$ for all tests. When comparing only two groups, paired or unpaired (as appropriate) Student's t-tests were used.

Results

Role of group I mGluRs in mGluR-LTD of large spines

It has been observed that mGluR-LTD preferentially occurs at large spines (Holbro et al., 2009; Oh et al., 2013). To test the role of the specific group I mGluRs in mGluR-LTD, I induced mGluR-LTD using a 5 minute application of 100 μM DHPG and used the specific inhibitors of $mGluR_1$ and $mGluR_5$ (MPEP and JNJ-16259685, respectively) to measure their contribution to mGluR-LTD at spines of different sizes (**Figure S1A ,B**). I found that in the absence of mGluR inhibitors, a 5 minute application of DHPG induced a depression of spine uEPSCs in large spines (**Figure 1A, B**; $p = 0.013$) but not in small spines ($p = 0.68$) as we had previously shown (Oh et al., 2013). I also found that the DHPG-induced depression of uEPSCs was blocked in large spines when $mGluR_5$ was inhibited (**Figure 1 A, B**; $p = 0.36$). Interestingly, small spines exhibited an LTD trend when $mGluR_5$ was blocked during mGluR-LTD induction (**Figure 1A, B**; $p = 0.11$). Blockade of $mGluR_1$ blocked mGluR-LTD in both large and small spines (**Figure 1A, B**; large spines: $p = 0.78$; small spines: $p = 0.84$). These results suggest that $mGluR_1$ and $mGluR_5$ are both involved in mGluR-LTD at large spines.

Discussion

Our lab had previously found that mGluR-LTD occurs preferentially at large dendritic spine synapses (Oh et al., 2013). Because $mGluR_1$ is not found in Ca1 neurons (Luján et al., 1996), we had hypothesized that mGluR-LTD was driven by $mGluR_5$. Consistent with our lab's previous

results, I found that $mGlur_5$ is required for mGluR-LTD at large dendritic spines (**Figure 1**). Surprisingly, there was a trend for small spines to undergo mGluR-LTD in the presence of the $mGluR_5$ inhibitor, MPEP. My results also show that in the presence of JNJ-16259685, large dendritic spines also failed to undergo mGluR-LTD. Although this is an intriguing result, other data from our lab (unpublished) suggests that while MPEP can block low-frequency uncaging (LFU)-induced large spine shrinkage in the presence of CPP, JNJ-16259685 did not. Furthermore, it has been previously reported that while $mGluR_5$ is present in the pyramidal cells of hippocampal area CA1, $mGluR_{1b/c}$ are primarily found in CA3 neurons and $mGluR_{1a}$ is found in GABAergic neurons (Baude et al., 1993; Luján et al., 1996). This may suggest that application of DHPG in the presence of JNJ-16259685, could be acting to block the mGluR-LTD of large spines by a mechanism that is not specific to the postsynaptic site. The expression of $mGluR_1$ in the CA3 neurons that synapse onto the CA1 neurons used in these experiments could mean that $mGluR_1$ is blocking the induction of mGluR-LTD through a presynaptic mechanism.

It is still unclear if mGluR-LTD is specifically induced by $mGluR_5$. While our previous pharmacological inhibition of group I mGluRs showed that small spines do not undergo DHPG-induced LTD, my results suggest that $mGluR_5$ may also play a role in preventing small spines from undergoing this form of LTD, as blocking this receptor led to a small reduction in the uEPSCs of small spines. It is possible that the dual inhibition of $mGluR_1$ and $mGluR_5$ occluded the effect that blocking $mGluR_5$ alone has on small spines after DHPG treatment. One key control that was not performed and may be a confounding variable in the observed role of $mGluR_1$ in mGluR-LTD, would be a vehicle control for JNJ-16259685. While all other drugs were dissolved in H_2O, JNJ-16259685 was solubilized in DMSO. DMSO has been shown to reduce the currents of both NMDA- and AMPA-type glutamate receptors (C. Lu & Mattson, 2001). The effect of DMSO cannot be ignored, as previous data from our lab has also shown that DMSO

can impair HFU-induced spine growth. If these results show that the lack of mGluR LTD in the presence of $mGluR_1$ inhibitors is not due to DMSO, it would be interesting to test whether $mGluR_1$ blockade prevents LFU induced uEPSC weakening. This could reveal whether my result is due to a divergence between spine shrinkage and synaptic weakening or a result of the different LTD-induction protocols used. Metabotropic glutamate receptor-mediated LTD at large spines requires activation of $mGluR_5$. The role of $mGluR_1$ in this form of LTD remains unclear. Further studies into the role of $mGluR_1$ may clarify explain these results.

Figures and Legends

Figure 1: Role of group I mGluRs in mGluR-LTD of large spines

(A) Representative single spines uEPSCs before and after DHPG treatment. **(B)** DHPG treatment induced LTD in large spines ($p = 0.013$; green dots/bars) but not small spines ($p = 0.68$; red dots/bars) in the vehicle condition. Blockade of $mGluR_5$ with MPEP blocked mGluR-LTD in large spines ($p = 0.36$) and small spines ($p = 0.11$). Blockade of $mGluR_1$ with JNJ-16259685 blocked mGluR-LTD in large spines ($p = 0.78$) and small spines ($p = 0.84$). n-values: vehicle: 7 cells, 7 biological replicates; MPEP: 8 cells, 8 biological replicates; JNJ: 6 cells, 6 biological replicates. Statistics: significance was determined using a paired Student's t-test. *$p < 0.05$, **$p < 0.01$, ***$p < 0.001$.

Figure 1

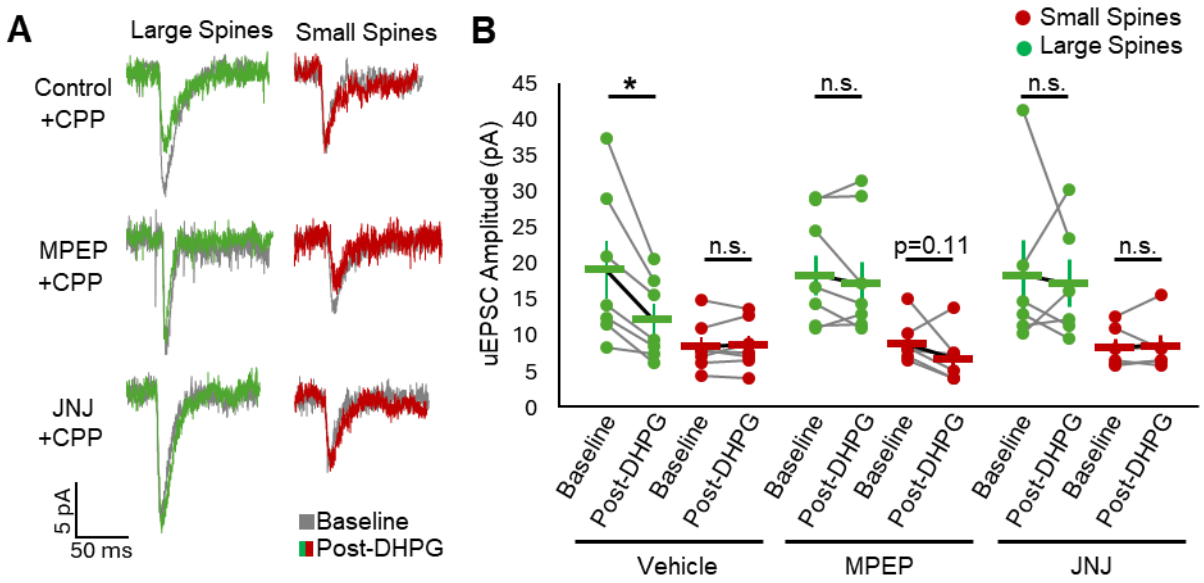
A
Large Spines
Small Spines
Control
+CPP
MPEP
+CPP
JNJ
+CPP
5 pA
50 ms
Baseline
Post-DHPG
B
Small Spines
Large Spines
uEPSC Amplitude (pA)
45
40
35
30
25
20
15
10
5
0
*
n.s.
n.s.
p=0.11
n.s.
n.s.
Baseline
Post-DHPG
Baseline
Post-DHPG
Baseline
Post-DHPG
Baseline
Post-DHPG
Baseline
Post-DHPG
Baseline
Post-DHPG
Vehicle
MPEP
JNJ

Figure S1: Relative sizes of spines used for Figure 1

(A) Relative spine sizes of large and small spines used in each experimental condition. **(B)** Distribution of relative spine sizes of all spines on imaged dendrites. Blue shaded boxes indicate the average relative size of large and small spines ± SE. n-values: vehicle: 7 cells, 7 biological replicates; MPEP: 8 cells, 8 biological replicates; JNJ: 6 cells, 6 biological replicates.

Figure S1

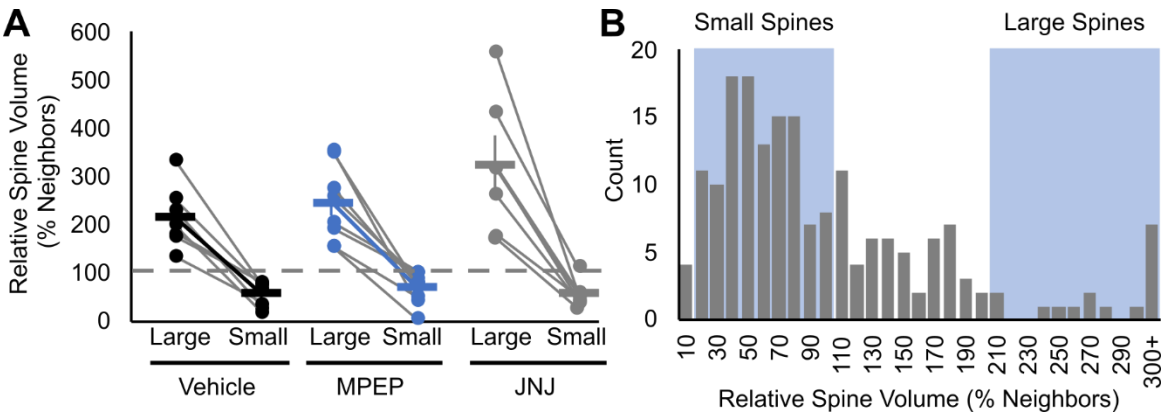
A
Relative Spine Volume (% Neighbors)
600
500
400
300
200
100
0
Large Small
Large Small
Large Small
Vehicle
MPEP
JNJ
B
Small Spines
Large Spines
Count
20
15
10
5
0
10 30 50 70 90 110 130 150 170 190 210 230 250 270 290 300+
Relative Spine Volume (% Neighbors)

References

Abraham, W. C., Jones, O. D., & Glanzman, D. L. (2019). Is plasticity of synapses the mechanism of long-term memory storage? *Npj Science of Learning*, *4*(1), 9. https://doi.org/10.1038/s41539-019-0048-y

Alagarsamy, S., Rouse, S. T., Junge, C., Hubert, G. W., Gutman, D., Smith, Y., & Conn, P. J. (2002). NMDA-induced phosphorylation and regulation of mGluR5. *Pharmacology Biochemistry and Behavior*, *73*(2), 299–306. https://doi.org/10.1016/S0091-3057(02)00826-2

Aow, J., Dore, K., & Malinow, R. (2015). Conformational signaling required for synaptic plasticity by the NMDA receptor complex. *Proceedings of the National Academy of Sciences*, *112*(47), 14711–14716. https://doi.org/10.1073/pnas.1520029112

Argunsah, A. Ö., & Israely, I. (2023). The temporal pattern of synaptic activation determines the longevity of structural plasticity at dendritic spines. *iScience*, *26*(6), 106835. https://doi.org/10.1016/j.isci.2023.106835

Astudillo, D., Karmelic, D., Casas, B. S., Otmakhov, N., Palma, V., & Sanhueza, M. (2020). CaMKII inhibitor 1 (CaMK2N1) mRNA is upregulated following LTP induction in hippocampal slices. *Synapse*. https://doi.org/10.1002/syn.22158

Bailey, C. H., Kandel, E. R., & Harris, K. M. (2015). Structural Components of Synaptic Plasticity and Memory Consolidation. *Cold Spring Harbor Perspectives in Biology*, *7*(7), a021758. https://doi.org/10.1101/cshperspect.a021758

Barcomb, K., Hell, J. W., Benke, T. A., & Bayer, K. U. (2016). The CaMKII/GluN2B Protein Interaction Maintains Synaptic Strength. *Journal of Biological Chemistry*, *291*(31), 16082–16089. https://doi.org/10.1074/jbc.M116.734822

Barnes, C., Jung, M., McNaughton, B., Korol, D., Andreasson, K., & Worley, P. (1994). LTP saturation and spatial learning disruption: Effects of task variables and saturation levels.

The Journal of Neuroscience, *14*(10), 5793–5806. https://doi.org/10.1523/JNEUROSCI.14-10-05793.1994

Barria, A., Derkach, V., & Soderling, T. (1997). Identification of the Ca2+/Calmodulin-dependent Protein Kinase II Regulatory Phosphorylation Site in the α-Amino-3-hydroxyl-5-methyl4-isoxazole-propionate-type Glutamate Receptor. *Journal of Biological Chemistry*, *272*(52), 32727–32730. https://doi.org/10.1074/jbc.272.52.32727

Bartol, T. M., Bromer, C., Kinney, J., Chirillo, M. A., Bourne, J. N., Harris, K. M., & Sejnowski, T. J. (2015). Nanoconnectomic upper bound on the variability of synaptic plasticity. *eLife*, *4*. https://doi.org/10.7554/eLife.10778

Basu, S., & Lamprecht, R. (2018). The Role of Actin Cytoskeleton in Dendritic Spines in the Maintenance of Long-Term Memory. *Frontiers in Molecular Neuroscience*, *11*. https://doi.org/10.3389/fnmol.2018.00143

Baude, A., Roberts, J. D. B., Mulvihill, E., Mcllhinney, R. A. J., & Somogyi, P. (1993). The Metabotropic Glutamate Receptor (mGluRla) Is Concentrated at Perisynaptic Membrane of Neuronal Subpopulations as Dekckd by Immunogold Reaction. *Neuron*, *11*, 771–787. https://doi.org/doi.org/10.1016/0896-6273(93)90086-7

Bayer, K. U., & Schulman, H. (2019). CaM Kinase: Still Inspiring at 40. *Neuron*, *103*(3), 380–394. https://doi.org/10.1016/j.neuron.2019.05.033

Bell, M. E., Bourne, J. N., Chirillo, M. A., Mendenhall, J. M., Kuwajima, M., & Harris, K. M. (2014). Dynamics of nascent and active zone ultrastructure as synapses enlarge during long-term potentiation in mature hippocampus: Nascent and Active Zone Structural Dynamics. *Journal of Comparative Neurology*, *522*(17), 3861–3884. https://doi.org/10.1002/cne.23646

Bellone, C., & Nicoll, R. A. (2007). Rapid Bidirectional Switching of Synaptic NMDA Receptors. *Neuron*, *55*(5), 779–785. https://doi.org/10.1016/j.neuron.2007.07.035

Bliss, T. V. P., & Collingridge, G. L. (1993). A synaptic model of memory: Long-term potentiation in the hippocampus. *Nature*, *361*(6407), 31–39. https://doi.org/10.1038/361031a0

Bliss, T. V. P., & Lømo, T. (1973). Long-lasting potentiation of synaptic transmission in the dentate area of the anaesthetized rabbit following stimulation of the perforant path. *The Journal of Physiology*, *232*(2), 331–356. https://doi.org/10.1113/jphysiol.1973.sp010273

Boettcher, M., Boettcher, J., Mietzsch, S., Krebs, T., Bergholz, R., & Reinshagen, K. (2018). The spaced learning concept significantly improves training for laparoscopic suturing: A pilot randomized controlled study. *Surgical Endoscopy*, *32*(1), 154–159. https://doi.org/10.1007/s00464-017-5650-6

Boros, B. D., Greathouse, K. M., Gentry, E. G., Curtis, K. A., Birchall, E. L., Gearing, M., & Herskowitz, J. H. (2017). Dendritic spines provide cognitive resilience against A lzheimer's disease. *Annals of Neurology*, *82*(4), 602–614. https://doi.org/10.1002/ana.25049

Bortolotto, Z. A., Bashir, Z. I., Davies, C. H., & Collingridge, G. L. (1994). A molecular switch activated by metabotropic glutamate receptors regulates induction of long-term potentiation. *Nature*, *368*(6473), 740–743. https://doi.org/10.1038/368740a0

Bortolotto, Z. A., Collett, V. J., Conquet, F., Jia, Z., van der Putten, H., & Collingridge, G. L. (2005). The regulation of hippocampal LTP by the molecular switch, a form of metaplasticity, requires mGlu5 receptors. *Neuropharmacology*, *49*, 13–25. https://doi.org/10.1016/j.neuropharm.2005.05.020

Bosch, M., Castro, J., Saneyoshi, T., Matsuno, H., Sur, M., & Hayashi, Y. (2014). Structural and Molecular Remodeling of Dendritic Spine Substructures during Long-Term Potentiation. *Neuron*, *82*(2), 444–459. https://doi.org/10.1016/j.neuron.2014.03.021

Bourne, J. N., & Harris, K. M. (2011). Coordination of size and number of excitatory and inhibitory synapses results in a balanced structural plasticity along mature hippocampal

CA1 dendrites during LTP. *Hippocampus*, *21*(4), 354–373. https://doi.org/10.1002/hipo.20768

Bourne, J. N., & Harris, K. M. (2012). Nanoscale analysis of structural synaptic plasticity. *Current Opinion in Neurobiology*, *22*(3), 372–382. https://doi.org/10.1016/j.conb.2011.10.019

Brenman, J. E., Christopherson, K. S., Craven, S. E., McGee, A. W., & Bredt, D. S. (1996). Cloning and Characterization of Postsynaptic Density 93, a Nitric Oxide Synthase Interacting Protein. *The Journal of Neuroscience*, *16*(23), 7407–7415. https://doi.org/10.1523/JNEUROSCI.16-23-07407.1996

Cane, M., Maco, B., Knott, G., & Holtmaat, A. (2014). The Relationship between PSD-95 Clustering and Spine Stability *In Vivo*. *The Journal of Neuroscience*, *34*(6), 2075–2086. https://doi.org/10.1523/JNEUROSCI.3353-13.2014

Cao, G., & Harris, K. M. (2014). Augmenting saturated LTP by broadly spaced episodes of theta-burst stimulation in hippocampal area CA1 of adult rats and mice. *Journal of Neurophysiology*, *112*(8), 1916–1924. https://doi.org/10.1152/jn.00297.2014

Chazeau, A., & Giannone, G. (2016). Organization and dynamics of the actin cytoskeleton during dendritic spine morphological remodeling. *Cellular and Molecular Life Sciences*, *73*(16), 3053–3073. https://doi.org/10.1007/s00018-016-2214-1

Cho, K.-O., Hunt, C. A., & Kennedy, M. B. (1992). The rat brain postsynaptic density fraction contains a homolog of the drosophila discs-large tumor suppressor protein. *Neuron*, *9*(5), 929–942. https://doi.org/10.1016/0896-6273(92)90245-9

Cook, S. G., Buonarati, O. R., Coultrap, S. J., & Bayer, K. U. (2021). CaMKII holoenzyme mechanisms that govern the LTP versus LTD decision. *Science Advances*, *7*(16), eabe2300. https://doi.org/10.1126/sciadv.abe2300

Corkin, S. (1965). Tactually-guided maze learning in man: Effects of unilateral cortical excisions and bilateral hippocampal lesions. *Neuropsychologia*, *3*(4), 339–351. https://doi.org/10.1016/0028-3932(65)90006-0

Coultrap, S. J., Buard, I., Kulbe, J. R., Dell'Acqua, M. L., & Bayer, K. U. (2010). CaMKII Autonomy Is Substrate-dependent and Further Stimulated by Ca^{2+} /Calmodulin. *Journal of Biological Chemistry*, *285*(23), 17930–17937. https://doi.org/10.1074/jbc.M109.069351

De Roo, M., Klauser, P., Mendez, P., Poglia, L., & Muller, D. (2008). Activity-Dependent PSD Formation and Stabilization of Newly Formed Spines in Hippocampal Slice Cultures. *Cerebral Cortex*, *18*(1), 151–161. https://doi.org/10.1093/cercor/bhm041

Derkach, V., Barria, A., & Soderling, T. R. (1999). Ca^{2+} /calmodulin-kinase II enhances channel conductance of α-amino-3-hydroxy-5-methyl-4-isoxazolepropionate type glutamate receptors. *Proceedings of the National Academy of Sciences*, *96*(6), 3269–3274. https://doi.org/10.1073/pnas.96.6.3269

Ehlers, M. D., Heine, M., Groc, L., Lee, M.-C., & Choquet, D. (2007). Diffusional Trapping of GluR1 AMPA Receptors by Input-Specific Synaptic Activity. *Neuron*, *54*(3), 447–460. https://doi.org/10.1016/j.neuron.2007.04.010

Ehrlich, I., Klein, M., Rumpel, S., & Malinow, R. (2007). PSD-95 is required for activity-driven synapse stabilization. *Proceedings of the National Academy of Sciences*, *104*(10), 4176–4181. https://doi.org/10.1073/pnas.0609307104

Ehrlich, I., & Malinow, R. (2004). Postsynaptic Density 95 controls AMPA Receptor Incorporation during Long-Term Potentiation and Experience-Driven Synaptic Plasticity. *The Journal of Neuroscience*, *24*(4), 916–927. https://doi.org/10.1523/JNEUROSCI.4733-03.2004

El-Hassar, L., Hagenston, A. M., D'Angelo, L. B., & Yeckel, M. F. (2011). Metabotropic glutamate receptors regulate hippocampal CA1 pyramidal neuron excitability via Ca^{2+} wave-dependent activation of SK and TRPC channels: cAMP regulates mGluR and Ca^{2+}

wave-mediated TRPC depolarization. *The Journal of Physiology*, *589*(13), 3211–3229. https://doi.org/10.1113/jphysiol.2011.209783

Favaro, P. D., Huang, X., Hosang, L., Stodieck, S., Cui, L., Liu, Y., Engelhardt, K.-A., Schmitz, F., Dong, Y., Löwel, S., & Schlüter, O. M. (2018). An opposing function of paralogs in balancing developmental synapse maturation. *PLOS Biology*, *16*(12), e2006838. https://doi.org/10.1371/journal.pbio.2006838

Frey, U., Krug, M., Reymann, K. G., & Matthies, H. (1988). Anisomycin, an inhibitor of protein synthesis, blocks late phases of LTP phenomena in the hippocampal CA1 region in vitro. *Brain Research*, *452*(1–2), 57–65. https://doi.org/10.1016/0006-8993(88)90008-X

Frey, U., Schollmeier, K., Reymann, K. G., & Seidenbecher, T. (1995). Asymptotic hippocampal long-term potentiation in rats does not preclude additional potentiation at later phases. *Neuroscience*, *67*(4), 799–807. https://doi.org/10.1016/0306-4522(95)00117-2

Fu, M., Yu, X., Lu, J., & Zuo, Y. (2012). Repetitive motor learning induces coordinated formation of clustered dendritic spines in vivo. *Nature*, *483*(7387), 92–95. https://doi.org/10.1038/nature10844

Fusi, S., Drew, P. J., & Abbott, L. F. (2005). Cascade Models of Synaptically Stored Memories. *Neuron*, *45*(4), 599–611. https://doi.org/10.1016/j.neuron.2005.02.001

Glas, A., Hübener, M., Bonhoeffer, T., & Goltstein, P. M. (2021). Spaced training enhances memory and prefrontal ensemble stability in mice. *Current Biology*, *31*(18), 4052-4061.e6. https://doi.org/10.1016/j.cub.2021.06.085

Gray, E. G. (1959a). AXO-SOMATIC AND AXO-DENDRITIC SYNAPSES OF THE CEREBRAL CORTEX: AN ELECTRON MICROSCOPE STUDY. *Journal of Anatomy*, *93*(4), 420–433.

Gray, E. G. (1959b). Electron Microscopy of Synaptic Contacts on Dendrite Spines of the Cerebral Cortex. *Nature*, *183*(4675), 1592–1593. https://doi.org/10.1038/1831592a0

Gray, J. A., Shi, Y., Usui, H., During, M. J., Sakimura, K., & Nicoll, R. A. (2011). Distinct Modes of AMPA Receptor Suppression at Developing Synapses by GluN2A and GluN2B:

Single-Cell NMDA Receptor Subunit Deletion In Vivo. *Neuron*, *71*(6), 1085–1101. https://doi.org/10.1016/j.neuron.2011.08.007

Gray, N. W., Weimer, R. M., Bureau, I., & Svoboda, K. (2006). Rapid Redistribution of Synaptic PSD-95 in the Neocortex In Vivo. *PLoS Biology*, *4*(11), e370. https://doi.org/10.1371/journal.pbio.0040370

Gross, G. G., Junge, J. A., Mora, R. J., Kwon, H.-B., Olson, C. A., Takahashi, T. T., Liman, E. R., Ellis-Davies, G. C. R., McGee, A. W., Sabatini, B. L., Roberts, R. W., & Arnold, D. B. (2013). Recombinant Probes for Visualizing Endogenous Synaptic Proteins in Living Neurons. *Neuron*, *78*(6), 971–985. https://doi.org/10.1016/j.neuron.2013.04.017

Grutzendler, J., Kasthuri, N., & Gan, W.-B. (2002). Long-term dendritic spine stability in the adult cortex. *Nature*, *420*(6917), 812–816. https://doi.org/10.1038/nature01276

Harris, K. M., Jensen, F. E., & Tsao, B. (1992). Three-dimensional structure of dendritic spines and synapses in rat hippocampus (CA1) at postnatal day 15 and adult ages: Implications for the maturation of synaptic physiology and long-term potentiation. *The Journal of Neuroscience*, *12*(9), 2685–2705.

Harris, K. M., & Stevens, J. K. (1989). Dendritic spines of CA 1 pyramidal cells in the rat hippocampus: Serial electron microscopy with reference to their biophysical characteristics. *The Journal of Neuroscience*, *9*(8), 2982–2997. https://doi.org/10.1523/JNEUROSCI.09-08-02982.1989

Harris, K., & Stevens, J. (1988). Dendritic spines of rat cerebellar Purkinje cells: Serial electron microscopy with reference to their biophysical characteristics. *The Journal of Neuroscience*, *8*(12), 4455–4469. https://doi.org/10.1523/JNEUROSCI.08-12-04455.1988

Harvey, C. D., & Svoboda, K. (2007). Locally dynamic synaptic learning rules in pyramidal neuron dendrites. *Nature*, *450*(7173), 1195–1200. https://doi.org/10.1038/nature06416

Hayashi, Y. (2022). Molecular mechanism of hippocampal long-term potentiation – Towards multiscale understanding of learning and memory. *Neuroscience Research*, *175*, 3–15. https://doi.org/10.1016/j.neures.2021.08.001

Hayashi, Y., Shi, S.-H., Esteban, J. A., Piccini, A., Poncer, J.-C., & Malinow, R. (2000). Driving AMPA Receptors into Synapses by LTP and CaMKII: Requirement for GluR1 and PDZ Domain Interaction. *Science*, *287*(5461), 2262–2267. https://doi.org/10.1126/science.287.5461.2262

Hayashi-Takagi, A., Yagishita, S., Nakamura, M., Shirai, F., Wu, Y. I., Loshbaugh, A. L., Kuhlman, B., Hahn, K. M., & Kasai, H. (2015). Labelling and optical erasure of synaptic memory traces in the motor cortex. *Nature*, *525*(7569), 333–338. https://doi.org/10.1038/nature15257

Hell, J. W. (2014). CaMKII: Claiming Center Stage in Postsynaptic Function and Organization. *Neuron*, *81*(2), 249–265. https://doi.org/10.1016/j.neuron.2013.12.024

Hill, T. C., & Zito, K. (2013). LTP-Induced Long-Term Stabilization of Individual Nascent Dendritic Spines. *Journal of Neuroscience*, *33*(2), 678–686. https://doi.org/10.1523/JNEUROSCI.1404-12.2013

Hofer, S. B., Mrsic-Flogel, T. D., Bonhoeffer, T., & Hübener, M. (2006). Prior experience enhances plasticity in adult visual cortex. *Nature Neuroscience*, *9*(1), 127–132. https://doi.org/10.1038/nn1610

Hofer, S. B., Mrsic-Flogel, T. D., Bonhoeffer, T., & Hübener, M. (2009). Experience leaves a lasting structural trace in cortical circuits. *Nature*, *457*(7227), 313–317. https://doi.org/10.1038/nature07487

Holbro, N., Grunditz, Å., & Oertner, T. G. (2009). Differential distribution of endoplasmic reticulum controls metabotropic signaling and plasticity at hippocampal synapses. *Proceedings of the National Academy of Sciences*, *106*(35), 15055–15060. https://doi.org/10.1073/pnas.0905110106

Hollmann, M., Hartley, M., & Heinemann, S. (1991). Ca2+ Permeability of KA-AMPA-Gated Glutamate Receptor Channels Depends on Subunit Composition. *Science*, *252*(5007), 851. Materials Science & Engineering Collection; Natural Science Collection.

Holtmaat, A. J. G. D., Trachtenberg, J. T., Wilbrecht, L., Shepherd, G. M., Zhang, X., Knott, G. W., & Svoboda, K. (2005). Transient and Persistent Dendritic Spines in the Neocortex In Vivo. *Neuron*, *45*(2), 279–291. https://doi.org/10.1016/j.neuron.2005.01.003

Honkura, N., Matsuzaki, M., Noguchi, J., Ellis-Davies, G. C. R., & Kasai, H. (2008). The Subspine Organization of Actin Fibers Regulates the Structure and Plasticity of Dendritic Spines. *Neuron*, *57*(5), 719–729. https://doi.org/10.1016/j.neuron.2008.01.013

Huang, Y., Colino, A., Selig, D., & Malenka, R. (1992). The influence of prior synaptic activity on the induction of long-term potentiation. *Science*, *255*(5045), 730–733. https://doi.org/10.1126/science.1346729

Huber, K. M., Gallagher, S. M., Warren, S. T., & Bear, M. F. (2002). Altered synaptic plasticity in a mouse model of fragile X mental retardation. *Proceedings of the National Academy of Sciences*, *99*(11), 7746–7750. https://doi.org/10.1073/pnas.122205699

Hutsler, J. J., & Zhang, H. (2010). Increased dendritic spine densities on cortical projection neurons in autism spectrum disorders. *Brain Research*, *1309*, 83–94. https://doi.org/10.1016/j.brainres.2009.09.120

Kasai, H., Ucar, H., Morimoto, Y., Eto, F., & Okazaki, H. (2023). Mechanical transmission at spine synapses: Short-term potentiation and working memory. *Current Opinion in Neurobiology*, *80*, 102706. https://doi.org/10.1016/j.conb.2023.102706

Kellermayer, B., Ferreira, J. S., Dupuis, J., Levet, F., Grillo-Bosch, D., Bard, L., Linarès-Loyez, J., Bouchet, D., Choquet, D., Rusakov, D. A., Bon, P., Sibarita, J.-B., Cognet, L., Sainlos, M., Carvalho, A. L., & Groc, L. (2018). Differential Nanoscale Topography and Functional Role of GluN2-NMDA Receptor Subtypes at Glutamatergic Synapses. *Neuron*, *100*(1), 106-119.e7. https://doi.org/10.1016/j.neuron.2018.09.012

Kelley, P., & Whatson, T. (2013). Making long-term memories in minutes: A spaced learning pattern from memory research in education. *Frontiers in Human Neuroscience*, *7*. https://doi.org/10.3389/fnhum.2013.00589

Kennedy, M. B. (1997). The postsynaptic density at glutamatergic synapses. *Trends in Neurosciences*, *20*(6), 264–268. https://doi.org/10.1016/S0166-2236(96)01033-8

Kleinjan, M. S., Buchta, W. C., Ogelman, R., Hwang, I.-W., Kuwajima, M., Hubbard, D. D., Kareemo, D. J., Prikhodko, O., Olah, S. L., Gomez Wulschner, L. E., Abraham, W. C., Franco, S. J., Harris, K. M., Oh, W. C., & Kennedy, M. J. (2023). Dually innervated dendritic spines develop in the absence of excitatory activity and resist plasticity through tonic inhibitory crosstalk. *Neuron*, *111*(3), 362-371.e6. https://doi.org/10.1016/j.neuron.2022.11.002

Kopec, C. D., Li, B., Wei, W., Jannic, B., & Roberto, M. (2006). Glutamate Receptor Exocytosis and Spine Enlargement during Chemically Induced Long-Term Potentiation. *Journal of Neuroscience*, *26*(7), 2000–2009. https://doi.org/10.1523/JNEUROSCI.3918-05.2006

Kopec, C. D., Real, E., Kessels, H. W., & Malinow, R. (2007). GluR1 Links Structural and Functional Plasticity at Excitatory Synapses. *Journal of Neuroscience*, *27*(50), 13706–13718. https://doi.org/10.1523/JNEUROSCI.3503-07.2007

Kornau, H.-C., Schenker, L. T., Kennedy, M. B., & Seeburg, P. H. (1995). Domain Interaction Between NMDA Receptor Subunits and the Postsynaptic Density Protein PSD-95. *Science*, *269*(5231), 1737–1740. https://doi.org/10.1126/science.7569905

Kramar, E. A., Babayan, A. H., Gavin, C. F., Cox, C. D., Jafari, M., Gall, C. M., Rumbaugh, G., & Lynch, G. (2012). Synaptic evidence for the efficacy of spaced learning. *Proceedings of the National Academy of Sciences*, *109*(13), 5121–5126. https://doi.org/10.1073/pnas.1120700109

Kudithipudi, D., Aguilar-Simon, M., Babb, J., Bazhenov, M., Blackiston, D., Bongard, J., Brna, A. P., Chakravarthi Raja, S., Cheney, N., Clune, J., Daram, A., Fusi, S., Helfer, P., Kay, L.,

Ketz, N., Kira, Z., Kolouri, S., Krichmar, J. L., Kriegman, S., … Siegelmann, H. (2022). Biological underpinnings for lifelong learning machines. *Nature Machine Intelligence*, *4*(3), 196–210. https://doi.org/10.1038/s42256-022-00452-0

Lambert, J. T., Hill, T. C., Park, D. K., Culp, J. H., & Zito, K. (2017). Protracted and asynchronous accumulation of PSD95-family MAGUKs during maturation of nascent dendritic spines: Accumulation of PSD-MAGUKs in New Spines. *Developmental Neurobiology*, *77*(10), 1161–1174. https://doi.org/10.1002/dneu.22503

Lauterborn, J. C., Schultz, M. N., Le, A. A., Amani, M., Friedman, A. E., Leach, P. T., Gall, C. M., Lynch, G. S., & Crawley, J. N. (2019). Spaced training improves learning in Ts65Dn and Ube3a mouse models of intellectual disabilities. *Translational Psychiatry*, *9*(1), 166. https://doi.org/10.1038/s41398-019-0495-5

Lee, M.-C., Yasuda, R., & Ehlers, M. D. (2010). Metaplasticity at Single Glutamatergic Synapses. *Neuron*, *66*(6), 859–870. https://doi.org/10.1016/j.neuron.2010.05.015

Lee, S.-J. R., Escobedo-Lozoya, Y., Szatmari, E. M., & Yasuda, R. (2009). Activation of CaMKII in single dendritic spines during long-term potentiation. *Nature*, *458*(7236), 299–304. https://doi.org/10.1038/nature07842

Lendvai, B., Stern, E. A., Chen, B., & Svoboda, K. (2000). Experience-dependent plasticity of dendritic spines in the developing rat barrel cortex in vivo. *Nature*, *404*(6780), 876–881. https://doi.org/10.1038/35009107

Lu, C., & Mattson, M. P. (2001). Dimethyl Sulfoxide Suppresses NMDA- and AMPA-Induced Ion Currents and Calcium Influx and Protects against Excitotoxic Death in Hippocampal Neurons. *Experimental Neurology*, *170*(1), 180–185. https://doi.org/10.1006/exnr.2001.7686

Lu, Y.-M., Jia, Z., Janus, C., Henderson, J. T., Gerlai, R., Wojtowicz, J. M., & Roder, J. C. (1997). Mice Lacking Metabotropic Glutamate Receptor 5 Show Impaired Learning and Reduced CA1 Long-Term Potentiation (LTP) But Normal CA3 LTP. *The Journal of*

Neuroscience, *17*(13), 5196–5205. https://doi.org/10.1523/JNEUROSCI.17-13-05196.1997

Luján, R., Nusser, Z., Roberts, J. D. B., Shigemoto, R., & Somogyi, P. (1996). Perisynaptic Location of Metabotropic Glutamate Receptors mGluR1 and mGluR5 on Dendrites and Dendritic Spines in the Rat Hippocampus. *European Journal of Neuroscience*, *8*(7), 1488–1500. https://doi.org/10.1111/j.1460-9568.1996.tb01611.x

Lynch, G., Kramár, E. A., Babayan, A. H., Rumbaugh, G., & Gall, C. M. (2013). Differences between synaptic plasticity thresholds result in new timing rules for maximizing long-term potentiation. *Neuropharmacology*, *64*, 27–36. https://doi.org/10.1016/j.neuropharm.2012.07.006

Magee, J. C., & Grienberger, C. (2020). Synaptic Plasticity Forms and Functions. *Annual Review of Neuroscience*, *43*(1), 95–117. https://doi.org/10.1146/annurev-neuro-090919-022842

Mammen, A. L., Kameyama, K., Roche, K. W., & Huganir, R. L. (1997). Phosphorylation of the α-Amino-3-hydroxy-5-methylisoxazole4-propionic Acid Receptor GluR1 Subunit by Calcium/ Calmodulin-dependent Kinase II. *Journal of Biological Chemistry*, *272*(51), 32528–32533. https://doi.org/10.1074/jbc.272.51.32528

Martin, S. J., Grimwood, P. D., & Morris, R. G. M. (2000). Synaptic Plasticity and Memory: An Evaluation of the Hypothesis. *Annual Review of Neuroscience*, *23*(1), 649–711. https://doi.org/10.1146/annurev.neuro.23.1.649

Matsuzaki, M., Ellis-Davies, G. C. R., Nemoto, T., Miyashita, Y., Iino, M., & Kasai, H. (2001). Dendritic spine geometry is critical for AMPA receptor expression in hippocampal CA1 pyramidal neurons. *Nature Neuroscience*, *4*(11), 1086–1092. https://doi.org/10.1038/nn736

Matsuzaki, M., Honkura, N., Ellis-Davies, G. C. R., & Kasai, H. (2004). Structural basis of long-term potentiation in single dendritic spines. *Nature*, *429*(6993), 761–766. https://doi.org/10.1038/nature02617

Matus, A. (2000). Actin-Based Plasticity in Dendritic Spines. *Science*, *290*(5492), 754–758. https://doi.org/10.1126/science.290.5492.754

Meyer, D., Bonhoeffer, T., & Scheuss, V. (2014). Balance and Stability of Synaptic Structures during Synaptic Plasticity. *Neuron*, *82*(2), 430–443. https://doi.org/10.1016/j.neuron.2014.02.031

Miesenböck, G., De Angelis, D. A., & Rothman, J. E. (1998). Visualizing secretion and synaptic transmission with pH-sensitive green fluorescent proteins. *Nature*, *394*(6689), 192–195. https://doi.org/10.1038/28190

Milner, B., Corkin, S., & Teuber, H.-L. (1968). Further analysis of the hippocampal amnesic syndrome: 14-year follow-up study of H.M. *Neuropsychologia*, *6*(3), 215–234. https://doi.org/10.1016/0028-3932(68)90021-3

Mongillo, G., Rumpel, S., & Loewenstein, Y. (2017). Intrinsic volatility of synaptic connections—A challenge to the synaptic trace theory of memory. *Current Opinion in Neurobiology*, *46*, 7–13. https://doi.org/10.1016/j.conb.2017.06.006

Moser, E. I. (1998). Impaired Spatial Learning after Saturation of Long-Term Potentiation. *Science*, *281*(5385), 2038–2042. https://doi.org/10.1126/science.281.5385.2038

Murakoshi, H., Wang, H., & Yasuda, R. (2011). Local, persistent activation of Rho GTPases during plasticity of single dendritic spines. *Nature*, *472*(7341), 100–104. https://doi.org/10.1038/nature09823

Nabavi, S., Kessels, H. W., Alfonso, S., Aow, J., Fox, R., & Malinow, R. (2013). Metabotropic NMDA receptor function is required for NMDA receptor-dependent long-term depression. *Proceedings of the National Academy of Sciences*, *110*(10), 4027–4032. https://doi.org/10.1073/pnas.1219454110

Nakahata, Y., & Yasuda, R. (2018). Plasticity of Spine Structure: Local Signaling, Translation and Cytoskeletal Reorganization. *Frontiers in Synaptic Neuroscience*, *10*, 29. https://doi.org/10.3389/fnsyn.2018.00029

Nakamoto, M., Nalavadi, V., Epstein, M. P., Narayanan, U., Bassell, G. J., & Warren, S. T. (2007). Fragile X mental retardation protein deficiency leads to excessive mGluR5-dependent internalization of AMPA receptors. *Proceedings of the National Academy of Sciences*, *104*(39), 15537–15542. https://doi.org/10.1073/pnas.0707484104

Ngo-Anh, T. J., Bloodgood, B. L., Lin, M., Sabatini, B. L., Maylie, J., & Adelman, J. P. (2005). SK channels and NMDA receptors form a Ca2+-mediated feedback loop in dendritic spines. *Nature Neuroscience*, *8*(5), 642–649. https://doi.org/10.1038/nn1449

Niethammer, M., Kim, E., & Sheng, M. (1996). Interaction between the C terminus of NMDA receptor subunits and multiple members of the PSD-95 family of membrane-associated guanylate kinases. *The Journal of Neuroscience*, *16*(7), 2157–2163. https://doi.org/10.1523/JNEUROSCI.16-07-02157.1996

Nishiyama, J., & Yasuda, R. (2015). Biochemical Computation for Spine Structural Plasticity. *Neuron*, *87*(1), 63–75. https://doi.org/10.1016/j.neuron.2015.05.043

Niswender, C. M., & Conn, P. J. (2010). Metabotropic Glutamate Receptors: Physiology, Pharmacology, and Disease. *Annual Review of Pharmacology and Toxicology*, *50*(1), 295–322. https://doi.org/10.1146/annurev.pharmtox.011008.145533

Oh, W. C., Hill, T. C., & Zito, K. (2013). Synapse-specific and size-dependent mechanisms of spine structural plasticity accompanying synaptic weakening. *Proceedings of the National Academy of Sciences*, *110*(4), E305–E312. https://doi.org/10.1073/pnas.1214705110

Oh, W. C., Parajuli, L. K., & Zito, K. (2015). Heterosynaptic Structural Plasticity on Local Dendritic Segments of Hippocampal CA1 Neurons. *Cell Reports*, *10*(2), 162–169. https://doi.org/10.1016/j.celrep.2014.12.016

Okabe, S., Miwa, A., & Okado, H. (2001). Spine Formation and Correlated Assembly of Presynaptic and Postsynaptic Molecules. *The Journal of Neuroscience*, *21*(16), 6105–6114. https://doi.org/10.1523/JNEUROSCI.21-16-06105.2001

Opazo, P., Labrecque, S., Tigaret, C. M., Frouin, A., Wiseman, P. W., De Koninck, P., & Choquet, D. (2010). CaMKII Triggers the Diffusional Trapping of Surface AMPARs through Phosphorylation of Stargazin. *Neuron*, *67*(2), 239–252. https://doi.org/10.1016/j.neuron.2010.06.007

Ottersen, O. P., & Landsend, A. S. (1997). Organization of Glutamate Receptors at the Synapse. *European Journal of Neuroscience*, *9*(11), 2219–2224. https://doi.org/10.1111/j.1460-9568.1997.tb01640.x

Paoletti, P., Bellone, C., & Zhou, Q. (2013). NMDA receptor subunit diversity: Impact on receptor properties, synaptic plasticity and disease. *Nature Reviews Neuroscience*, *14*(6), 383–400. https://doi.org/10.1038/nrn3504

Parvez, S., Ramachandran, B., & Frey, J. U. (2010). Properties of subsequent induction of long-term potentiation and/or depression in one synaptic input in apical dendrites of hippocampal CA1 neurons in vitro. *Neuroscience*, *171*(3), 712–720. https://doi.org/10.1016/j.neuroscience.2010.09.018

Penzes, P., Cahill, M. E., Jones, K. A., VanLeeuwen, J.-E., & Woolfrey, K. M. (2011). Dendritic spine pathology in neuropsychiatric disorders. *Nature Neuroscience*, *14*(3), 285–293. https://doi.org/10.1038/nn.2741

Perez-Alvarez, A., Yin, S., Schulze, C., Hammer, J. A., Wagner, W., & Oertner, T. G. (2020). Endoplasmic reticulum visits highly active spines and prevents runaway potentiation of synapses. *Nature Communications*, *11*(1), 5083. https://doi.org/10.1038/s41467-020-18889-5

Petersen, C. C. H., Malenka, R. C., Nicoll, R. A., & Hopfield, J. J. (1998). All-or-none potentiation at CA3-CA1 synapses. *Proceedings of the National Academy of Sciences*, *95*(8), 4732–4737. https://doi.org/10.1073/pnas.95.8.4732

Plant, K., Pelkey, K. A., Bortolotto, Z. A., Morita, D., Terashima, A., McBain, C. J., Collingridge, G. L., & Isaac, J. T. R. (2006). Transient incorporation of native GluR2-lacking AMPA receptors during hippocampal long-term potentiation. *Nature Neuroscience*, *9*(5), 602–604. https://doi.org/10.1038/nn1678

Pologruto, T. A., Sabatini, B. L., & Svoboda, K. (2003). ScanImage: Flexible software for operating laser scanning microscopes. *BioMedical Engineering OnLine*, *2*(1), 13. https://doi.org/10.1186/1475-925X-2-13

Rosoklija, G., Toomayan, G., Ellis, S. P., Keilp, J., Mann, J. J., Latov, N., Hays, A. P., & Dwork, A. J. (2000). Structural Abnormalities of Subicular Dendrites in Subjects With Schizophrenia and Mood Disorders: Preliminary Findings. *Archives of General Psychiatry*, *57*(4), 349. https://doi.org/10.1001/archpsyc.57.4.349

Sans, N., Petralia, R. S., Wang, Y.-X., Blahos, J., Hell, J. W., & Wenthold, R. J. (2000). A Developmental Change in NMDA Receptor-Associated Proteins at Hippocampal Synapses. *The Journal of Neuroscience*, *20*(3), 1260–1271. https://doi.org/10.1523/JNEUROSCI.20-03-01260.2000

Sanz-Clemente, A., Matta, J. A., Isaac, J. T. R., & Roche, K. W. (2010). Casein Kinase 2 Regulates the NR2 Subunit Composition of Synaptic NMDA Receptors. *Neuron*, *67*(6), 984–996. https://doi.org/10.1016/j.neuron.2010.08.011

Scheefhals, N., & MacGillavry, H. D. (2018). Functional organization of postsynaptic glutamate receptors. *Molecular and Cellular Neuroscience*, *91*, 82–94. https://doi.org/10.1016/j.mcn.2018.05.002

Schnell, E., Sizemore, M., Karimzadegan, S., Chen, L., Bredt, D. S., & Nicoll, R. A. (2002). Direct interactions between PSD-95 and stargazin control synaptic AMPA receptor

number. *Proceedings of the National Academy of Sciences*, *99*(21), 13902–13907. https://doi.org/10.1073/pnas.172511199

Scoville, W. B., & Milner, B. (1957). LOSS OF RECENT MEMORY AFTER BILATERAL HIPPOCAMPAL LESIONS. *Journal of Neurology, Neurosurgery & Psychiatry*, *20*(1), 11–21. https://doi.org/10.1136/jnnp.20.1.11

Seese, R. R., Wang, K., Yao, Y. Q., Lynch, G., & Gall, C. M. (2014). Spaced training rescues memory and ERK1/2 signaling in fragile X syndrome model mice. *Proceedings of the National Academy of Sciences*, *111*(47), 16907–16912. https://doi.org/10.1073/pnas.1413335111

Shibata, A. C. E., Ueda, H. H., Eto, K., Onda, M., Sato, A., Ohba, T., Nabekura, J., & Murakoshi, H. (2021). Photoactivatable CaMKII induces synaptic plasticity in single synapses. *Nature Communications*, *12*(1), 751. https://doi.org/10.1038/s41467-021-21025-6

Smolen, P., Zhang, Y., & Byrne, J. H. (2016). The right time to learn: Mechanisms and optimization of spaced learning. *Nature Reviews Neuroscience*, *17*(2), 77–88. https://doi.org/10.1038/nrn.2015.18

Snyder, E. M., Nong, Y., Almeida, C. G., Paul, S., Moran, T., Choi, E. Y., Nairn, A. C., Salter, M. W., Lombroso, P. J., Gouras, G. K., & Greengard, P. (2005). Regulation of NMDA receptor trafficking by amyloid-β. *Nature Neuroscience*, *8*(8), 1051–1058. https://doi.org/10.1038/nn1503

Sobczyk, A., & Svoboda, K. (2007). Activity-Dependent Plasticity of the NMDA-Receptor Fractional Ca2+ Current. *Neuron*, *53*(1), 17–24. https://doi.org/10.1016/j.neuron.2006.11.016

Stein, I. S., Gray, J. A., & Zito, K. (2015). Non-Ionotropic NMDA Receptor Signaling Drives Activity-Induced Dendritic Spine Shrinkage. *Journal of Neuroscience*, *35*(35), 12303–12308. https://doi.org/10.1523/JNEUROSCI.4289-14.2015

Stein, I. S., Park, D. K., Flores, J. C., Jahncke, J. N., & Zito, K. (2020). Molecular Mechanisms of Non-ionotropic NMDA Receptor Signaling in Dendritic Spine Shrinkage. *The Journal of Neuroscience*, *40*(19), 3741–3750. https://doi.org/10.1523/JNEUROSCI.0046-20.2020

Stoppini, L., Buchs, P.-A., & Muller, D. (1991). A simple method for organotypic cultures of nervous tissue. *Journal of Neuroscience Methods*, *37*(2), 173–182. https://doi.org/10.1016/0165-0270(91)90128-M

Sun, Q., & Turrigiano, G. G. (2011). PSD-95 and PSD-93 Play Critical But Distinct Roles in Synaptic Scaling Up and Down. *The Journal of Neuroscience*, *31*(18), 6800–6808. https://doi.org/10.1523/JNEUROSCI.5616-10.2011

Sun, Y., Smirnov, M., Kamasawa, N., & Yasuda, R. (2021). Rapid Ultrastructural Changes in the PSD and Surrounding Membrane after Induction of Structural LTP in Single Dendritic Spines. *The Journal of Neuroscience*, *41*(33), 7003–7014. https://doi.org/10.1523/JNEUROSCI.1964-20.2021

Taft, C. E., & Turrigiano, G. G. (2014). PSD-95 promotes the stabilization of young synaptic contacts. *Philosophical Transactions of the Royal Society B: Biological Sciences*, *369*(1633), 20130134. https://doi.org/10.1098/rstb.2013.0134

Takumi, Y., Ramírez-León, V., Laake, P., Rinvik, E., & Ottersen, O. P. (1999). Different modes of expression of AMPA and NMDA receptors in hippocampal synapses. *Nature Neuroscience*, *2*(7), 618–624. https://doi.org/10.1038/10172

Tomita, S., Stein, V., Stocker, T. J., Nicoll, R. A., & Bredt, D. S. (2005). Bidirectional Synaptic Plasticity Regulated by Phosphorylation of Stargazin-like TARPs. *Neuron*, *45*(2), 269–277. https://doi.org/10.1016/j.neuron.2005.01.009

Trachtenberg, J. T., Chen, B. E., Knott, G. W., Feng, G., Sanes, J. R., Welker, E., & Svoboda, K. (2002). Long-term in vivo imaging of experience-dependent synaptic plasticity in adult cortex. *Nature*, *420*(6917), 788–794. https://doi.org/10.1038/nature01273

Traynelis, S. F., Wollmuth, L. P., McBain, C. J., Menniti, F. S., Vance, K. M., Ogden, K. K., Hansen, K. B., Yuan, H., Myers, S. J., & Dingledine, R. (2010). Glutamate Receptor Ion Channels: Structure, Regulation, and Function. *Pharmacological Reviews*, *62*(3), 405–496. https://doi.org/10.1124/pr.109.002451

Van De Ven, G. M., Siegelmann, H. T., & Tolias, A. S. (2020). Brain-inspired replay for continual learning with artificial neural networks. *Nature Communications*, *11*(1), 4069. https://doi.org/10.1038/s41467-020-17866-2

Van De Ven, G. M., Tuytelaars, T., & Tolias, A. S. (2022). Three types of incremental learning. *Nature Machine Intelligence*, *4*(12), 1185–1197. https://doi.org/10.1038/s42256-022-00568-3

Venkitaramani, D. V., Moura, P. J., Picciotto, M. R., & Lombroso, P. J. (2011). Striatal-enriched protein tyrosine phosphatase (STEP) knockout mice have enhanced hippocampal memory. *European Journal of Neuroscience*, *33*(12), 2288–2298. https://doi.org/10.1111/j.1460-9568.2011.07687.x

Won, S., Incontro, S., Nicoll, R. A., & Roche, K. W. (2016). PSD-95 stabilizes NMDA receptors by inducing the degradation of STEP $_{61}$. *Proceedings of the National Academy of Sciences*, *113*(32). https://doi.org/10.1073/pnas.1609702113

Won, S., Levy, J. M., Nicoll, R. A., & Roche, K. W. (2017). MAGUKs: Multifaceted synaptic organizers. *Current Opinion in Neurobiology*, *43*, 94–101. https://doi.org/10.1016/j.conb.2017.01.006

Woods, G. F., Oh, W. C., Boudewyn, L. C., Mikula, S. K., & Zito, K. (2011). Loss of PSD-95 Enrichment Is Not a Prerequisite for Spine Retraction. *Journal of Neuroscience*, *31*(34), 12129–12138. https://doi.org/10.1523/JNEUROSCI.6662-10.2011

Woods, G., & Zito, K. (2008). Preparation of Gene Gun Bullets and Biolistic Transfection of Neurons in Slice Culture. *Journal of Visualized Experiments*, *12*, 675. https://doi.org/10.3791/675

Yang, G., Pan, F., & Gan, W.-B. (2009). Stably maintained dendritic spines are associated with lifelong memories. *Nature*, *462*(7275), 920–924. https://doi.org/10.1038/nature08577

Yang, S.-N., Tang, Y.-G., & Zucker, R. S. (1999). Selective Induction of LTP and LTD by Postsynaptic [Ca^{2+}]$_i$ Elevation. *Journal of Neurophysiology*, *81*(2), 781–787. https://doi.org/10.1152/jn.1999.81.2.781

Yasuda, R., Hayashi, Y., & Hell, J. W. (2022). CaMKII: A central molecular organizer of synaptic plasticity, learning and memory. *Nature Reviews Neuroscience*, *23*(11), 666–682. https://doi.org/10.1038/s41583-022-00624-2

Yuste, R. (2015). The discovery of dendritic spines by Cajal. *Frontiers in Neuroanatomy*, *9*. https://doi.org/10.3389/fnana.2015.00018

Zhang, Y.-P., Holbro, N., & Oertner, T. G. (2008). Optical induction of plasticity at single synapses reveals input-specific accumulation of αCaMKII. *Proceedings of the National Academy of Sciences*, *105*(33), 12039–12044. https://doi.org/10.1073/pnas.0802940105